Enhancing post-fire forest recovery monitoring through a remote sensing perspective

Alba Viana Soto

Tesis Doctoral

Directores:
Francisco Javier Salas Rey
Mariano García Alonso

Departamento de Geología, Geografía y Medio Ambiente
Programa de Doctorado en Tecnologías de la Información Geográfica

Universidad de Alcalá

Universidad de Alcalá

Programa de Doctorado en Tecnologías de la Información Geográfica

Enhancing post-fire forest recovery monitoring through a remote sensing perspective

Tesis doctoral con mención internacional presentada por:

Alba Viana Soto

Directores:

Dr. Francisco Javier Salas Rey

Dr. Mariano García Alonso

Alcalá de Henares, 2022

A mi familia

“Nothing in life is to be feared, it is only to be understood.

Now is the time to understand more, so that we may fear less.”

– Marie Curie

Acknowledgements

Cuando inicié este camino del doctorado allá por octubre de 2018 no podía imaginar todo lo que esta aventura traería, personal y profesionalmente. Pero creo que cada uno de nosotros somos el resultado de las personas que nos rodean y de las experiencias que vivimos, así que voy a intentar agradecer a todas aquellas personas que me han acompañado en este camino.

En primer lugar me gustaría comenzar agradeciendo a mis directores de Tesis, Javier Salas y Mariano García. Gracias por la confianza depositada en mí desde el primer minuto, por el apoyo de todos estos años, porque sin su valiosa ayuda no habría sido posible la realización de esta tesis. Cuando hablo de directores no puedo dejar de agradecer a Inmaculada Aguado, quien me dio la oportunidad de sumergirme en este apasionante campo de la investigación en teledetección cuando realizaba el máster y también ha estado dirigiendo esta Tesis aunque no fuese oficialmente sobre el papel. A todos ellos que han confiado en mí y en este trabajo, a menudo más que yo misma, gracias por guiarme y enseñarme tanto en estos años, más allá de lo profesional, por su calidad humana.

I would like to thank the Earth Observation team from the Humboldt-Universität zu Berlin, especially Patrick Hostert, for giving me the opportunity and his support to do this stay, as well as Akpona Okujeni and Dirk Pflugmacher. I thank all of them for their support during the whole stay, for the enriching discussions and their interest in the research ongoing. I am also grateful to Sander Veraverbeke and his team from the Vrije Universiteit Amsterdam for the chance of doing a second stay and dive into their fascinating research on fire-climate interactions in boreal forests. I feel fortunate to have had the opportunity of doing such awesome stays during my PhD.

Me gustaría dar las gracias al Ministerio de Ciencia, Innovación y Universidades por haber financiado la realización de esta tesis y al proyecto SERGISAT, en el marco del cual inicié esta investigación. Destacada mención merecen todos los miembros del Grupo de Investigación en Teledetección Ambiental (GITA) de la

Universidad de Alcalá, y en especial Emilio Chuvieco. Gracias por haberme hecho sentir parte de tan maravilloso grupo, por crear ese clima de trabajo y colaboración tan enriquecedor. También quiero mostrar mi agradecimiento al trabajo de la Comisión Académica del Programa de Doctorado en TIG y a la Escuela de Doctorado por la gestión e impartición de cursos de formación esenciales.

Este trabajo es también parte de mis compañeros de doctorado, con los que he compartido grandes momentos de risas, de estrés, de alegrías, y de obstáculos que hemos superado en compañía. Tarek, Ignacio, Macarena, Rubén, Gonzalo, Geovanna, Ramón, Pablo, Roberto, Amin... Y gracias especialmente a Silvia y a Andrea, a quienes la casualidad ha puesto en mi camino en cursos de formación y cuando transitaba por otros países. A mis compañeros de Complutig, especialmente a Dani por darme la primera oportunidad, y a Laura por estar más allá del trabajo y los cambios que vinieron.

Tampoco puedo dejar de agradecer a mis orígenes en la universidad. A Augusto Pérez-Alberti, geógrafo incansable que desde el primer momento consiguió que mi pasión por la Geografía creciese todavía más, por transmitirme sus ganas de seguir descubriendo.

A mis amigos Eva, Adrián, Alba, Sandra, Ana, por estar a pesar de los kilómetros y por sus consejos por muy lejano que también les resultase este trabajo. Pero sobre todo gracias por hacerme disfrutar, por hacerme sentir que con ellos siempre estoy en casa.

A mis padres, Aura y Luis, y a mi hermano Diego, sin los que no habría podido llegar hasta aquí. Gracias por su inspiración y su apoyo incondicional, por creer en mí y en el camino que elegí. A Javi, por compartir cada día conmigo en este caótico mundo de la investigación, por crecer y mejorar juntos, por ser y estar.

Gracias, grazas, thanks, danke, dank je

Contents

Abstract

Forests are essential for human well-being, providing a wide range of benefits like climate regulation, biodiversity conservation, watershed protection and prevention of soil erosion. Although forests have historically been modulated by a multitude of disturbances, they now face unprecedented challenges due to changes in climate and land use. In Mediterranean forests, fire is one of the most common disturbance agents, shaping their structure, composition and functioning. Mediterranean species exhibit adaptive mechanisms to resist and recover, thus being considered fire-resilient ecosystems. Nonetheless, recovery may be hampered by the expected increasing exposure to more frequent and severe fire events. Yet, estimating recovery poses a challenge as it is a dynamic process spanning different spatial and temporal scales. Providing systematic and spatio-temporally explicit information is therefore pivotal to better understand changes in vegetation dynamics in response to fire disturbance.

The overall objective of this thesis is to contribute to the understanding of post-fire forest recovery in Mediterranean ecosystems using remotely sensed data from active and passive sensors. The main goal is conducted through the following specific objectives:

1. To obtain the post-fire recovery trajectories from Landsat time series.
2. To appraise recovery rates and driving factors of forest recovery.
3. To analyse forest structural changes along the post-fire recovery process by combining LiDAR and Landsat data.
4. To quantify changes in cover composition at the subpixel level from unmixing Landsat data.

These objectives are addressed through three papers that have been published in relevant scientific journals. In Paper I we approached the objectives 1 and 2. Through two case studies in Mediterranean pine forests in Spain, we characterised post-fire spectral recovery dynamics at successional stages. We

identified different categories of spectral recovery trajectories using temporal segmentation of Landsat time series (1994–2018) and K-means clustering. *LandTrendr* algorithm was used to derive trajectory metrics from Tasseled Cap Wetness (TCW), sensitive to canopy structure, and Tasseled Cap Angle (TCA), related to vegetation cover gradients. Different categories of post-fire trajectories revealed processes of continuous recovery (continuous recovery, continuous recovery with slope changes, continuous recovery stabilised) and non-continuous recovery. As fire-prone ecosystems, vegetation quickly colonised the space after fire by displaying higher recovery rates in the short-term, but this does not imply the recovery to the pre-fire forest conditions two decades after fire. We further evaluated the influence of environmental and contextual factors on recovery rates. The modelling results indicated that recovery rates were strongly related to fire severity in the short term, whereas climatic conditions in relation to drought were more determinant in the long-term.

In paper II we approached the third objective and combined LiDAR data and Landsat imagery to provide insights on the return of forest structure after fire in fire-prone Mediterranean pine forests in the SE of Spain. We addressed the extrapolation of forest structural variables (Vegetation Cover, Tree Cover, Mean Height and heterogeneity) over three decades (1990-2020) using a Support Vector Regression model (SVR). Model performances to estimate LiDAR-derived structural variables using Landsat images and topographic variables was high, showing stability of the estimations both temporally and spatially. Time-series of structural recovery underlined that less than 50% of burned pixels completely recovered to a pre-fire structure 26 years after fire, suggesting an ongoing recovery process.

In paper III we approached the fourth objective and developed a methodology to quantify changes in woody-vegetation (tree and shrub) cover composition using a regression-based unmixing approach from Landsat Spectral Temporal Metrics (STM). We used synthetically mixed training data from Landsat STM as input for a SVR model to disentangling tree and shrub cover dynamics in Mediterranean

forests, yielding spatio-temporally explicit information on post-fire forest compositional recovery. Our findings suggest that successional dynamics of tree and shrub strongly depended on pre-fire conditions since the majority of the burned areas tended to the pre-fire composition. However, areas shifting from tree to shrub dominance were found 26 years after fire, indicating ongoing transitions that may constitute a successional stage or would prevail in a mature stage. Our results emphasise the utility of unmixing Landsat data to gather information on shifts in composition along the recovery process.

Providing retrospective information on post-fire recovery dynamics can potentially support post-fire forest management by acknowledging the spatio-temporal patterns of forest recovery. Enhancing forest resilience and adaptation pose a challenge for forest managers because Mediterranean forests highly subjected to fire occurrence are also those that face changes in fire regimes along with susceptibility to other disturbances. Estimations of post-fire recovery from remotely sensed data can therefore provide a basis for forest management strategies to better cope with climate change and facilitate decision-makers the selection of management alternatives.

Resumen

Los bosques son esenciales para el bienestar humano, ya que proporcionan una amplia gama de beneficios como la regulación del clima, la conservación de la biodiversidad, la protección de las cuencas hidrográficas y la prevención de la erosión del suelo. Aunque históricamente los bosques han sido modulados por una multitud de perturbaciones, en la actualidad se enfrentan a retos sin precedentes debido a cambios en el clima y los usos del suelo. En los bosques mediterráneos, el fuego es uno de los agentes de perturbación más comunes, dando forma a su estructura, composición y el funcionamiento. Las especies mediterráneas presentan mecanismos de adaptación para resistir y recuperarse, por lo que se consideran ecosistemas resilientes al fuego. Sin embargo, la capacidad de recuperación puede verse comprometida ante el esperado incremento de exposición a eventos de incendios más frecuentes y severos. Con todo, la estimación de la recuperación supone un reto, ya que se trata de un proceso dinámico que abarca diferentes escalas espaciales y temporales. Proporcionar información sistemática y espacio-temporalmente explícita es, por tanto, esencial para una mejor compresión de los cambios en la dinámica de la vegetación en respuesta a la acción del fuego.

El objetivo general de esta tesis es contribuir a la comprensión de la recuperación forestal post-incendio en ecosistemas mediterráneos utilizando datos de teledetección de sensores activos y pasivos. El objetivo principal se aborda a través de los siguientes objetivos específicos:

1. Obtener las trayectorias de recuperación post-incendio a partir de las series temporales de Landsat.
2. Evaluar las tasas de recuperación y los factores que influyen en la recuperación del bosque.
3. Analizar los cambios estructurales del bosque a lo largo del proceso de recuperación post-incendio combinando datos LiDAR y Landsat.

4. Cuantificar los cambios en la composición de la cubierta a nivel de subpixel a partir de la desmezcla de datos Landsat.

Estos objetivos se abordan a través de tres artículos que se han publicado en revistas científicas relevantes. En el artículo I abordamos los objetivos 1 y 2. A través de dos estudios de caso en pinares mediterráneos en España, caracterizamos la dinámica de recuperación espectral post-incendio en las diferentes etapas sucesivas. Identificamos diferentes categorías de trayectorias de recuperación espectral utilizando la segmentación temporal de las series temporales de Landsat (1994-2018) y la agrupación mediante K-means. Se utilizó el algoritmo *LandTrendr* para derivar las métricas de trayectorias a partir de los componentes de Tasseled Cap de humedad (TCW), sensible a la estructura del dosel, y el componente angular (TCA), relacionado con los gradientes de la cubierta vegetal. Las diferentes categorías de trayectorias post-incendio revelaron procesos de recuperación continua (recuperación continua, recuperación continua con cambios de pendiente, recuperación continua estabilizada) y recuperación no continua. Al tratarse de ecosistemas propensos al fuego, la vegetación colonizó rápidamente el espacio tras el incendio mostrando mayores tasas de recuperación a corto plazo, aunque ello no implica la recuperación de las condiciones del bosque previas al incendio dos décadas después del mismo. Además, se evaluó la influencia de los factores ambientales y contextuales en las tasas de recuperación. Los resultados de la modelización indicaron que las tasas de recuperación estaban fuertemente relacionadas con la severidad del incendio a corto plazo, mientras que las condiciones climáticas en relación con la sequía fueron más determinantes a largo plazo.

En el artículo II abordamos el tercer objetivo y combinamos datos LiDAR e imágenes Landsat para proporcionar información sobre la recuperación de la estructura forestal después del incendio en pinares mediterráneos propensos al fuego en el SE de España. Abordamos la extrapolación de las variables estructurales del bosque (cobertura de vegetación, cobertura de arbolado, altura media y heterogeneidad) a lo largo de tres décadas (1990-2020) utilizando un

modelo de *Support Vector Regression* (SVR). El rendimiento del modelo para estimar las variables estructurales derivadas de LiDAR utilizando imágenes Landsat y variables topográficas fue alto, mostrando estabilidad de las estimaciones tanto temporal como espacialmente. Las series temporales de recuperación estructural subrayaron que menos del 50% de los píxeles quemados recuperaron completamente a la estructura anterior al incendio 26 años después, lo que sugiere un proceso de recuperación en curso.

En el artículo III abordamos el cuarto objetivo y desarrollamos una metodología para cuantificar los cambios en la composición de la cubierta vegetal leñosa (arbolado y matorral) utilizando un enfoque de desmezcla basado en la regresión de las Métricas Spectro-Temporales de Landsat (STM). Utilizamos datos de entrenamiento mezclados sintéticamente a partir de Landsat STM como entrada para un modelo SVR para desentrañar la dinámica de la cubierta de arbolado y matorral en los bosques mediterráneos, proporcionando información espacio-temporalmente explícita sobre la recuperación de la composición de los bosques después del incendio. Nuestros resultados sugieren que la dinámica del arbolado y del matorral depende en gran medida de las condiciones previas al incendio, ya que una gran mayoría de la superficie quemada tiende a la composición anterior al incendio. Sin embargo, se encontraron áreas que cambiaron de un dominio del arbolado a un dominio de matorral 26 años después del incendio, indicando transiciones en curso que pueden constituir una etapa transitoria o que podrían prevalecer en una etapa madura. Nuestros resultados enfatizan la utilidad de la desmezcla de datos Landsat para recopilar información sobre los cambios en la composición a lo largo del proceso de recuperación.

Proporcionar información retrospectiva sobre la dinámica de recuperación tras los incendios puede potencialmente apoyar la gestión forestal tras los incendios al reconocer los patrones espacio-temporales de la recuperación forestal. La mejora de la resiliencia y la adaptación de los bosques suponen un reto para los gestores forestales, ya que los bosques mediterráneos altamente sujetos a la ocurrencia de incendios son también los que se enfrentan a cambios en los

regímenes de incendios junto con la susceptibilidad de otras perturbaciones. La estimación de la recuperación tras el incendio a partir de datos de teledetección puede, por tanto, proporcionar una base a las estrategias de gestión forestal para afrontar el cambio climático y facilitar a los responsables de la toma de decisiones la selección de alternativas de gestión.

List of abbreviations

ALS	Airborne Laser Scanning
ARD	Analysis Ready Data
CVH	Coefficient of Variation of Height
DEM	Digital Elevation Model
ETM+	Enhanced Thematic Mapper Plus
FAO	Food and Agriculture Organization
FORCE	Framework for Operational Radiometric Correction for Environmental Monitoring
GEE	Google Earth Engine
IGN	National Geographic Institute of Spain
LAI	Leaf Area Index
LandTrendr	Landsat-based detection of Trends in Disturbance and Recovery
LaSRC	Landsat Surface Reflectance Code
LEDAPS	Landsat Ecosystem Disturbance Adaptive Processing System
LiDAR	Light Detection and Ranging
LTS	Landsat Time Series
MFE	Forest Map of Spain
MH	Mean Height
NIR	Near Infrared
OLI	Orbital Land Imager
PNOA	National Plan for Aerial Orthophotography of Spain
RI	Recovery Indicator
RMSE	Root Mean Square Error
SI	Spectral Indices
SNFI	Second National Forest Inventory of Spain
STM	Spectral Temporal Metrics
SVR	Support Vector Regression
SWIR	Short Wavelength Infrared
TC	Tree Cover
TCT	Tasselled Cap Transformations
TM	Thematic Mapper
USGS	United States Geological Survey
VC	Vegetation Cover

List of tables

Chapter 2

Chapter 3

Appendices

List of figures

Chapter 1

Chapter 3

Chapter 4

Chapter 5

Appendices

Chapter 1. Introduction

1.1. The role of fire in forest ecosystems

Forests are complex ecosystems covering nearly one third of the Earth's land surface (FAO, 2020). Forests provide numerous ecosystem services and play a pivotal role in the Earth System contributing to climate regulation by storing water and carbon (Fahey et al., 2010), biodiversity conservation, and thereby human well-being (Hernández-Blanco et al., 2022). From ages, forests have been modulated by multitude of disturbance agents, strongly influencing the composition, structure and ecosystem functioning (White and Pickett, 1985). Natural disturbances like fire, windthrow, insects and diseases, along with human activities have acted continuously over time shaping current ecosystems (Seidl et al., 2017).

Fires are one of the most widespread natural disturbances (Bowman et al., 2020) that have been present since plants colonised land over 400 million years ago (Scott and Glasspool, 2006), and humans have expanded their use for land management (Pausas and Keeley, 2009). They are key phenomena in the dynamics of global ecosystems (Chuvieco, 2009) directly influencing Earth System's processes through their impacts on vegetation, the carbon cycle, climate (Archibald et al., 2018) and contributing the maintenance of biodiversity (Pausas and Ribeiro, 2017). As fire constitutes an essential component of forest ecosystems, plants have developed adaptive traits to survive and recover, which vary depending on the fire regime (McLauchlan et al., 2020; Pausas and Keeley, 2014a). Nonetheless, forests worldwide are currently facing unprecedented challenges due to changes in climate and land use and other anthropogenic actions (McDowell et al., 2020). Forests are therefore under increasing pressure, resulting in augmented vegetation stress, carbon and biodiversity losses, or changes in soil and hydrology (Aponte et al., 2016; Seidl et al., 2017).

Fire disturbance regimes have profoundly changed in recent decades (Pausas and Keeley, 2009), with climate shifts acting as one of the major drivers (Seidl et al., 2011; Stephens et al., 2013), along with changes in vegetation structure and productivity (Pausas and Keeley, 2014b). Alterations in fire regimes, regarding

their frequency, intensity, size, type, severity and seasonality (Flannigan et al., 2009) can potentially undermine ecosystems recovery dynamics or even prevent recovery (Anderson-Teixeira et al., 2013; Johnstone et al., 2016). Climate change projections indicate an increase in the frequency and severity of forest fires as a result of extreme weather conditions and more severe and prolonged droughts, particularly in water-limited areas (Bowman et al., 2020; Jones et al., 2022; Stephens et al., 2013). Beyond an increase in fire occurrence and area burned, numerous studies suggest that fire seasons are lengthening and this trend is expected to continue in a warmer world (Flannigan et al., 2009; Senande-Rivera et al., 2022). Furthermore, forests will have to adapt not only to changes in fire activity and climate dynamics (Anderson-Teixeira et al., 2013), but also to increased risk of extreme weather events, such as prolonged droughts, storms and floods (IPCC, 2018). The high exposure of forests to global change is likely to hamper future forest recovery after disturbances (Anderson-Teixeira et al., 2013; Qiu et al., 2022). Consequently, improving the understanding of forest ecosystems' response to global environmental changes has become especially important at global and local scales for designing adaptation and mitigation strategies (Ibáñez et al., 2019; Keenan, 2015; Lindner et al., 2010).

1.2. Fire in Mediterranean ecosystems

Mediterranean-type climate regions (MTC), comprising the Mediterranean Basin, California, southern Australia, the Cape Region of South Africa and central Chile, are particularly subjected to fire occurrence (Keeley et al., 2011; Moreira et al., 2020). These areas share similar climate and structurally similar plant communities, comprised of woodlands and sclerophyllous shrublands (Keeley et al., 2011). Fire activity underpins the dynamics of Mediterranean ecosystems worldwide, exerting an evolutionary pressure on plants (Pausas and Keeley, 2014a), so that many species have developed adaptive traits to resist and recover after fire (Keeley, 2012; Ne'eman and Osem, 2021).

In the European context, Mediterranean basin countries concentrate around 85% of the total burned area (San-Miguel-Ayanz et al., 2021). Around 25% of forested areas are dominated by Mediterranean pine forests, (FOREST EUROPE, 2020), forming ecologically and culturally valuable landscapes. These pine forests mostly resulted from reforestation of abandoned lands during the nineteenth and twentieth centuries (Pausas et al., 2004; Vadell et al., 2016). A high proportion of Mediterranean pine forests are currently composed of dense stands and low structural heterogeneity (Ruiz-Benito et al., 2012), which makes them vulnerable not only to extreme wildfires, but also to other disturbances (droughts, pest, pathogens) (Lindner et al., 2010; Senf and Seidl, 2021).

Pine dominated ecosystems as those comprised of *Pinus halepensis* Mill. and *Pinus pinaster* Ait. are largely threatened by wildfires (Fernandes et al., 2008). Nonetheless, adaptive mechanisms as resprouting from surviving individuals and seedling recruitment (Keeley, 2012; Ne'eman and Osem, 2021) have long enable them to recover after fire, leading to rapid cover of vegetation, with post-fire communities presenting similar characteristics to those prior to the fire (Keeley and Pausas, 2022). After a fire event, a phase of establishment and regeneration is initiated with the resprouting of remnant vegetation and the recruitment of new individuals from seeds released from serotinous cones (Tapias et al., 2001; Thanos and Daskalakou, 2000) (*Figure 1.1*). This first stand initiation phase is characterised by seedling growth and competitive interactions between pine seedlings and resprouting shrubs (Calvo et al., 2008; Pausas et al., 2002). In a later successional phase, pine individuals which survive to competition tend to expand, leading to pine canopy dominance (De las Heras et al., 2012).

Despite the high fire resilience of Mediterranean ecosystems, fire can become a destructive force under changing fire regimes and climatic conditions (Pausas and Fernández-Muñoz, 2012), which may jeopardise the natural forest recovery dynamics (González-De Vega et al., 2016). Obligate seeders as *Pinus halepensis* and *Pinus pinaster* (Calvo et al., 2008; Moya et al., 2008) are especially vulnerable in the face of increasing anthropogenic fire frequency

(Keeley and Pausas, 2022). Natural regeneration strongly depend on the amount of seeds stored in the canopy seed bank linked to the immaturity risk period, and the quantity of seeds available after fire (Tapias et al., 2001; Thanos and Daskalakou, 2000). Shorter fire return intervals can undermine natural seedling recruitment (Taboada et al., 2017) since recovery and maturity, both structurally and functionally, is estimated to require at least 20-30 years (De las Heras et al., 2012; Trabaud, 1994). Therefore, fire recurrence can negatively affect the ecosystem if the minimum time interval of immaturity risk (estimated in 15 years, Eugenio et al., 2006) is exceeded, promoting ecosystem transitions in Mediterranean forests (Karavani et al., 2018; Vasques et al., 2022).

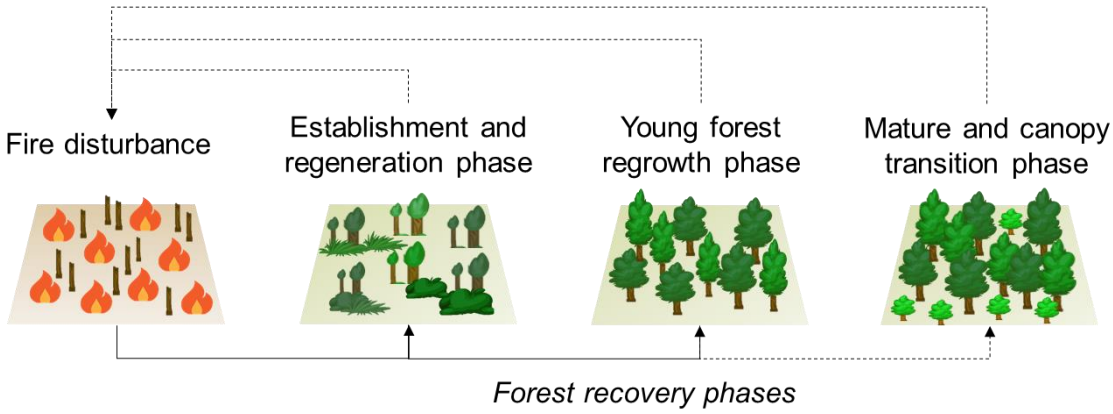

Figure 1.1. Diagram of post-fire recovery phases in relation to stand development stages (adapted from Oliver and Larson, 1996).

1.3. Earth observation for forest monitoring

Detailed knowledge of forest dynamics is essential for enhancing forest resilience to fire. Field data measurements of vegetation physical parameters are highly valuable when studying forests ecosystems, but cost-effective methodologies to support forest resilience strategies at different spatio-temporal scales are needed. Remote sensing sensors enable to systematically monitoring forest recovery processes, providing spatio-temporally explicit information on ecosystems dynamics (Lechner et al., 2020). Given the challenge involved in

monitoring continuously changing environments, remote sensing techniques are increasingly used for characterising forest recovery as they provide global information at a variety of spectral, spatial and temporal resolutions (Banskota et al., 2014; Chu and Guo, 2013; Gómez et al., 2019).

Remotely sensed data have been used to investigate a variety of aspects regarding fire and ecosystems interactions: before fire occurrence, to estimate fire danger conditions, to monitor fire position and combustion characteristics, and after fire to analyse fire effects on vegetation and regeneration (Chuvieco et al., 2020). Contributions of remote sensing techniques to forest monitoring comprise a wide range of sensors and methods. Remote sensing uses the electromagnetic radiation recorded by sensors onboard satellites, planes and unmanned aerial vehicles (UAVs) in different spectral regions (*Figure 1.2*). These sensors provide valuable information about the Earth's surface through the different interactions between the electromagnetic radiation and cover types depending on the wavelength observed. Passive sensors use the solar irradiance as source of energy, which is either reflected by the Earth's surface and atmosphere, or absorbed and re-emitted. Active sensors, such as radar and LiDAR, in turn, have their own source of radiation and thus are independent of sunlight.

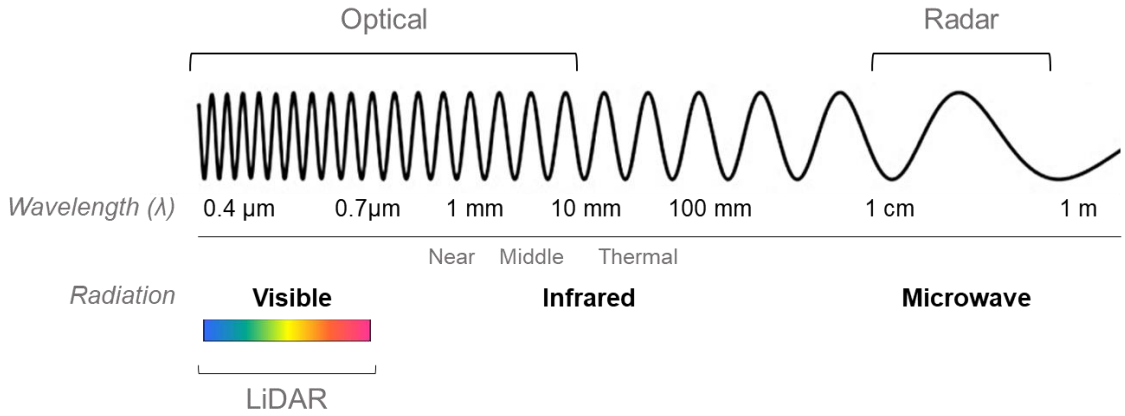

Figure 1.2. Electromagnetic spectrum covered by remote sensing systems (adapted from Chuvieco, 2016).

Furthermore, the range of methods for forest monitoring has broadened exponentially in the last decades, including machine learning and deep learning algorithms (Lary et al., 2016; Yuan et al., 2020), synergies between optical and LiDAR (Coops et al., 2021; García et al., 2011), between optical and radar (Baumann et al., 2018; García et al., 2018), more sophisticated change detection algorithms (Zhu, 2017) and cloud-computing environments (Gorelick et al., 2017).

In the following sections the main characteristics of optical and LiDAR data that were considered in this thesis are explained in the context of forest monitoring.

1.3.1. Optical data

Passive optical sensors have been most commonly used for analysing vegetation dynamics (Hirschmugl et al., 2017). Optical sensors vary in the number of bands and the width of these bands, determining the spectral resolution. While multispectral sensors have a limited number of bands, hyperspectral sensors have hundreds of much narrower bands. Data obtained from optical multispectral sensors also vary in terms of spatial and temporal resolution depending on the satellite orbit characteristics. Multispectral sensors from leading space missions vary from medium spatial resolution (10-30 m) such as the Landsat mission (Wulder et al., 2016) or Sentinel 2 from the Copernicus program of the European Space Agency (ESA) (Berger et al., 2012), with revisit periods of 5-16 days, to coarser spatial resolution of MODIS data onboard Terra-Aqua (Salomonson et al., 2002) or Sentinel 3, (250-500 m) but with daily revisit periods.

The opening of the Landsat archive in 2008 undoubtedly changed the way of observing Earth's ecosystems (Wulder et al., 2012a). Landsat sensors, with 50 years of observations (Wulder et al., 2022), provide retrospective information on forest dynamics, having the spatial, spectral and temporal characteristics adequate to analyse dynamic processes as recovery (Bright et al., 2019; Frazier et al., 2015; Griffiths et al., 2014; Hislop et al., 2018). Landsat sensors have evolved from initially four broad bands (MSS) to increasingly narrower and

numerous wavelength ranges (TM, ETM+, OLI and OLI2), extracting information from the visible, infrared and thermal since the launch of Thematic Mapper (TM) on Landsat 4 in 1982. Landsat's continuity and improved reprocessing to ensure geometric consistency, well-radiometric calibration and harmonization among sensors are especially important because it renders a unique measurement record for comprehensively tracking vegetation changes (Kennedy et al., 2014).

1.3.2. LiDAR data

LiDAR remote sensing data have garnered much attention due to their wide range of applications in forestry. LiDAR sensors provide detailed information on many structural properties as the height and vertical distribution of the forest canopy (Lefsky et al., 2002). Lidar instruments measure the distance between the sensor and the target surface based on the elapsed time between the emitted laser pulses and reflected energy. Based on their recorded characteristics can be classified as discrete return, which record single or multiple returns (*Figure 1.3*), or full waveform recording, which digitise the entire reflected energy from a return, resulting in complete vertical profiles (Wulder et al., 2012b).

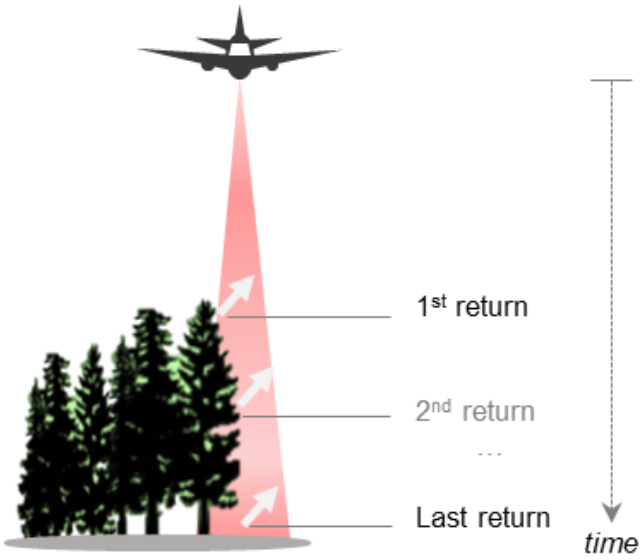

Figure 1.3. Schema of discrete return LiDAR systems in forest mapping (adapted from Montealegre, 2017).

Although LiDAR data have been used less than optical data for forest monitoring, mainly due to lower spatio-temporal coverage, cost and higher processing complexity, software and hardware developments along with new spaceborne LiDAR missions have largely expanded their use in recent years. Spaceborne LiDAR instruments recently launched as the Global Ecosystem Dynamics Investigation (GEDI) on the International Space Station (ISS; Dubayah et al., 2020) and the Advanced Topographic Laser Altimeter System (ATLAS) onboard the Ice, Cloud, and land Elevation Satellite 2 (ICESat-2; Neumann et al., 2019) are currently providing near-global observations. However, products derived have several limitations for practical applications that need further enhancement (Mulverhill et al., 2022; Potapov et al., 2021) such as un-sampled areas, local-scale analysis and data fusion with optical imagery for the spatiotemporally extrapolation (Coops et al., 2021).

Airborne laser scanning (ALS) on planes or helicopters is one of the most common types of LiDAR (Maltamo et al., 2014). ALS data are well suited to characterise forest attributes (Bottalico et al., 2017; Wulder et al., 2012b; Zhao et al., 2011) and vegetation structural recovery (Gordon et al., 2017; Martín-Alcón et al., 2015) over both local-scale and large areas. In the case of the Spanish territory, two LiDAR coverages for the period 2008-2015 (1st coverage) and from 2015 up to date (2nd coverage) have been acquired by the National Plan for Aerial Orthophotography of Spain (PNOA). These LiDAR data collected using small-footprint discrete-return sensors (*Figure 1.3*) have proved their ability to estimate forest attributes across Mediterranean forests in Spain (Gelabert et al., 2020; Montealegre et al., 2016; Tijerín et al., 2022). The availability of free ALS data makes Spain a particular case for the synergies between ALS data and optical imagery to obtain vegetation parameters of forest conditions over time and space.

1.4. Measures of forest disturbance and recovery

Disturbance and recovery processes characterise forest current state and temporal dynamics. There is no single definition of post-disturbance forest

recovery, but it commonly relates to the return of forest characteristics following a disturbance event (Frolking et al., 2009). Furthermore, definitions of recovery and resilience are often disparate depending on the research field. Engineering resilience is mainly defined as recovery of the system, ecological resilience considers both resistance and recovery of the system, whereas socio-ecological resilience includes resistance, recovery and adaptive capacity (Nikinmaa et al., 2020). From a remote sensing perspective, engineering definition of the resilience is commonly taken, referring to the time a system takes for variables to return to their pre-disturbance equilibrium (Reynolds, 1975). Recovery of the ecosystem is therefore measured as the speed towards pre-disturbance state or the degree of return to pre-disturbance conditions (Nikinmaa et al., 2020) (*Figure 1.4*). Yet, estimating recovery is as challenging as it is complex to define and multiple approaches from optical and LiDAR data have been proposed (Pérez-Cabello et al., 2021).

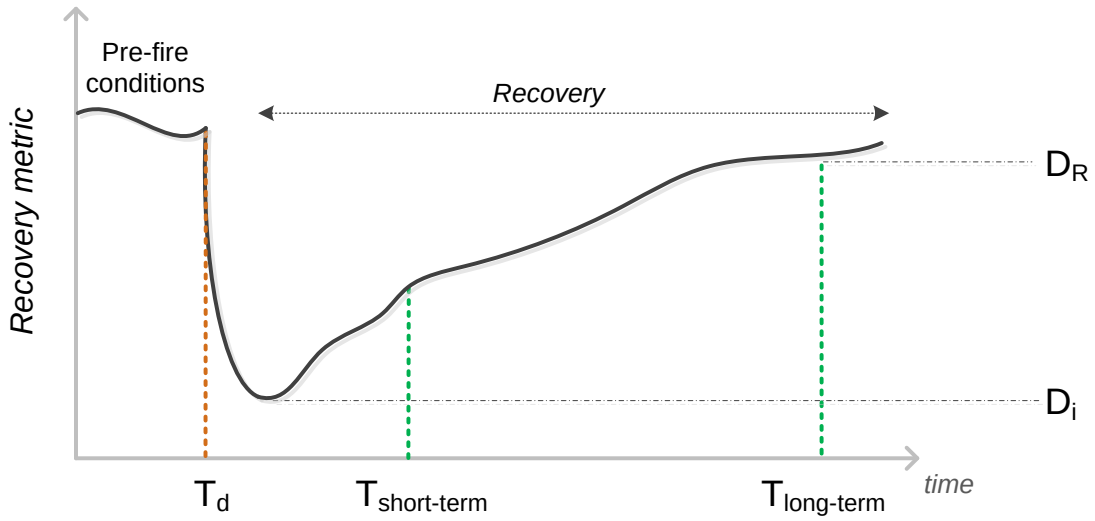

Figure 1.4. Outline of the dynamics of forest disturbance-recovery. T_d: time when disturbance occurr; $T_{short-term}$: initial recovery; $T_{long-term}$: moment in time in which recovery stabilises; D_I: lowest value derived from the impact of disturbance; D_R: value of the recovery as function of time.

Spectral recovery estimated from optical imagery is an indirect measure of the recovery. Disturbance and subsequent recovery are detected by the changes in spectral properties derived from changes in structure and composition of the forest. Stand-replacing disturbances like fire result in a significant removal of

vegetation, leaving the ground exposed. Immediately after fire, disturbed areas have low reflectance in the NIR and high reflectance in the visible and SWIR wavelengths due to the lack of absorption from vegetation and the exposure of soil (Escuin et al., 2008). Once the recovery process is initiated, reflectance in the NIR increase since vegetation have higher reflectance than soil in the NIR (Nilson and Peterson, 1994). Spectral Indices (SI) have been designed to enhance these different spectral responses of vegetation at different wavelengths and have been extensively used for assessing post-disturbance recovery with remotely sensed data (Banskota et al., 2014; Chu and Guo, 2013; Pérez-Cabello et al., 2021). Landsat time series analysis and change detection algorithms (Hirschmugl et al., 2017; Zhu, 2017) commonly use SI as inputs. Recent research on spectral recovery estimations have emphasised the advantages of using multiple indices and metrics to provide a more comprehensive assessment of recovery (Hislop et al., 2018; Pickell et al., 2016; White et al., 2017).

In turn, the necessity to provide insights on forest structural recovery has led to the emergence of new methodologies for assessing changes over time using LiDAR data (Coops et al., 2021). As LiDAR data are collected for limited extensions and specific moments on time at the national and regional level, the spatiotemporal extrapolation is unavoidable (Matasci et al., 2018; White et al., 2022). However, uncertainties regarding the performance of models for predicting LiDAR-derived metrics still remain depending on the nature of LiDAR data, ecosystem's characteristics and algorithms employed.

Despite numerous studies address the analysis of disturbance and post-fire recovery processes from remotely sensed data, the connections between remote sensing and ecological understanding of forest recovery are not conclusive to date and highly variable across ecoregions. It is therefore essential to further research these dynamics in order to meet the challenges posed by climate change. Sustainable management of post-fire actions requires understanding and better estimate natural recovery that can be decisive for anticipating and enhancing ecosystem resilience (Keenan, 2015; Lindner et al., 2014).

Chapter 2. Hypothesis, objectives and outline of the thesis

2.1. Hypothesis

Given that vegetation response following fire can be described and analysed from spectral information of satellite images and changes in forest structure can be quantified from LiDAR data, we hypothesise that:

- The use of Landsat time series provides multi-decadal information on spectral recovery. Rates of recovery can be derived considering pre-fire and post-fire values at successional recovery stages.
- Post-fire forest recovery dynamics can be further influenced by environmental and contextual factors. These factors vary across both time and space, and, therefore, recovery rates will differ.
- The integration of LiDAR data and Landsat imagery enables the assessment of changes in forest structure over both time and space. Structure recovery will be slower than either spectral or compositional recovery.
- Spectral unmixing techniques yield information on forest composition at the sub-pixel level. Cover dominance of vegetation types changes along the recovery process and transitions from pre-fire dominance may occur.

2.2. Objectives

Despite the efforts to provide meaningful information on post-fire recovery from remotely sensed data, key gaps remain open regarding connections between spectral indicators and ecological understanding of forest recovery and further enhancement of the integration of different sensors (Bartels et al., 2016; Pérez-Cabello et al., 2021). This thesis aims to contribute to the understanding of post-fire forest recovery in Mediterranean ecosystems using remotely sensed data from active and passive sensors. In order to achieve this objective, the following objectives were pursued:

1. To obtain the post-fire recovery trajectories from Landsat time series. We identify classes of spectral recovery trajectories by applying a trajectory segmentation approach to Landsat imagery.

2. To appraise recovery rates and driving factors. We define recovery patterns according to the spectral recovery rates and their relation to severity, topography, environmental and climatic factors.

3. To analyse forest structural changes along the post-fire recovery process. We combine LiDAR data and Landsat imagery to characterise the recovery of structural attributes over both time and space.

4. To quantify changes in cover composition at the subpixel level. We implement a spectral unmixing approach to disentangling post-fire woody-vegetation cover dynamics from Landsat imagery.

2.3. Outline of the thesis

This doctoral thesis is presented as a compendium of articles except for the overall Introduction chapter and Synthesis chapter. All other chapters have been published in international journals indexed in Journal Citation Reports (JCR) and Scopus (*Table 2.1*).

In Chapter 1 we introduce the main issues addressed in this thesis and provide a theoretical background and state of the art, which leads to the hypothesis and objectives described in Chapter 2. The objectives stated are addressed in the main part of the thesis, which comprises three papers.

In Paper I (Chapter 3), we approach the objectives 1 and 2. We identify spectral recovery trajectories using temporal segmentation of Landsat time series and evaluate the influence of pre-fire conditions, severity, topography and post-fire climate on recovery rates for each recovery category at successional stages.

In Paper II (Chapter 4), we address the extrapolation of LiDAR-derived metrics to Landsat imagery to provide insights on the return of forest structure after fire (Objective 3).

In Paper III (Chapter 5), we perform a regression-based unmixing approach to unravel the shifts in post-fire forest cover composition from Landsat imagery (Objective 4).

Chapter 6 summarises the key findings and discusses the relevance of the results to forest recovery assessment as well as the potential limitations of the research. Moreover, it outlines the future research directions.

Table 2.1. Publication index and chapters. Impact factor corresponds to Journal Citation Report.

Publication	**Impact factor**	**Chapter**
Viana-Soto, A., Aguado, I., Salas, J., & García, M. (2020). Identifying post-fire recovery trajectories and driving factors using landsat time series in fire-prone Mediterranean pine forests. *Remote Sensing*, 12(9), 1499.	4.848	3
Viana-Soto, A., García, M., Aguado, I., & Salas, J. (2022). Assessing post-fire forest structure recovery by combining LiDAR data and Landsat time series in Mediterranean pine forests. *International Journal of Applied Earth Observation and Geoinformation*, 108, 102754.	7.672	4
Viana-Soto, A., Okujeni, A., Pflugmacher, D., García, M., Aguado, I., & Hostert, P. (2022). Quantifying post-fire shifts in woody-vegetation cover composition in Mediterranean pine forests using Landsat time series and regression-based unmixing. *Remote Sensing of Environment*, 281, 113239.	13.850	5

Chapter 3. Temporal segmentation of Landsat time series to identify post-fire recovery patterns

Based on:

Viana-Soto, A., Aguado, I., Salas, J., & García, M. (2020). Identifying post-fire recovery trajectories and driving factors using Landsat time series in fire-prone Mediterranean pine forests. *Remote Sensing*, 12(9), 1499. https://doi.org/10.3390/rs12091499

Abstract

Wildfires constitute the most important natural disturbance of Mediterranean forests, driving vegetation dynamics. Although Mediterranean species have developed ecological post-fire recovery strategies, the impacts of climate change and changes in fire regimes may endanger their resilience capacity. This study aims at assessing post-fire recovery dynamics at different stages in two large fires that occurred in Mediterranean pine forests (Spain) using temporal segmentation of the Landsat time series (1994–2018). Landsat-based detection of Trends in Disturbance and Recovery (LandTrendr) was used to derive trajectory metrics from Tasseled Cap Wetness (TCW), sensitive to canopy moisture and structure, and Tasseled Cap Angle (TCA), related to vegetation cover gradients. Different groups of post-fire trajectories were identified through K-means clustering of the Recovery Ratios (RR) from fitted trajectories: continuous recovery, continuous recovery with slope changes, continuous recovery stabilised and non-continuous recovery. The influence of pre-fire conditions, fire severity, topographic variables and post-fire climate on recovery rates for each recovery category at successional stages was analysed through Geographically Weighted Regression (GWR). The modelling results indicated that pine forest recovery rates were highly sensitive to post-fire climate in the mid and long-term and to fire severity in the short-term, but less influenced by topographic conditions (adjusted R-squared ranged from 0.58 to 0.88 and from 0.54 to 0.93 for TCA and TCW, respectively). Recovery estimation was assessed through orthophotos, showing a high accuracy (Dice Coefficient ranged from 0.81 to 0.97 and from 0.74 to 0.96 for TCA and TCW, respectively). This study provides new insights into the post-fire recovery dynamics at successional stages and driving factors. The proposed method could be an approach to model the recovery for the Mediterranean areas and help managers in determining which areas may not be able to recover naturally.

***Keywords*:** post-fire recovery, Landsat, time series, LandTrendr, K-means, driving factors, Mediterranean, pine forests.

3.1. Introduction

Wildfires constitute one of the most widespread and important natural disturbances of forest ecosystems, playing a paramount role in the dynamics of the terrestrial system (Bowman et al., 2009). Forest fires impact at a wide range of scales causing ecological, economic and human health impacts (Aponte et al., 2016; Chuvieco, 2009). Specifically in Europe, the Mediterranean region registers the highest number of fires and burned areas (San-Miguel-Ayanz et al., 2019), with around 85% of the total burnt area (San-Miguel-Ayanz et al., 2013).

Notwithstanding, Mediterranean ecosystems are adapted to fire recurrence as it constitutes the most important natural disturbance, driving vegetation dynamics (Peterson, 2014). Mediterranean species have developed post-fire ecological strategies including resprouting capacity, seed bank persistence and increased dispersal capacity (De las Heras et al., 2012; González-De Vega et al., 2018). Nevertheless, land use changes and the impacts of climate change may affect the dynamics of post-fire ecological succession in the immediate future (Aponte et al., 2016; Pausas and Keeley, 2009). Although large fire (i.e. ≥ 500 ha) occurrence for the European Mediterranean region does not show a strong increasing trend in the recent decades (San-Miguel-Ayanz et al., 2013), climate change projections indicate an increase in the frequency and intensity of megafires, as a result of more extended and severe seasonal droughts (Stephens et al., 2013), which will impact ecosystems' species composition and functioning (Aponte et al., 2016). Forest ecosystems must adapt not only to changes in average climatic variables, but also to a wide variability with higher risk of extreme climatic events, such as prolonged droughts. Thus, forest management in European Mediterranean countries is challenging due to the vulnerability of natural regrowth capability of these ecosystems (González-De Vega et al., 2016; Lindner et al., 2010).

Time-series of satellite data have long been used for retrospectively generating information on forest disturbance and recovery dynamics (Gitas et al., 2012). The opening of the Landsat archive in 2008, now available geometrically and

radiometrically corrected, provided new opportunities for improved understanding of the mechanisms of forest changes (Banskota et al., 2014; Wulder et al., 2019). Several studies have addressed the spatial and temporal analysis of post-fire vegetation dynamics through different forest ecosystems: Mediterranean (Fernández-Manso et al., 2016; Meng et al., 2015), boreal (Ireland and Petropoulos, 2015; Pickell et al., 2016), Siberian (Chu et al., 2017; Shvetsov et al., 2019), temperate (Griffiths et al., 2014), tropical (DeVries et al., 2015), savannah (Lhermitte et al., 2011) or across different ecozones at the regional or national scale (Bright et al., 2019; Frazier et al., 2018; Kennedy et al., 2012; White et al., 2017).

The use of Landsat Time Series (LTS) for change detection has increased substantially in recent years as new methodological approaches have emerged (Zhu, 2017). Early approaches characterised post-fire recovery dynamics by applying linear regression functions to spectral trajectories obtained from Landsat time-series (Hope et al., 2007; Röder et al., 2008). More recently, several change detection algorithms have been developed and widely used in analysing forest changes, such as *Landsat-based detection of Trends in Disturbance and Recovery* (LandTrendr) (Kennedy et al., 2010) and *Vegetation Change Tracker* (VCT) (Huang et al., 2010), to provide change information on an annual time-scale (Zhu, 2017). Others include, *Breaks For Additive Seasonal and Trend* (BFAST) (Verbesselt et al., 2010) and *Continuous Monitoring of Forest Disturbance Algorithm* (CMFDA) (Zhu et al., 2012), which use a high frequency of time-series. The trajectory-based segmentation algorithm LandTrendr enables the characterization of distinct subtrends within a simplified representation of the spectral trajectory, which provides the essential information needed to identify abrupt disturbances in forests (e.g. fire and harvest), as well as slowly evolving processes (e.g. regrowth and defoliation). The utility of LandTrendr has been demonstrated in different regions for assessing disturbance and recovery dynamics (Bright et al., 2019; Kennedy et al., 2012; Nguyen et al., 2018).

Several spectral measures can be derived from LTS and used as inputs for segmentation algorithms such as spectral indices or Tasseled Cap Transformations (TCT). Some spectral indices focused more on the red and near-infrared bands, making them sensitive to canopy greenness and photosynthetic activity, such as the Normalised Difference Vegetation Index (NDVI) employed for characterizing post-fire recovery (Ireland and Petropoulos, 2015; Meng et al., 2015; Viana-Soto et al., 2017), whereas other indices using the SWIR bands are more sensitive to vegetation moisture and forest structure (Hislop et al., 2018), such as the Normalised Burn Ratio (NBR) (Key and Benson, 2006), commonly used for recovery assessment (Bright et al., 2019; Morresi et al., 2019; Pickell et al., 2016). TCT are created via linear transformations using defined coefficients (Crist, 1985) and have been widely used for studying forest changes (Frazier et al., 2015; Gómez et al., 2011; Nguyen et al., 2018; Pflugmacher et al., 2014). TCT components correspond to the physical characteristics of vegetation: Brightness (TCB) is related to the pixel albedo of the land surface and values are typically high after a stand replacing disturbance; Greenness (TCG) is a contrast between the visible and near-infrared bands, being sensitive to green vegetation (Pickell et al., 2016), and Wetness (TCW) is a contrast of the visible and near-infrared with the SWIR bands, making it sensitive to canopy moisture and structure (Hansen et al., 2001). Several metrics can be derived from TCT such as TC Angle (TCA), which is related to the vegetation cover within the TCB-TCG spectral plane (Powell et al., 2010). Considering that spectral indices are sensitive to different vegetation conditions, the use of TCT components and derived metrics enables the characterization of different forest conditions (Frazier et al., 2015; Gómez et al., 2012; Hislop et al., 2018; Pickell et al., 2016).

Although the dynamics of post-fire vegetation recovery has been studied through different forest ecosystems, few studies have investigated the recovery driving factors in Mediterranean ecosystems (Martín-Alcón and Coll, 2016; Meng et al., 2015; Röder et al., 2008; Viana-Soto et al., 2017) and fewer have focused on characterizing successional recovery stages (Bartels et al., 2016; Oliver and Larson, 1996), which are key to understanding forest changes for sustainable

forest management. This study assesses the post-fire recovery dynamics at different stages in fire-prone Mediterranean pine forests. The specific objectives of this study were: (1) to identify the different post-fire recovery trajectories using temporal segmentation of LTS; (2) to analyse the recovery patterns for each trajectory group through stages; and (3) to appraise the environmental and contextual drivers of the recovery process.

3.2. Study area

This research is based on two large fires that occurred in the summer of 1994 (*Figure 3.1*): The Yeste Fire (August 7th), which burned 11,685 ha of wooded area and the Requena Fire (July 5th), which burned 16,373 ha of wooded area For this study, we selected sections that had neither burned in subsequent fires nor been reforested after the main disturbance of 1994 in order to ensure the analysis of natural recovery only.

Both study areas are located in the Southeast of the Iberian Peninsula, in the Mediterranean biogeographic region, which is characterised by mean annual precipitations of 600-700 mm with soil hydrological deficit in summer and mean annual temperatures around 15^{o}C. These areas were dominated by anthropogenic coniferous forests, mainly composed by species of the genus *Pinus* along with certain deciduous species of the genus *Quercus*, and , sclerophyll species such as *Rosmarinus*, *Thymus*, or *Juniperus* species in the understory (Rivas-Martínez, 1981). Due to the differences in post-fire ecological strategies to recover, we selected those patches dominated by *Pinus halepensis* and *Pinus pinaster* according to the Second National Forest Inventory of Spain (SNFI) (Ministerio de Agricultura Pesca y Alimentación, 1990). Both species are obligate seeders since they have serotinous cones that enable the natural post-fire regeneration (De las Heras et al., 2012; Fernández-García et al., 2019). The post-fire recovery stages which can be identified in a Mediterranean pine forest 24 years after fire, range from the stand initiation (establishment phase including remnant pines, herbaceous and pine seeding processes)(González-De Vega et

al., 2018) to the stem exclusion (a young regrowth forest composed by shrubs and tree plantlets) (Eugenio et al., 2006; Moya et al., 2018; Oliver and Larson, 1996). Since competition between shrubs and trees starts immediately following fire (Bartels et al., 2016; Crotteau et al., 2013), vegetation recovery in this study refers to both tree and shrub recovery.

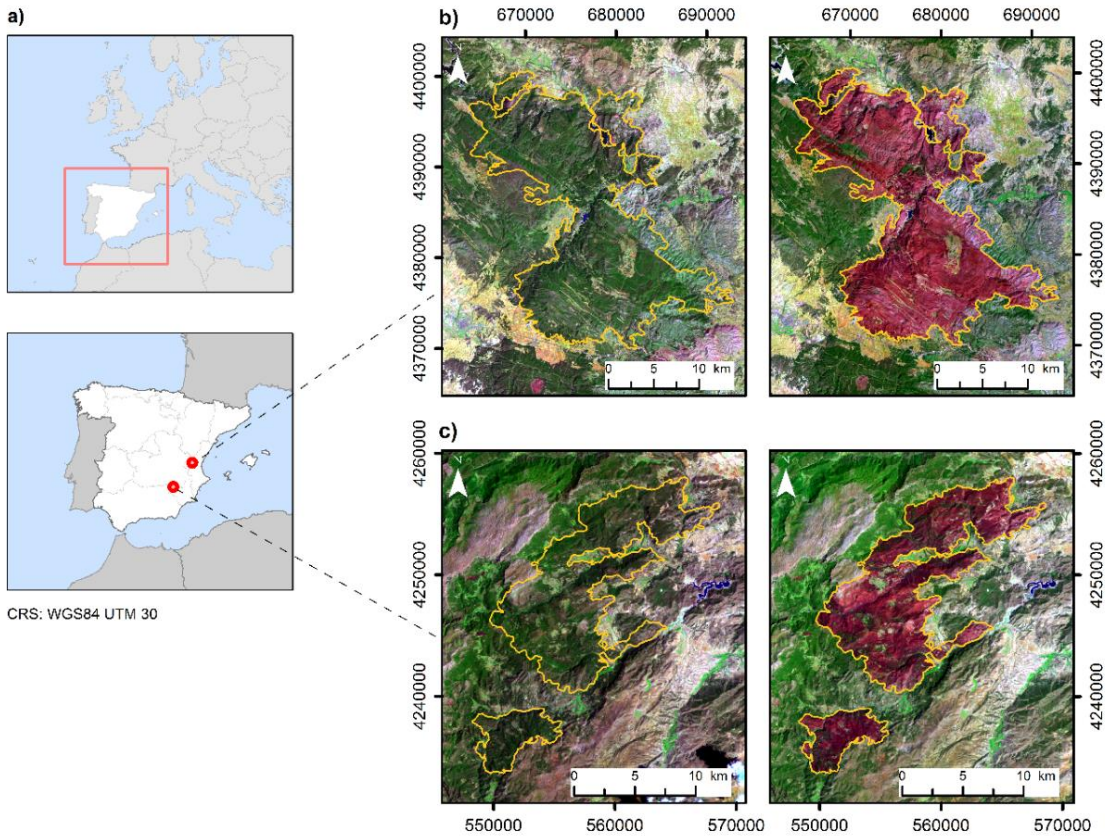

Figure 3.1. Study areas located in the Iberian Peninsula: Requena above, Yeste below; (a) Location of the study areas; (b) Pre- and post-fire Landsat composition for Requena RGB (SWIR2, NIR, Blue); (c) Pre- and post-fire Landsat composition for Yeste RGB (SWIR2, NIR, Blue).

3.3. Materials and methods

A flowchart of the methodology is depicted in *Figure 3.2*. Firstly, annual composites were created for the available time-series. Secondly, spectral indices and TCT was performed to delineate burned areas and derive trajectory metrics

of forested pixels based on the LandTrendr segmentation algorithm (Kennedy et al., 2010). Fitted trajectories were categorised according to the change magnitude and duration represented in the sequence of segments of each trajectory using a K-means algorithm. Finally, we analysed the environmental and contextual drivers of the recovery process. The accuracy assessment of the recovery classes was carried out by visual assessment of vegetation cover in randomly distributed sample plots, in reference to high-resolution orthophotos.

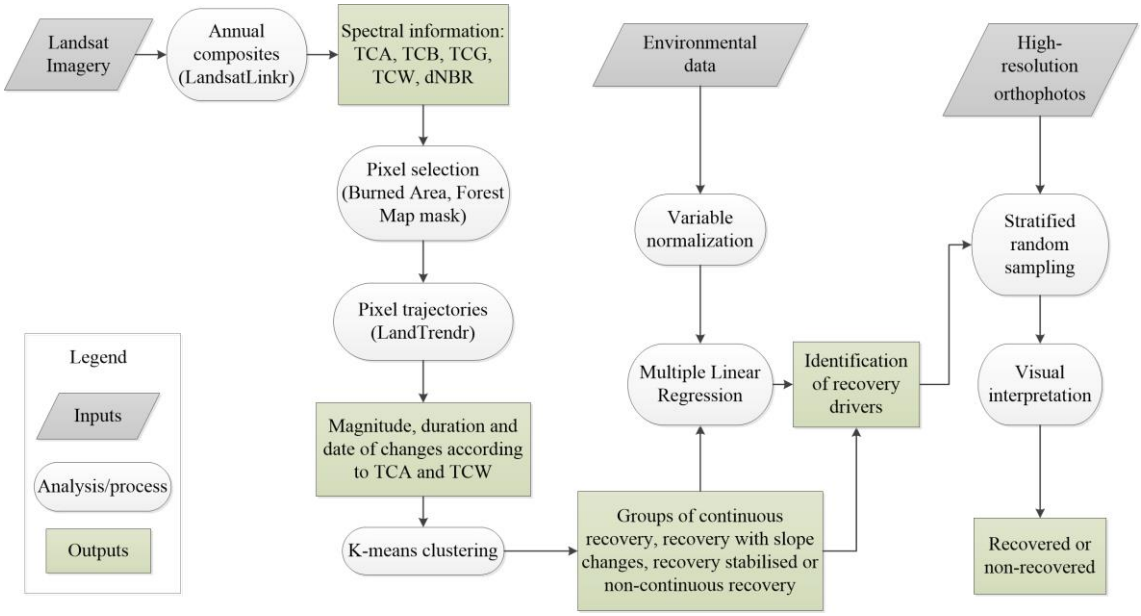

Figure 3.2. Flowchart of the methodology.

3.3.1. Data

We downloaded the Landsat TM/ETM+/OLI images from the United States Geological Survey (USGS) Earth Explorer server to build the time-series covering the period 1990–2018, including 4 years pre-fire (Path/Row: 200/033, 199/032, 199/033). We selected images from Tier 1 Surface Reflectance products generated from the Landsat Ecosystem Disturbance Adaptive Processing System (LEDAPS) software (Masek et al., 2006) for TM and ETM + images and Landsat 8 Surface Reflectance Code (LaSRC) for the OLI dataset (Vermote et al., 2016). We prioritised scenes with less than 10% cloud-cover, within the

summer period to minimise the effect of phenological changes. To delimit fire perimeters and to assess fire severity we used two Landsat 5 TM images acquired in 1994 for the Yeste Fire (July 22th pre-fire, August 23th post-fire) and for the Requena Fire (June 29th pre-fire, 16thAugust post-fire) (*Figure 3.1*). Fire perimeters were constructed by applying the USGS thresholds (Key and Benson, 2006) to the differenced Normalised Burn Ratio (dNBR) (Miller and Thode, 2007).

Spatial reference to vegetation types was based upon the Forest Map of Spain which was made between 1986 and 1997 through aerial photographs and field work (Ministerio de Agricultura Pesca y Alimentación). Topographic variables were built from the LiDAR-based Digital Elevation Model (25-m spatial resolution) from the National Geographic Institute of Spain (IGN). As climatic information we used the Standardised Precipitation-Evapotranspiration Index (SPEI) (Vicente-Serrano et al., 2017), a multi-scalar drought index that calculates the effect of potential evapotranspiration (PET) on drought severity. Compared to other drought indices, the SPEI has the advantage of combining multi-scalar character with the capacity to include the effects of temperature variability (Vicente-Serrano et al., 2010). Data are available for the entire time-series (1990-2018) at 1-km resolution. We also downloaded the orthophotos at 0.5-m resolution from the Aerial Orthophotography National Plan, as reference data to assess recovery through time-series (Years 2002, 2009, 2010, 2017 and 2018) (IGN).

3.3.2. Landsat Time Series

Summer time-series was created for the 28-year time period using the closest cloud-free image to the mid of the summer season: Requena median Julian day 209; Yeste median Julian day 218. The temporal window used to select the images spanned ±38 days around the reference date (*Figure 3.3*) in order to ensure consistency through the time-series.

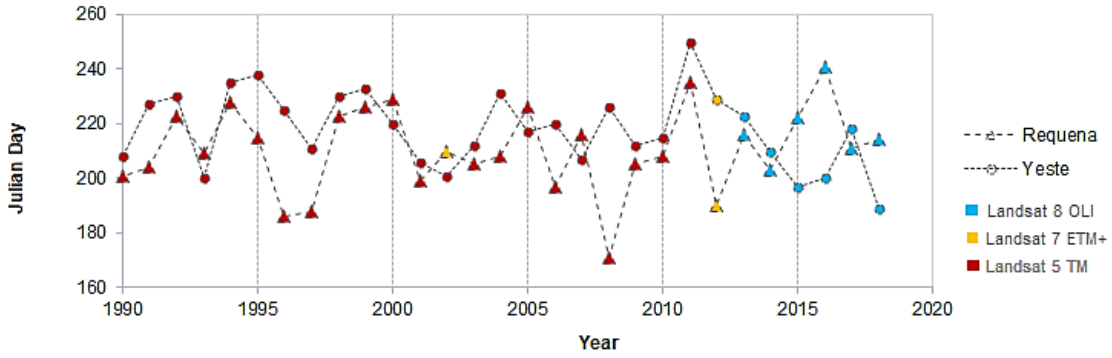

Figure 3.3. Scene selection dates according to the Julian Day.

We used the R package LandsatLinkr (Braaten et al., 2017; Vogeler et al., 2018) to create annual cloud-free image stacks and calculate the TCT components using the coefficients defined for reflectance data (Crist, 1985): Brightness (TCB), Greenness (TCG) and Wetness (TCW). Subsequently, the angular component of the TCT (TCA) was computed as follows (Powell et al., 2010):

$$TCA = \tan^{-1}\left(\frac{TCG}{TCB}\right) \quad (1)$$

3.3.3. Trajectory segmentation and clustering

To extract recovery trajectories, we applied the LandTrendr trajectory-based segmentation algorithm (Kennedy et al., 2010) to TCA and TCW time-series. In this study we opted to use the TCA due to its relation with the percentage of vegetation cover in coniferous and mixed forests (Gómez et al., 2012; Powell et al., 2010), and the TCW since it is sensitive to canopy moisture and structure (Frazier et al., 2015; Hansen et al., 2001). LandTrendr goes through the time-series and creates a fitted trajectory as a sequence of line segments for each pixel. Firstly, the vertices of each segments were established from an iterative regression process using Ordinary Least Squares (OLS) by estimating the years of change using the TCA and TCW time-series. Then, the trajectories are iteratively simplified from a selection process using the angle criterion until a number of segments equal to or less than a user-defined threshold were obtained

(segmentation process) (Kennedy et al., 2010). We set this threshold to the maximum available (6) as we attempted to unravel multiple recovery trends. In a second step, the spectral values at candidate vertices are estimated (fitting process), generating a trajectory of connected segments for each pixel. The best model was chosen based on the p-value according to the F-statistics ($p < 0.05$). Further details on the segmentation process can be found in Kennedy et al. (2010) (Kennedy et al., 2010).

From the derived trajectories, we selected the change magnitude and duration of the segments, at the pixel level, as parameters for the classification. We calculated a recovery ratio (RR) for each segment (Eq. 2), which allows us to describe the recovery rates through time or alternatively for each successional stage defined by the number of segments (*Figure 3.4*).

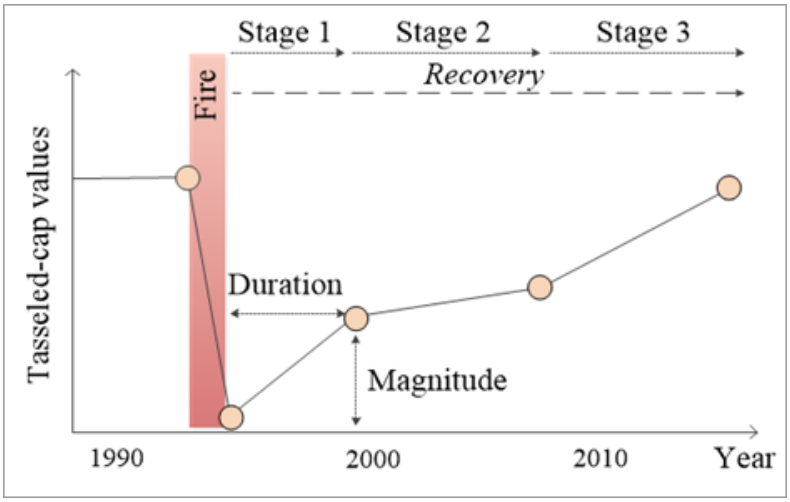

Figure 3.4. Example of fitted trajectory.

$$\mathrm{RR} = \frac{\text{Magnitude of Change}_x}{\text{Duration of Change}_x} \quad (2)$$

We performed an unsupervised clustering method, since our first objective was to unravel the different vegetation recovery patterns. K-means clustering (Hartigan and Wong, 1979) is one of the most popular unsupervised machine learning algorithms and has been previously applied to summarise vegetation

types and changes (Gouveia et al., 2010). K-means allowed us to group the trajectories (defined by the RR of the segments) in k groups, minimizing the sum of the distances between each trajectory and the centroid of a given class. To define the optimal number of classes we employed the Elbow Method, which is based on the percentage of variance explained as a function of the number of clusters (Purnima and Arvind, 2014). This process has been carried out with the scikit-learn library of Python (Pedregosa et al., 2011). The clusters obtained were overlapped to the LandTrendr outputs to characterise the categories (see *Table 3.3*).

3.3.4. Assessing driving factors of vegetation recovery

We aimed to explain the influence of fire severity, pre-fire conditions, topographic and climatic variables on recovery ratios through regression analysis. Six explanatory variables obtained from the Landsat imagery as well as auxiliary data sources (see 3.3.1) were derived to model post-fire recovery (*Table 3.1*). For the variables that did not meet the assumptions of normality of the residuals and homogeneity of variance, we used log-transformed or rank-transformed data.

Previous studies have shown strong effects of fire severity on post-fire vegetation recovery (Crotteau et al., 2013; González-De Vega et al., 2016; Meng et al., 2015). Fire severity, defined as the degree of ecosystem change caused by a fire with respect to the pre-fire situation (Lentile et al., 2006), was evaluated through the dNBR (Miller and Thode, 2007):

$$dNBR = NBR_{pre-fire} - NBR_{post-fire} \quad (3)$$

$$NBR = \frac{(NIR-SWIR2)}{(SWIR2+NIR)} \text{ (Key and Benson, 2006)} \quad (4)$$

Previous work has also addressed the important role of topography in explaining variations in forest establishment following fire (Chu et al., 2017; Ireland and Petropoulos, 2015; Röder et al., 2008). Other studies have established the

relevance of the post-fire climate (Bright et al., 2019; Meng et al., 2015; Viana-Soto et al., 2017) since it is related to water availability, and pre-fire vegetation conditions (Chu et al., 2017) due to its relationship with post-fire seed availability (González-De Vega et al., 2016). Regarding the drought index (SPEI), the 3 month-scale (cumulative from June, July, August) was selected since vegetation activity responds predominantly to short drought time-scales (Vicente-Serrano et al., 2013) and because maximum Pearson correlation coefficients between SPEI aggregated from summer season and TCA-TCW time-series were recorded for both study areas.

Table 3.1. List of variables used in the regression analysis.

Variable		**Units**	**Description**
Dependent	Recovery Ratio$_x$ (RR-TCA$_x$ RR-TCW$_x$)	Z value	Represents the slope of the fitted trajectory at each segment
Explanatory			
Pre-fire conditions	TCA$_{90-93}$ or TCW$_{90-93}$	Z value	TCA shows the percent vegetation cover and TCW the moisture and structure before the fire
Fire severity	dNBR	Values between −1 and 1	Represents the short-term post-fire effects on vegetation cover and structure. Severity thresholds proposed by the USGS (Key and Benson, 2006): Low: 0.1≤dNBR<0.27 Moderate-low: 0.27≤dNBR<0.44 Moderate-high: 0.44≤dNBR<0.66 High: ≥0.66
Topography	Elevation	Meters	
	Slope	Percent	
	Aspect	Values between 0 and 1	(TRASP) (Roberts and Cooper, 1989). Values of 0 correspond to cooler, wetter north-northeastern aspects; values of 1 correspond to hotter, dryer south-southwestern aspects
Climatic Anomalies	Drought index	Z value	(SPEI) (Vicente-Serrano et al., 2017). Positive values mean positive water balance and negative values indicate drought conditions

Firstly, an exploratory regression analysis was carried out to diagnose the suitability of the selected variables. Due to the presence of spatial autocorrelation and heteroscedasticity in our data (significance of Koenker statistics at 95% confidence level), we executed a Geographically Weighted Regression (GWR) (Brunsdon et al., 2010; Fotheringham et al., 2003), a local regression model which considers spatial heterogeneity in data relationships. Model fitting was conducted using optimised Adaptive Bi-square Kernel bandwidth (according to the Corrected Akaike Information Criterion) (Hurvich et al., 1998).

3.3.5. Recovery assessment

We evaluated the recovery through TCA and TCW trajectories in the short, mid and long-term as Key and Benson (2006) (Key and Benson, 2006) proposed to burn severity assessment: 2002 (8 years post-fire), 2009-2010 (15-16 years post-fire), and 2017-2018 (23-24 years post-fire), with 80% of the pre-fire value of TCA and TCW as recovery threshold (Pickell et al., 2016).

We carried out a stratified validation based on the recovery categories identified with a sample size of 500 plots randomly selected at each phase for each index (a total of 3000 reference plots). Vegetation recovery was evaluated by visual analysis of high resolution orthophotos. To facilitate the visual interpretation, we divided the 30-m pixel of Landsat images equally with a 6 m by 6 m grid (25 cells in one 30-m pixel) and overlaid the grids onto the orthophotos (*Figure 3.5*), similarly to Zhao et al. (2016). As an approximation to the pre-fire fractional cover due to the lack of pre-fire orthophotos, we established as reference the pre-fire fractional cover obtained from the SNFI (mean cover of 42.9% and 47.9% for Requena and Yeste, respectively). A disturbed pixel was considered to have recovered if the tree and shrub cover was at least 40% (i.e., 10/25) (*Figure 3.5a* and *3.5b*). Otherwise, that pixel was interpreted as having not recovered (*Figure 3.5c*).

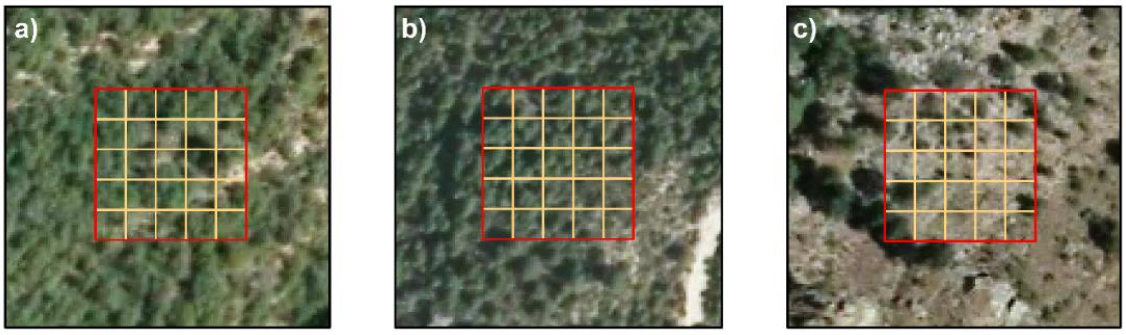

Figure 3.5. Examples of high resolution orthophotos of recovered (a, b) and non-recovered pixels (c) in 5 by 5 grids.

Four accuracy metrics derived from confusion matrices were computed to validate our vegetation recovery classification (*Table 3.2*), the omission error (OE) (Eq. 5), the commission error (CE) (Eq. 6), the overall accuracy (OA) (Eq. 7) and the Dice coefficient (DC) (Eq. 8) (Congalton and Green, 1999).

Table 3.2. Confusion matrix example.

	Reference data		
Estimation	Recovered	Non-recovered	Row total
Recovered	P11	P12	P1+
Non-recovered	P21	P22	P2+
Col. total	P+1	P+2	N
OE	P21/P+1		(5)
CE	P12/P1+		(6)
OA	P11+P22/N		(7)
DC	2P11/(P1++P+1)		(8)

3.4. Results

3.4.1. Classification of post-fire trajectories

Four different categories were identified for TCA (CR, CRSC, CRS, and NCR) and five for TCW (CR, CR2, CRSC, CRSC2 and CRS). The main characteristics of the categories describing recovery are defined in *Table 3.3*.

Table 3.3. Recovery categories definition.

Category	Acronym	Stages	Description
Continuous Recovery	CR CR2	1 2	Pixels show a continuous increase in the TCA and TCW values since the year of fire (CR) or since the first year post-fire (CR2).
Continuous Recovery with Slope Changes	CRSC CRSC2	4 3	Continuous recovery follows disturbance but slope changes occur through the time-series. Changes occur at a different time for TCA and TCW (CRSC and CRSC2).
Continuous Recovery Stabilised	CRS	2	Continuous recovery which slow down or stop 4-5 years after fire.
Non-continuous Recovery	NCR	3	Recovery process is interrupted in the mid-term followed by a second phase of continuous recovery (only found with TCA).

Recovery dynamics in TCA and TCW tended to be spatially clustered, indicating strong spatial effects (*Figure 3.6*). Moreover, there are differences in terms of the magnitude of change, as well as the year in which changes detected between TCA and TCW occurred, and both fires. For the Requena Fire we observed greater homogeneity, with CR as the main category, whereas for the Yeste Fire the CRSC category predominates.

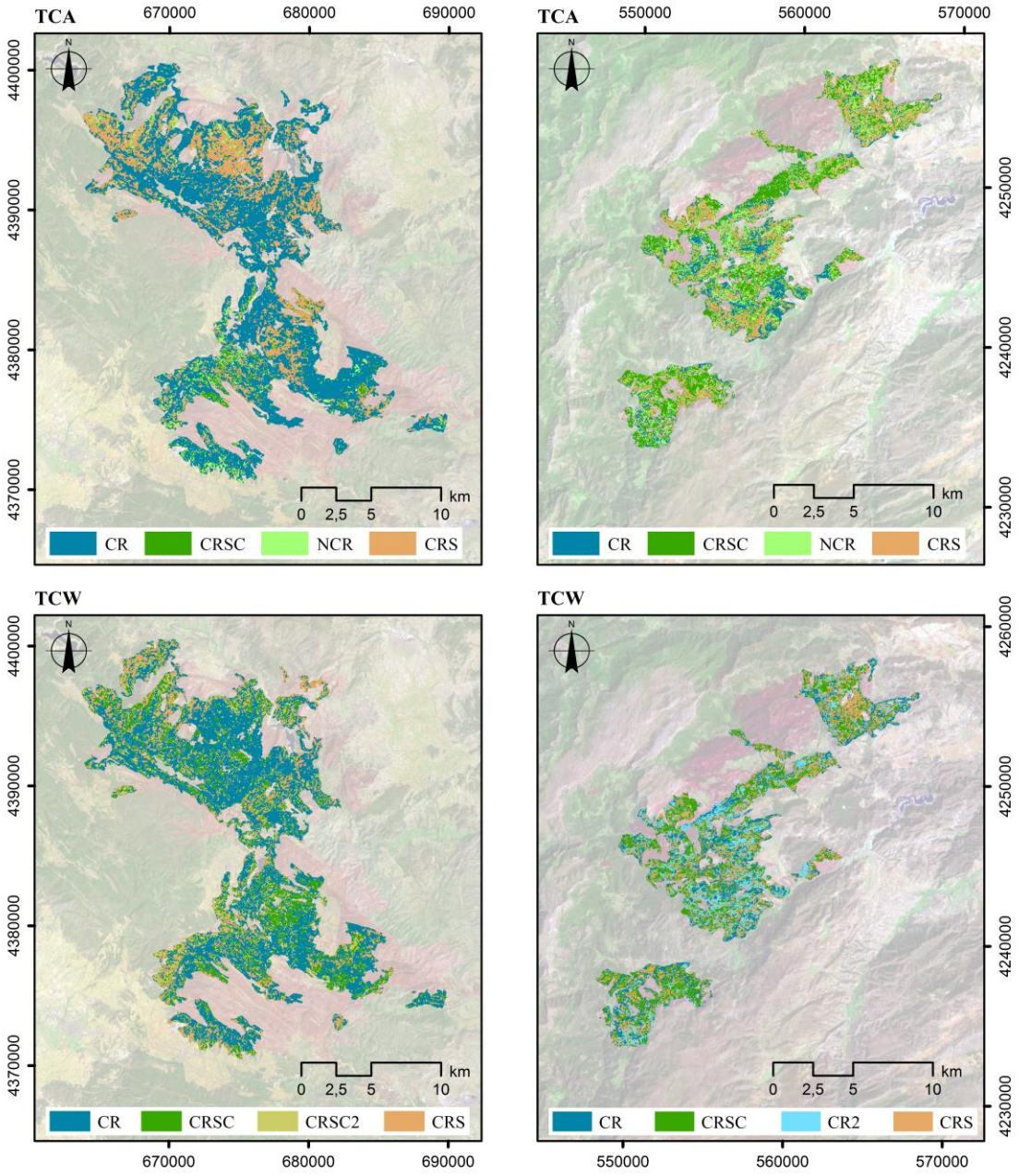

Figure 3.6. Maps of trajectory categories according to TCA (a) and TCW (b). Requena (left), Yeste (right).

The plots in *Figure 3.7* show the mean fitted trajectories of recovery categories from the TCA and the TCW. In the pre-fire period, the TCA and TCW trajectories did not show significant changes, indicating relative stability in forest cover until the occurrence of fire. Nevertheless, the trend is negative in the case of TCA trajectories which could be due to loss of vegetation vigour before the fires

occurred. The structure seems to have not changed in the pre-fire period according to stable values in TCW trajectories.

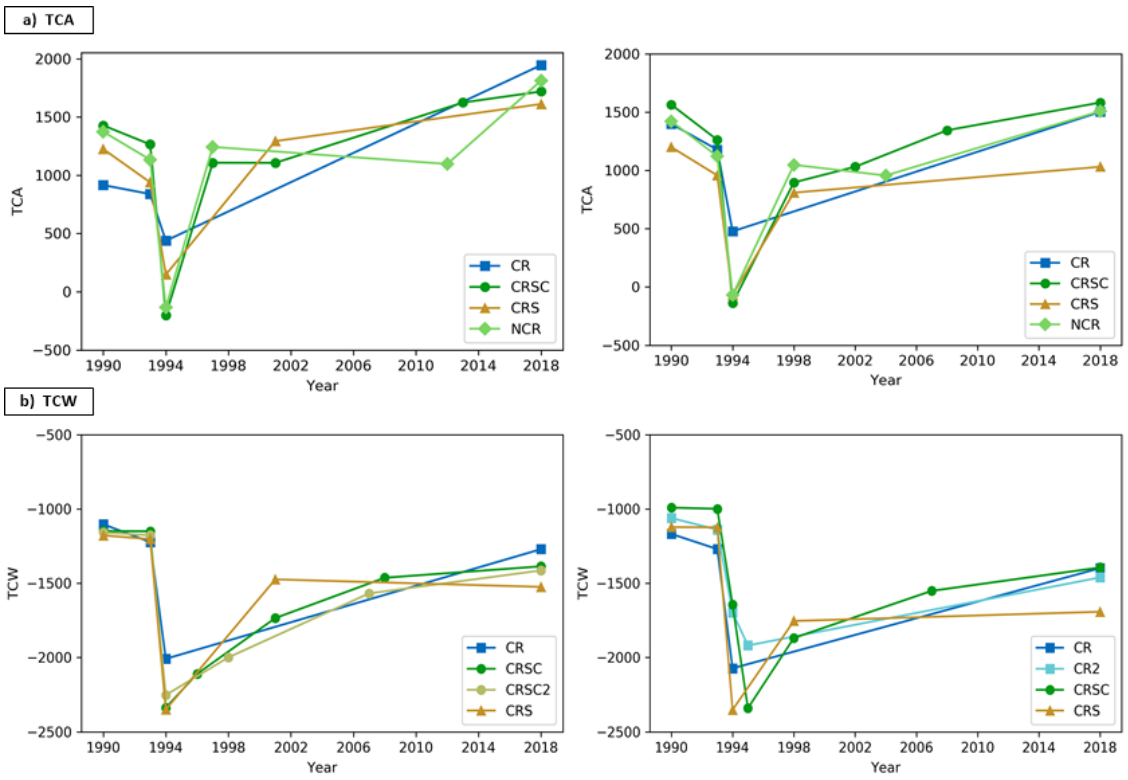

Figure 3.7. Time-series of mean fitted trajectories for each category: (a) TCA, (b) TCW; Requena (left), Yeste (right).

Although burned areas were generally characterised by an increase in spectral values after the fire events, the mean TCA and TCW trajectories showed differences in vegetation recovery between the two fires and across time-series. TCA showed faster recovery, with high slopes in trajectories in the short-term, because it is associated with the percent of vegetation cover, whereas TCW showed slower recovery since it is related to the vegetation structure and moisture

Regarding the TCA categories, same trends were found in both fires and post-fire mean values tended to overtake pre-fire values in the mid-term. Even so, recovery rates were higher in Requena, as the post-fire mean values reached the pre-fire values before 2005, whereas in Yeste the pre-fire values were reached around 2010. CR pixels correspond to lower disturbance magnitude whereas in

CRSC, CRS and NCR the magnitude of change is clearly higher. In the cases of CRSC and NCR the recovery rates were high even though the recovery dynamic was interrupted. CRS showed a particular trajectory as it stabilised in the mid-term and maintained the values across a subsequent phase of slight recovery.

According to the TCW categories, different trends were found between fires with the exception of CR and CRS pixels. In the case of the Yeste Fire the categories CR2 and CRSC continued to decrease until one year after the fire. In the case of Requena Fire, two different categories of CRSC were found since breakpoints in the recovery process occurred in different years. In spite of the trend toward pre-fire values none of the TCW trajectories reached pre-fire conditions after 24 years.

3.4.2. Assessing drivers of post-fire vegetation recovery

We summarised the results from regression analysis for TCA and TCW in *Tables S3.1* and *S3.2 (Appendices - Appendix 1)*, respectively. All of the aforementioned variables for predicting the Recovery Ratio (RR-TCA_x and RR-TCW_x) at each stage were statistically significant at the 95% level. The successional stages correspond to the segments of the fitted trajectories from each category.

With regards to the relationship between the RR-TCA_x and the predictor variables, different responses were found between the categories but also common trends among recovery classes (*Table S3.1*). There was a positive influence of pre-fire conditions since a higher percent of vegetation cover prior to the fire will lead to a higher percent of vegetation cover also after the fire. In addition, climate was positively related to RR-TCA_x in all stages. Positive water balance resulted in a higher ratio of percent vegetation cover. The coefficients varied for the different stages since post-fire climate increases its explanatory power until stage 3 and drops in the long-term. In relation to severity, high recovery rates were related to high severities whereas low ratios were associated with low-burned pixels. Regarding topographic variables, coefficients varied

according to the stage and category. Elevation showed a negative relation as a result of the limiting effects of temperature on vegetation growth, being more important in the short-term and decreasing through subsequent stages. The slope showed a weaker, negative influence as well as the aspect since cooler, wetter north-northeastern aspects (i.e. lower aspect values according to TRASP) were preferred.

The relationship between the RR-TCWx and the predictor variables showed different responses reflecting changes in forest structural complexity (*Table S3.2.*). In this case, a negative relationship with pre-fire values was found because the greater complexity of the forest structure (i.e. higher TCW), the lower the recovery ratio, indicating slower recovery processes of remnant trees and seeding in contrast to the quicker recovery of shrubs. With regard to severity higher values also lead to higher recovery rates. Concerning topographic variables, the slightly positive relationship of the slope might be attributed to pine forest distribution preferably in the foothills. Identically to TCA, elevation and aspect relationship tended to be negative although in the mid-term stages south-southwestern aspects lead to higher recovery rates. Post-fire climate conditions showed a positive or negative relationship depending on the stage. Enough available moisture post-fire is important for seed germination but abrupt changes in the climate conditions seem to reduce the recovery ratio in the long-term.

The relative importance of the explanatory variables for each trajectory category was assessed through t-statistics (*Figures 3.8* and *3.9*). Post-fire climate in terms of drought had high predictive power in most of the stages and categories according to both TCA and TCW regression analysis. This power increased in the mid-term and long-term while all other variables decreased. Fire severity had the second largest power for explaining percent vegetation cover in the short-term, although its power diminished in the estimation of the recovery in terms of forest structure. Pre-fire conditions also had a higher importance in the short-term, since the seed bank and the seeding processes will depend on the pre-fire forest cover and structure. Topographic variables showed the lowest explanation

power. Elevation had higher relative importance in the case of TCA compared to TCW, in which aspect was the most important topographic variable in all stages.

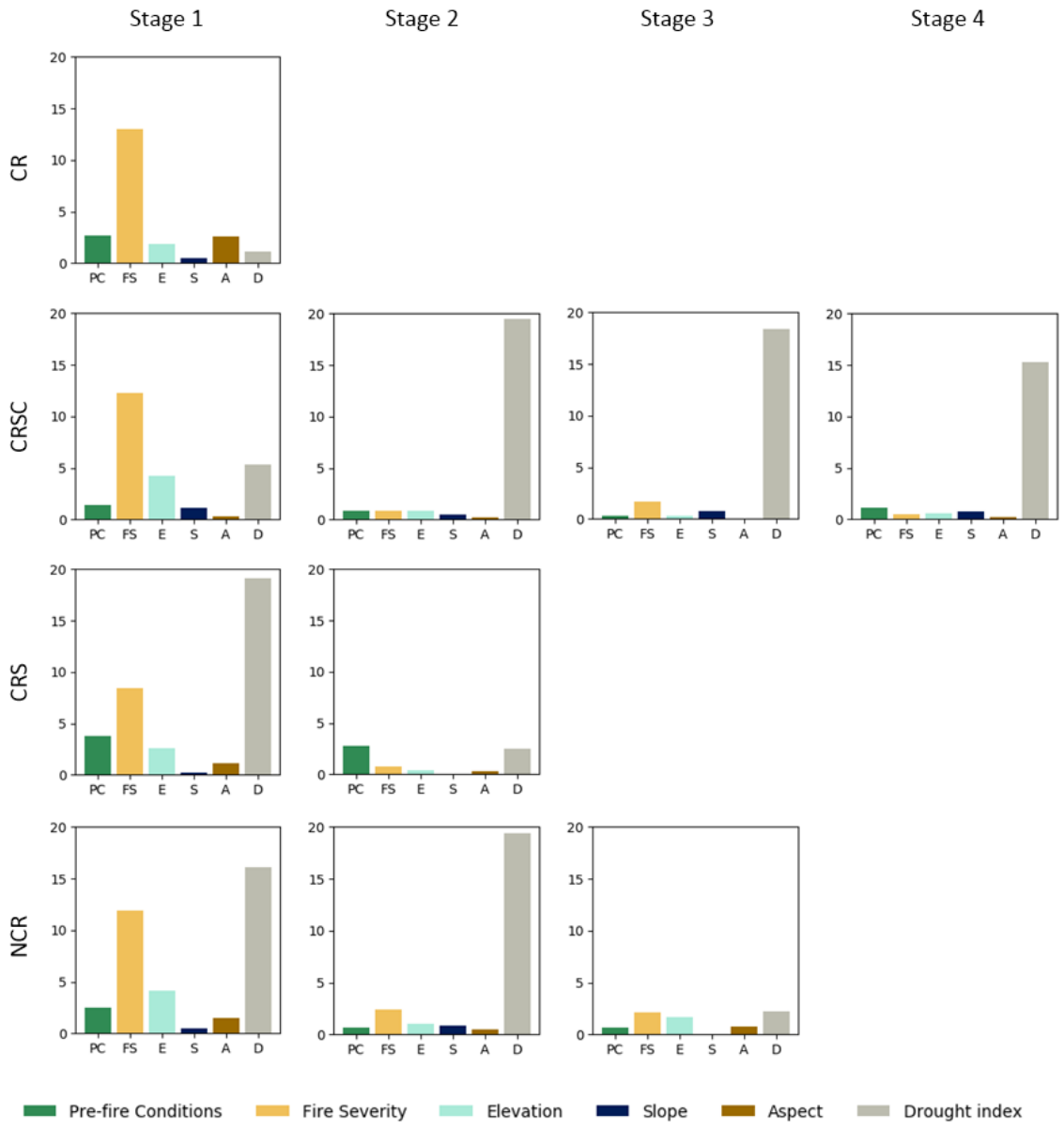

Figure 3.8. Relative importance of explanatory variables in TCA regression analysis.

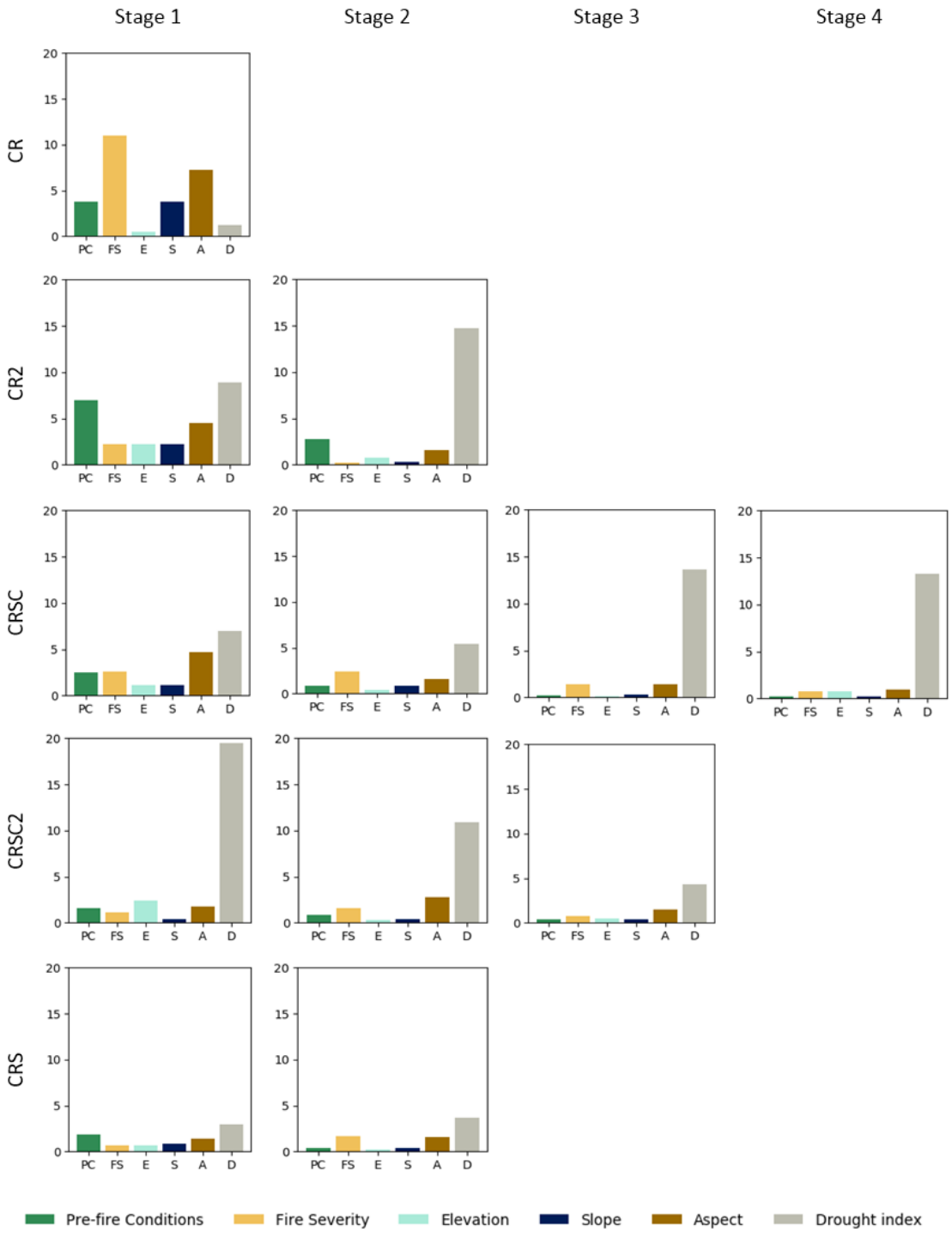

Figure 3.9. Relative importance of explanatory variables in TCW regression analysis.

3.4.3. Recovery estimation assessment

According to the recovered and non-recovered definitions, all categories showed high accuracy, with OA values ranging from 0.7 to 0.94 (*Table 3.4*). The OE and CE of the recovery categories varied, with the highest errors in the short-term (OE of 0.36 for TCW and CE of 0.22 for TCA). Post-fire recovery estimated by TCA shows more balanced errors, although with higher CE due to early successional recovery processes of herbs and shrubs. In contrast, recovery estimated by means of TCW shows higher OE since it is more sensitive to moisture and structure than early soil colonization of herbs. In both cases, more stable recovery classes (CR and CRS) showed higher accuracy than the more disrupted ones (CRSC). DC increases through the time-series since forest cover and structure are more clearly defined.

Table 3.4. Error metrics for recovery estimations according to TCA and TCW.

		2002				2009-2010				2017-2018			
		OA	**DC**	**OE**	**CE**	**OA**	**DC**	**OE**	**CE**	**OA**	**DC**	**OE**	**CE**
TCA	CR	0.86	0.91	0.07	0.11	0.90	0.94	0.04	0.07	0.95	0.97	0.00	0.05
	CRSC	0.70	0.84	0.14	0.19	0.82	0.90	0.09	0.11	0.87	0.93	0.07	0.07
	CRS	0.79	0.86	0.05	0.22	0.86	0.92	0.08	0.08	0.94	0.97	0.02	0.05
	NCR	0.74	0.81	0.16	0.20	0.88	0.93	0.10	0.04	0.92	0.96	0.03	0.05
TCW	CR	0.91	0.85	0.21	0.04	0.84	0.88	0.20	0.02	0.93	0.96	0.08	0.00
	CR2	0.82	0.74	0.36	0.13	0.86	0.85	0.21	0.08	0.89	0.93	0.13	0.00
	CRSC	0.82	0.78	0.33	0.06	0.87	0.89	0.15	0.01	0.82	0.91	0.16	0.01
	CRSC2	0.82	0.82	0.29	0.04	0.86	0.91	0.16	0.00	0.88	0.92	0.14	0.00
	CRS	0.86	0.87	0.17	0.10	0.77	0.93	0.12	0.01	0.89	0.93	0.10	0.04

OA – Overall Accuracy; DC - Dice coefficient; OE - omission error; and CE - commission error.

3.5. Discussion

3.5.1. Post-fire recovery trajectories from LTS

Characterizing post-fire recovery processes is challenging due to the variety of factors driving vegetation recovery, resulting in different recovery dynamics. Post-fire vegetation recovery estimated from spectral data is not a direct measure of actual forest regrowth. However, trends of forest recovery can be quantified by linking spectral change metrics with a reference dataset (Bartels et al., 2016). Here, we identified different recovery categories according to TCA and TCW recovery ratios at different stages through a 24-year-series in Mediterranean pine forests.

Time-series analysis from Landsat data using the LandTrendr segmentation algorithm has been suitable to capture the different post-fire recovery trends. The trajectories extracted revealed continuous and non-continuous recovery processes, allowing us to identify slight changes in the slowly evolving recovery process. This was of great importance in determining slow but more stable recovery processes (CR, CR2) compared to other faster, but also interrupted, recovery processes (CRSC, CRSC2, CRS, NCR), indicating changes in greenery and forest structure throughout the recovering process. Other studies which also employed a Landsat trajectory-based approach with LandTrendr were able to identify different patterns of vegetative regrowth depending on the state, owner category and ecoregion in North America (Kennedy et al., 2012) or set recovery levels across sclerophyll forest in Australia (Nguyen et al., 2018). Even though several studies have addressed the analysis of post-fire recovery trends, our findings highlight the importance of defining and grouping recovery patterns to facilitate the understanding of recovery processes.

TCA and TCW have been proved useful to characterise both vegetation cover (TCA) and forest structure (TCW). TCW trajectories were much more gradual, while TCA trajectories tended to saturate around 5 years post-disturbance. Frazier et al. (2015) and Nguyen et al. (2018) also concluded that the TCW

contained more detail on the vegetation structure and regrowth in the regeneration processes since it is highly correlated to stand age and structural complexity in mature forest stands. The wetness values rise with an increasing amount of canopy (Hansen et al., 2001), making it more suitable for analysing mid and long-term recovery. Alternatively, initial increases in vegetation cover were well-characterised with shorter visible and near-infrared wavelengths as used in TCA (Gómez et al., 2012; Pflugmacher et al., 2014; Schroeder et al., 2011). In contrast to the canopy layer, recovery of the understory through both resprouting and seeding is quicker (Eugenio et al., 2006; González-De Vega et al., 2018). Thus, TCA was more suitable for tracking early stages, suggesting greater sensitivity toward shrub recovery and changes in vegetation condition rather than structure.

The Recovery Ratio (RR) varied across the stages and for each category (*Figure 3.7*). Generally, the recovery rates of TCA and TCW were greatest shortly after the fire (Stage 1 in CRSC, CRSC2, CRS and NCR), decreasing afterwards, due to the early post-fire colonization of annual herbs and shrubs (Crotteau et al., 2013; González-De Vega et al., 2018). In the following stages (2, 3 and 4), the RR according to both TCA and TCW was lower, associated with stem exclusion processes in a young regrowth forest characterised by intense competition among regenerated species (De las Heras et al., 2012; Fernández-García et al., 2019; Oliver and Larson, 1996). Our results agree with other studies which also obtained higher recovery rates in the short-term according to spectral vegetation indices in Mediterranean forests (Morresi et al., 2019) and NBR trajectories in pine, mixed conifer and conifer-oak forest (Bright et al., 2019). .

Accordingly, the recovery time for the fitted mean trajectories also varied across categories. TCA categories tended to reach mean pre-fire values quicker, as it tends to saturate earlier (short-mid-term) due to the influence of herbaceous vegetation on TCA. Specifically, in the Requena Fire, the TCA trajectories tended to overtake pre-fire values in the long-term, possibly because these are fire-adapted forests in which fire creates favourable conditions for vegetation

germination and regeneration (De las Heras et al., 2012). Nevertheless, TCW trajectories did not reach the previous values 24 years after the fire, suggesting that burned areas did not recover the complexity of the pre-fire forest structure. This agrees with the interval of minimum 15 years to consider a *Pinus halepensis* forest recovered after a fire proposed by Eugenio et al. (2006) (Eugenio et al., 2006) since post-fire populations of seeder species does not overpass the reproductive juvenile phase up to 12–20 years after fire (Thanos and Daskalakou, 2000) and thus, canopy seed bank is not completely fulfilled (González-De Vega et al., 2016). Some studies in Mediterranean ecosystems reported recovery times from remote sensing which fit with our findings (Viana Soto et al., 2019). In this sense, Gouveia et al. (2010) found recovery times of vegetation cover around 3-5 years according to NDVI (highly correlated with TCA), and Fernández-Manso et al. (2016) estimated the time of vegetation cover with VRI between 7 and 20 years depending on fire severity level. However, the estimated recovery times with NBR, which is highly correlated with TCW, were generally longer compared to NDVI (Morresi et al., 2019).

Some of the limitations for the modelling of post-fire vegetation recovery using optical data are related to saturation at high LAI values. Previous studies found that the saturation of optical indices is reached after 20 years in Mediterranean environments (Tanase et al., 2011). Likewise, Schroeder et al. (2011), Pickell et al. (2016), Viana-Soto et al. (2017) and Hislop et al. (2018) found post-fire recovery of NDVI or TCA returning back to pre-fire levels rapidly (i.e. around 5-7 years post-fire). Structural information derived from airborne LiDAR data would enable a better characterization of the recovery trajectories and to improve our understanding post-fire vegetation recovery (Bolton et al., 2015; Martín-Alcón et al., 2015).

3.5.2. Accuracy assessment of post-fire recovery

Accuracy assessment of post-fire recovery is often avoided because historical reference datasets are scarce and field data are costly and time-consuming

(Banskota et al., 2014). Here, we used a human interpretation approach to derive reference data of recovered and non-recovered areas, which has been widely employed to derive reference data for disturbance and recovery mapping (Cohen et al., 2010; DeVries et al., 2015; Nguyen et al., 2018; Zhao et al., 2016).

All classes showed high accuracy, with increasing OA and DC from the short-term to the long-term since forest cover and structure are more clearly defined 24 years post-fire. DC values were slightly lower in the long-term for TCW compared to TCA, which might indicate a recovery process that evolves to a secondary forest with higher shrub domain (González-De Vega et al., 2016). This could also be related to the uncertainty associated with signal sensitivity to changes in vegetation cover and biomass (Storey et al., 2020). Moreover, the highest accuracy in the more stable categories (CR), in contrast to the more variable (CRSC), also highlights the difficulty in establishing the level of recovery for those more dynamic areas. Nguyen et al. (2018) also pointed out the challenge of determining the post-disturbance recovery level, and identified recovery levels from NBR trajectories after fires according to whether pre-fire conditions were reached or not. Here, we did not distinguish among recovery levels as we were unable to accurately characterise the pre-fire forest structure due to the lack of high-resolution imagery, for which a more extensive reference dataset would also be needed.

The main source of error stemming from OE for both TCA and TCW in the recovered pixels. Our results showed that the TCW had higher accuracy for the non-recovered areas but omitted pixels that had already recovered. Zhao et al. (2016) also found higher OE in the recovered class regarding post-fire and post-harvest forest recovery. Similarly, DeVries et al. (2015) assessed post-harvest regrowth in tropical forests obtaining lower CE in the regrowth class but the highest OE. On the other hand, TCA showed higher CE, as it is more sensitive to fast detection of early recovering processes but also tends to saturate earlier as Schroeder et al. (2011) reported.

3.5.3. Assessment of post-fire recovery drivers

Regression modelling of TCA and TCW recovery ratios for the recovery categories identified showed a varied influence of environmental factors, fire severity and pre-fire conditions. The results indicated post-fire climate as one of the most important factors for vegetation recovery in Mediterranean pine forests in Spain. Likewise, Meng et al. (2015), Liu (2016) and Viana-Soto et al. (2017) found that climate conditions in the first post-fire seasons were critical for predicting short-term recovery. Tree regeneration after disturbances in Mediterranean ecosystems could be limited under post-fire drought events since droughts constrain seedling establishment and growth (De las Heras et al., 2012; Fernández-García et al., 2019). Bright et al. (2019) also reported that post-fire climate explained substantial variation of the degree to which vegetation greenness recovered after a fire. Further analysis between trajectories and post-fire climate revealed that stages of recovery slowdown and even breakpoints coincided with negative SPEI values (i.e. dry or very dry periods). The year of the fires was followed by a slightly humid period which supported the recovery. However, 5 years after the fires, a new drought event interrupted the recovery, as can be observed very clearly in the stabilisation of the recovery in the CRS category from 1999-2000, not only in the TCA trajectories but also in TCW trajectories. The effect of this drought event was also noticeable in the categories of CRSC and CRSC2. Furthermore, the impact of post-fire climate on the recovery process was also shown in the mid-term and long-term. In the case of the Yeste Fire, an extreme drought event in 2005 coincided with the breakpoints in NCR and CRSC, whereas in the Requena fire this event was not as severe as it was in 2012, coinciding with the breakpoints in NCR and CRSC2.

Fire severity was also a key factor in the short-term recovery of pine forests. Some studies also found that fire severity was decisive in recovery dynamics both in mixed-conifer forests (Meng et al., 2015) and pine forests (Ireland and Petropoulos, 2015) due to its relation to pine seedling densities after fire, depending on pre-fire vegetation composition, seedling mortality and

reestablishment processes (Crotteau et al., 2013; Fernández-García et al., 2019; González-De Vega et al., 2018). In this study, the areas were burned at high severity (dNBR > 0.66) as forested areas tended to experience a higher severity compared to herbaceous and shrublands. Moderate-high severity was only found in those pixels of CR, which showed a slower but stable recovery trend. In agreement with the results reported by Shvetsov et al. (2019), a positive relationship between recovery rate and fire severity was found, since recovery rates were higher for the higher severity areas than for high-moderate severity (corresponding to successful recovery). Moderate fire severity sites might result in higher soil organic matter mineralisation, and thus in higher post-fire soil fertility that produces faster growth in pine seedlings (Pausas et al., 2002). Bright et al. (2019) also found that areas burned at higher severities recovered at faster rates, possibly because they are fire-adapted forest in which fire creates favourable conditions for vegetation germination and regeneration. Nevertheless, some studies in Mediterranean pine forest reported that conversion from forest to shrubland occurred in the most xeric sites (south-facing areas) (Martín-Alcón and Coll, 2016) or in those areas with a high severity (González-De Vega et al., 2016). In this sense, Baudena et al. (2019) predicted that future potential increases in aridity may drive these fire-prone ecosystems past a tipping point, after which closed forest structure would be replaced by open shrublands.

Topographic variables can also influence post-fire vegetation recovery through its effects on local microclimate, soil and hydrological processes (Chu et al., 2017; Ireland and Petropoulos, 2015). Wittenberg et al. (2007) and Ireland and Petropulous (2015) found that north facing aspects exhibit higher rates of vegetation recovery compared to south facing aspects as we found in the short-term recovery in CRS, NCR and CR categories according to TCA, but also in CRSC according to TCW. The negative influence of elevation was also detected in Mediterranean pine forest (Viana-Soto et al., 2017) and red fir forests (Meng et al., 2015) that might be attributed to the decreased temperature with elevation. In contrast, Chu et al. (2017) and Shvetsov et al. (2019) reported that topographic variables were the least important factors in explaining the regeneration rate in

Siberian forests. In our study, recovery in relation to topographic position did not show any clear pattern. This could be due to the fact that most of the pixels were located at either upper or mid-slope in the foothills and very few were bottom slopes.

Although we found that post-fire climate was the most important variable in explaining post-fire recovery in the mid and long-term, other variables not included could be influencing the recovery process. Further analysis would consider the influence of historical management legacies as well as the distance to seed banks in the post-fire recovery patterns.

3.6. Conclusion

Time-series analysis from a temporal segmentation approach allowed us to unravel and characterise different post-fire recovery trajectories. Although several studies have addressed the estimation of post-fire recovery rates, fewer have been done in defining and characterizing the differences among recovery trends in Mediterranean pine forests. Here, we identified different recovery categories according to TCA trajectories and TCW trajectories, which enabled us to define slow but more stable recovery processes (CR, CR2) compared to other faster but also interrupted recovery processes (CRSC, CRSC2, CRS, NCR). The appraisal of the environmental and contextual drivers of the recovery process showed that fire severity is important to predict the RR in the short-term but post-fire climate in terms of drought better explained the RR in the mid and long-term.

The thermophilous pine forests are the most affected by wildfires in Europe. Increased wildfire activity is expected to continue under warmer and drier conditions, making post-fire vegetation recovery of concern to researchers and forest managers. Since these forests may not be allowed the time to develop into a mature forest that would be able to recover rapidly, the resilience of these ecosystems will therefore be significantly reduced. Hence, a better understanding of fire regimes and forest recovery patterns in different environmental and climatic

conditions is needed for developing forest management strategies that enhance forest resilience.

3.7. Acknowledgments

A.V.-S. was supported by a doctoral fellowship from the Spanish Ministry of Science, Innovation and Universities with reference FPU17/03260.

Author contribution

Alba Viana-Soto: Conceptualization, Methodology, Formal analysis, Writing – original draft. Mariano García: Conceptualization, Methodology, Writing – review & editing. Inmaculada Aguado: Conceptualization, Methodology, Writing – review & editing. Javier Salas: Conceptualization, Writing – review & editing.

Chapter 4. Assessing post-fire structure recovery by combining LiDAR and Landsat data

Based on:

Viana-Soto, A., García, M., Aguado, I., & Salas, J. (2022). Assessing post-fire forest structure recovery by combining LiDAR data and Landsat time series in Mediterranean pine forests. *International Journal of Applied Earth Observation and Geoinformation*, *108*, 102754. https://doi.org/10.1016/j.jag.2022.102754

Abstract

Understanding post-fire recovery dynamics is critical for effective management that enhance forest resilience to fire. Mediterranean pine forests have been largely affected by wildfires, but the impacts of both changes in land use and climate endanger their capacity to naturally recover. Multispectral imagery is commonly used to estimate post-fire recovery, yet changes in forest structure must be considered for a comprehensive evaluation of forest recovery. In this research, we combine Light Detection and Ranging (LiDAR) with Landsat imagery to extrapolate forest structure variables over a 30-year period (1990-2020) to provide insights on how forest structure has recovered after fire in Mediterranean pine forests. Forest recovery was evaluated attending to vegetation cover (VC), tree cover (TC), mean height (MH) and heterogeneity (CVH). Structure variables were derived from two LiDAR acquisitions from 2016 and 2009, for calibration and independent spatial and temporal validation. A Support Vector Regression model (SVR) was calibrated to extrapolate LiDAR-derived variables using a series of Landsat imagery, achieving an R^2 of 0.78, 0.64, 0.70 and 0.63, and a relative RMSE of 24.4%, 30.2%, 36.5% and 27.4% for VC, TC, MH and CVH, respectively. Models showed to be consistent in the temporal validation, although a wider variability was observed, with R^2 ranging from 0.51 to 0.74. A different response to fire was revealed attending to forest cover and height since vegetation cover recovered to a pre-fire state but mean height did not 26-years after fire. Less than 50% of the area completely recovered to the pre-fire structure within 26 years, and the area subjected to fire recurrence showed signs of greater difficulty in initiating the recovery. Our results provide valuable information on forest structure recovery, which can support the implementation of mitigation and adaptation strategies that enhance fire resilience.

Keywords: Post-fire recovery, canopy cover, height, LiDAR, Landsat, support vector regression (SVR).

4.1. Introduction

Forest fires are one of the recurrent disturbances in Mediterranean biomes, shaping forest structure and composition (Keeley, 2012). Fire activity is particularly intense in Southern Europe, where half a million hectares are burnt every year (Rigo et al., 2017) causing ecological, economic and human health impacts (Bowman et al., 2017). Since fire is an integral component of the Mediterranean ecosystems (Pausas and Keeley, 2014a), plant species have developed diverse post-fire ecological strategies to recover including resprouting, seed bank persistence and dispersal capacity (De las Heras et al., 2012). Nonetheless, impacts of both changes in land use and climate, and the resulting alterations in fire regimes, may endanger their natural capability to recover (Pausas and Keeley, 2014a). Therefore, Mediterranean forests must adapt to new induced fire regimes with an increase in the frequency and intensity of fires, as a result of drier and longer droughts (Seidl et al., 2017; Turco et al., 2018). Consequently, the vulnerability of these ecosystems to not naturally recover is likely to increase, requiring forest management to focus on their resilience to fire (Ibáñez et al., 2019).

In this forthcoming situation, post-fire recovery has emerged as an important indicator of ecosystem resilience (González-De Vega et al., 2016; Nikinmaa et al., 2020), defined as the time the system needs to reach the pre-disturbance values. Remote sensing offers a powerful alternative to field methods for monitoring forest recovery based on the spectral response of vegetation at multiple spatial and temporal scales (Pérez-Cabello et al., 2021). The Landsat archive, with more than four decades of observations, has become the most widely used imagery source to monitor forest disturbances and subsequent recovery (Chuvieco et al., 2020). These datasets have both temporal and spatial characteristics appropriate to analyse dynamic processes as recovery, giving an overview of successional forest changes following a disturbance (Kennedy et al., 2014). Spectral indices and Tasseled Cap Transformations (TCT) have long been used to estimate parameters related to vegetation recovery (Hislop et al., 2018;

Pickell et al., 2016; White et al., 2017). More recently, time-series analysis has become increasingly important to characterise post-fire vegetation recovery, taking advantage of the development of change detection algorithms (Zhu, 2017) and cloud computing capabilities through the Google Earth Platform (Gorelick et al., 2017). Particularly, the use of recovery trajectories from time-series analysis provides essential information to identify abrupt disturbances and subsequent recovery processes (Bright et al., 2019; Frazier et al., 2015; Nguyen et al., 2018; Viana-Soto et al., 2020).

Notwithstanding, changes in forest structure in combination to the spectral signal of recovery must be considered for a comprehensive evaluation of forest resilience to fire (Bartels et al., 2016; Kennedy et al., 2014). LiDAR sensors are capable of penetrating through vegetation and recording forest structural characteristics (Lefsky et al., 2002). Previous studies have successfully used LiDAR data for estimating forest attributes (Bottalico et al., 2017; Zhao et al., 2011), quantify post-disturbance structural characteristics (Bolton et al., 2015; McCarley et al., 2017), fire severity assessment (García et al., 2020; Montealegre et al., 2014) and vegetation recovery analysis (Gordon et al., 2017; Martín-Alcón et al., 2015). The use of low-density LiDAR data has also proved its ability to estimate forest attributes in Mediterranean forests (Gelabert et al., 2020; Tijerín et al., 2022), providing a suitable representation of the post-fire forest conditions attending to both vertical structure and horizontal continuity of vegetation (Kane et al., 2010). Estimates of vegetation cover and height as well as structural heterogeneity provide valuable information on how the dominance of shrub and tree strata is shifting within the recovery process (Bartels et al., 2016).

Considering that airborne LiDAR data availability is limited in space and time, combining it with Landsat imagery to temporally and spatially extrapolate LiDAR-derived structural variables emerges as a promising approach to model post-fire recovery regarding forest structure (Ahmed et al., 2015; García et al., 2017; Matasci et al., 2018; Pflugmacher et al., 2014; Senf et al., 2019; Zald et al., 2016). The lack of a direct relationship between structure and reflectance can be solved

by non-parametric machine learning methods (Ahmed et al., 2014; García et al., 2017, 2011). In fact, the use of machine learning algorithms for combining multisource remotely sensed data have greatly increased due to their ability to model complex relationships between the dependent and independent variables and no assumption of data distribution (Lary et al., 2016), even in cases of high dimensionality and relatively small sample sizes. A diversity of machine learning regression algorithms has been used to address the extrapolation procedure, such as Random Forests (Martín-Alcón et al., 2015; Senf et al., 2019), k-Nearest Neighbour (Ahmed et al., 2015; Matasci et al., 2018) or Support Vector Regression (SVR) (García et al., 2017). From these, SVR has been proved an effective tool to capture complex non-linear relationships between the dependent and the explanatory variables, and thus enabling the extrapolation of LiDAR-derived canopy cover and height based on Landsat images (García et al., 2017; Zhao et al., 2011). However, attempts to extrapolate over time are limited due to the difficulty to achieve a stability of the estimates among sensors and across different environmental conditions (Matasci et al., 2018). Our understanding on how LiDAR-to-Landsat extrapolation will perform in high structurally heterogeneous and opened landscapes as the Mediterranean forests using LiDAR collected at low point densities remains incomplete.

In this current research, we aimed at combining LiDAR data and Landsat imagery to provide insights on how forest structure has recovered after fire in Mediterranean pine forests over a 30-year period. The specific objectives were:

i) to assess the feasibility of temporally extrapolating LiDAR-based cover, height and canopy heterogeneity using Landsat data based on a support vector regression (SVR) approach
ii) to generate a 30-year series of forest structural variables based on the temporal extrapolation of LiDAR based estimates using Landsat imagery
iii) to characterise post-fire forest structure recovery from the generated time-series of structure variables

4.2. Study area

The study site is located in the Mediterranean semi-arid region from southeastern Spain (*Figure 4.1*). The Yeste Fire occurred in the summer of 1994 (7th August), which burned 11,685 ha of pine dominated. Average annual rainfall is 600–700 mm and the average annual temperature is around 15 °C, subjected to soil hydrological deficit in summer (Ninyerola et al., 2005). *Pinus halepensis* Mill. and *Pinus pinaster* Ait. dominate in those relatively young semi-natural forests resulting from plantations carried out in the mid-20th century (Pausas et al., 2004). Both species are obligate seeders, requiring a minimum of 15 years and up to 30 years to reach reproductive maturity. The understory is mainly composed by shrub species such as *Thymus* L., *Rosmarinus* L. or *Juniperus* L., but *Quercus ilex* L. occurs in the understory at some areas. Fire recurrence in the northwest sector in 2017 (27th July, with approximately 3,000 ha burned) makes this site of particular interest. Patches dominated by *P. halepensis* and *P. pinaster* in the overstory were selected according to the Forest Map of Spain (MFE) (1:50.000), including those forested pixels that were burned as well as unburned from a buffer of 2 km from the fire perimeter, which represented the natural dynamics of the ecosystem. Other cover types present in the scene were masked.

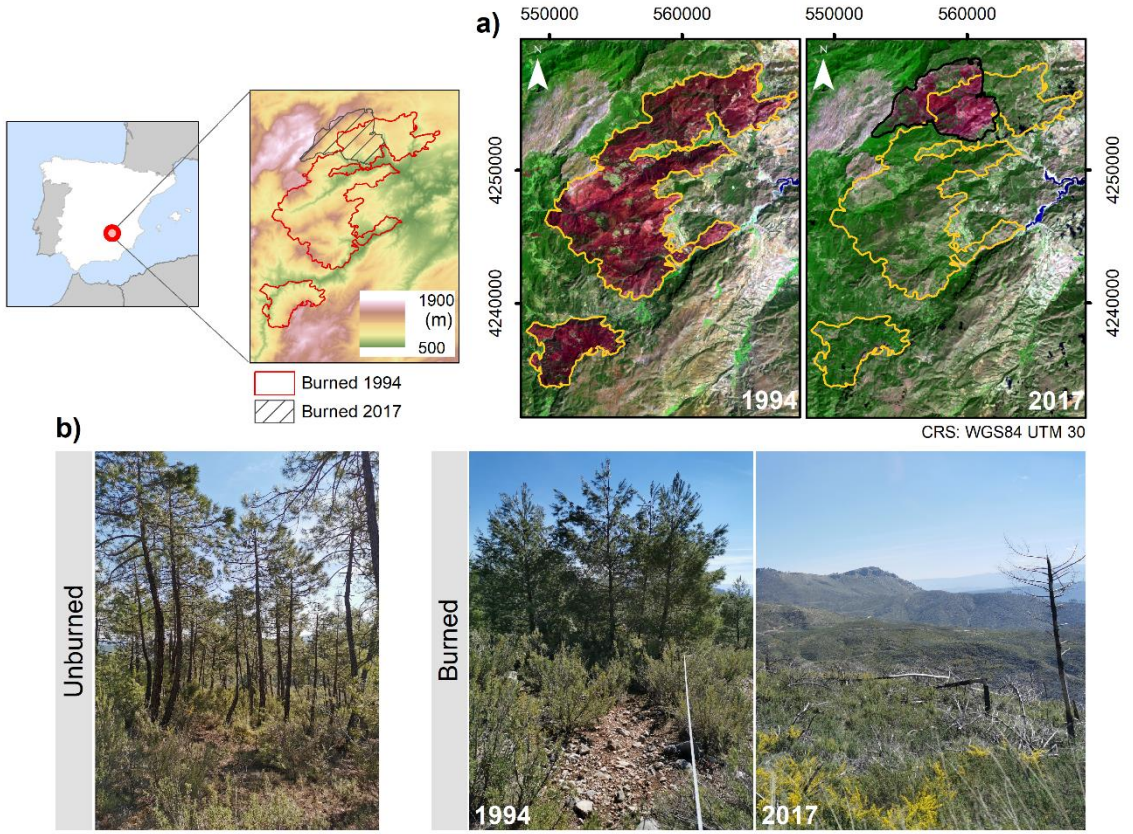

Figure 4.1. Location of the study area: a) post-fire Landsat images (RGB composition: SWIR2, NIR, Blue) from August 1994 (left) and August 2017 (right); b) Examples of Pinus forest from unburned and burned plots (photographs were taken in March 2021).

4.3. Materials and methods

The main methodological steps are shown in *Figure 4.2*. Firstly, we computed a set of forest structure variables from LiDAR data for two different dates, 2009 and 2016. Then, we extracted a series of predictor variables (Landsat spectral bands, indices and transformations, and topographic variables) to model the LiDAR-derived structure variables from a SVR approach. The SVR model was calibrated and applied to a 30-year series of Landsat imagery to generate a time-series of forest structure attributes. We validated the estimations both temporally and spatially from an independent sample of LiDAR-derived estimates.

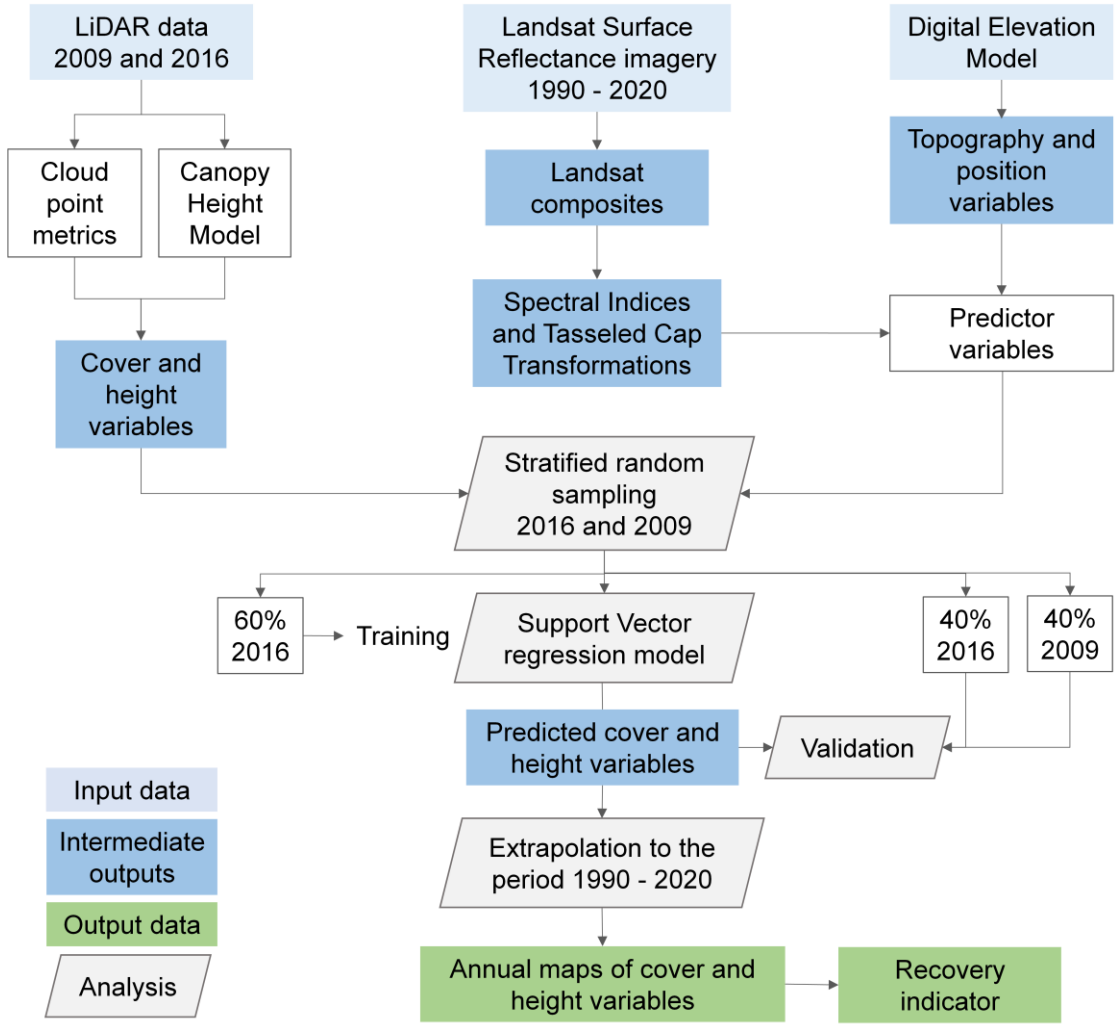

Figure 4.2. Workflow of the methodology for the modelling forest cover and height using Landsat imagery and LiDAR data.

4.3.1. Data acquisition and processing

LiDAR data

Airborne Laser Scanner (ALS) data were acquired in 2009 (September - November) and 2016 (August - September) by the National Plan for Aerial Orthophotography of Spain (PNOA) and distributed by the National Geographic Institute of Spain (IGN). Data were acquired using small-footprint discrete-return airborne sensors (LEICA ALS50 and ALS60), with a maximum scan angle of 50°, at a scanning frequency of 70 Hz (minimum of 40 Hz), and a minimum pulse

frequency of 45 kHz. The maximum flight height was 3000 m above ground level. The point density of the study area was 0.5 pts/m^2, with a vertical accuracy of 0.30 m (2009) and 0.20 m (2016). Data processing and subsequent statistical metrics computation were carried out using the U.S. Forest Service's FUSION software v3.80 (McGaughey, 2018).

We calculated a set of forest structural variables from LiDAR data at 30-m resolution to match the spatial resolution of the Landsat data: vegetation cover, tree cover, mean height, and coefficient of variation of height. Cover metrics were extracted directly from the cloud point using the "GridMetrics" command at a 30-m spatial resolution using all the returns (Morsdorf et al., 2006). Vegetation Cover (VC), defined as the percentage of ground covered by the vertical projection of vegetation for a given pixel (Jennings et al., 1999), was calculated as the ratio of vegetation returns above 0.3 m to all returns (Eq. 1). This height threshold was selected to avoid ground points in relation to the vertical accuracy (Gelabert et al., 2020). Similarly, the Tree Cover (TC) was computed using a 2 m height threshold (Shi et al., 2018), which was enough to exclude shrubs and herbs.

$$Cover = \frac{Returns\ above\ Hthreshold}{Total\ all\ returns}\ x\ 100 \quad (1)$$

Metrics of forest height were derived from the Canopy Height Model (CHM) constructed by subtracting the terrain heights (DEM) to the points. The DEM was previously generated by interpolating the points classified as ground. Canopy height for each 30-m cell was computed by averaging the contained pixels of the original CHM computed at 2-m spatial resolution. Subsequently, we calculated the coefficient of variation of height (CVH) by dividing the standard deviation of height (STDH) to the mean height (MH) to assess the vertical structural heterogeneity.

Landsat data

Annual Landsat composites for the period 1990-2020 were generated through the Google Earth Engine platform (Gorelick et al., 2017) using a medoid selection process choosing the pixel closest to the median among images (Flood, 2013). Landsat TM, ETM + and OLI Surface Reflectance images were selected according to a target period (31st August - 15th October) to minimise the effect of phenological changes, filtering by cloud cover (less than 20%). Inter-sensor harmonization was carried out due to differences among the spectral characteristics of Landsat ETM+ and OLI datasets (Vogeler et al., 2018). We normalised Landsat TM and ETM+ to Landsat OLI from a multilinear regression approach (Roy et al., 2016). We applied the topographic correction SCS+C (Soenen et al., 2005) to remove the effect of the terrain slope. The SCS+C is based on the Sun-Canopy-Sensor correction proposed by (Gu and Gillespie, 1998), specifically designed for forested areas (Chance et al., 2016; García et al., 2011).

Apart from the Landsat spectral bands, we computed a set of spectral indices to encompass the diversity of vegetation characteristics: the Normalised Difference Vegetation Index (NDVI) (Tucker, 1979), the Enhanced Vegetation Index (EVI) (Huete et al., 2002), the Normalised Difference Water Index (NWMI) (Gao, 1996), and the Normalised Burn Ratio (NBR) (Key and Benson, 2006). Tasselled Cap Transformations (Brightness, Greenness and Wetness) (Crist, 1985) were calculated using the coefficients derived by Baig et al. (2014) and then the Tasseled Cap Angle (TCA) (Powell et al., 2010) and Tasseled Cap Distance (TCD) (Duane et al., 2010) were computed from brightness and greenness components. TCA is sensitive to the gradient of vegetation cover (Gómez et al., 2011), and TCD is related to vegetation composition and structure (Pflugmacher et al., 2014).

Topographic data

Topographic variables were derived from the LiDAR-based Digital Elevation Model (DEM) (25-m spatial resolution) from the National Geographic Institute (IGN) of Spain, as they are known to be related to forest vegetation distribution: elevation, slope and transformed aspect (TRASP, Roberts and Cooper, 1989) (Eq. 2). The post-processing of this DEM included the removal of possible artefacts and gap filling.

$$TRASP = \frac{1 - (\cos(aspect - 30))}{2} \quad (2)$$

where aspect is in degrees. TRASP ranges from 0 to 1: values of 0 correspond to cooler, wetter north-northeast aspects, whereas values of 1 correspond to hotter, dryer south-southwestern aspects.

4.3.2. Predictor variables and sample selection

LiDAR-derived variables to describe structural recovery (Vegetation Cover-VC-, Tree Cover-TC-, Mean Height -MH- and Coefficient of Variation of Height -CVH-) were set as response variables, and Landsat variables (bands and spectral indices), topography and position were set as predictors. A sample of 10,000 pixels was selected for the model training and validation by a stratified random sampling method. Outliers were previously removed to provide meaningful training and validation pixels considering 3 standard deviations from the mean value of the target variable. We stratified the dataset depending on the response variable histogram distribution to ensure all strata were represented in the train-test and validation datasets. Mean height was stratified in equal intervals of 0.5 m in a range of 0 to 15 m while cover variables were stratified in equal intervals of 5% in a range of 0 to 100 %. We then carried out a spatial random selection within each strata avoiding forested edge pixels considering a distance of 100 m from the borders. The 2016 data sample was split into 60% for calibration of the model (i.e. 6,000 pixels) and 40% for independent validation. In addition, to

evaluate the temporal robustness of the model, we extracted an independent sample from the 2009 dataset for the temporal validation, with a size equal to the sample used for the spatial validation.

4.3.3. Support vector regression modelling

We calibrated a Support Vector Regression model (SVR) (Smola and Scholkopf, 2004) to estimate forest cover and height from predictor variables using the module of Scikit-learn in Python (Pedregosa et al., 2011). SVR is a supervised learning algorithm designed to solve regression problems, which can deal with non -linearity by transforming the data into higher-dimensional space using a kernel function. SVR attempts to find an optimal loss function deviating from the target (training data) less than a value ε while being as flat as possible (Smola and Scholkopf, 2004). SVR was selected for the extrapolation as it has been demonstrated an effective tool to model forest canopy height (García et al., 2018; Pourshamsi et al., 2021) with a good generalization capability (Awad and Khanna, 2015). Input data were scaled to prevent variables of higher numerical ranges dominating variables of lower numerical ranges. We used the radial basis function kernel and performed a grid search using 5-fold cross validation for the parameter tuning (Xu and Goodacre, 2018).

4.3.4. Model evaluation and performance

The performance of the SVR models was evaluated both temporally and spatially. The spatial assessment was conducted using the reserved validation sample from the reference year (2016) (4,000 samples), and the temporal assessment using a sample from the independent LiDAR acquisition collected in 2009 (4,000 samples). Models were assessed by comparing predicted to observed values using a series of goodness of fit measures, including the coefficient of determination R^2, mean absolute error (MAE), root mean squared error (RMSE), relative root mean square error (rRMSE) and bias (i.e., average of predicted minus observed values) for each response variable.

$$MAE = \frac{1}{N}\sum_{i=1}^{N}|Predicted_i - Observed_i| \quad (3)$$

$$RMSE = \sqrt{\frac{1}{N}\sum_{i=1}^{N}(Predicted_i - Observed_i)^2} \quad (4)$$

$$rRMSE = \frac{RMSE}{Mean\ Observed_i}\ 100 \quad (5)$$

4.3.5. Characterisation of post-fire structural recovery

Post-fire recovery was quantified using a relative indicate of recovery within each of the estimated structural variables (VC, TC, MH and CVH). Similarly to Kennedy et al. (2012) and White et al. (2017), the Recovery Indicator (RI) was defined as the ratio of the post-fire recovery (Δ Recovery) by the magnitude of the fire (Δ Disturbance) (*Figure 4.3*):

$$RI_{(VC,TC,MH,CVH)} = \frac{\Delta\ Recovery}{\Delta\ Disturbance} \quad (6)$$

Where Δ Recovery is the change in the forest structural variable value at a defined year following fire:

$$\Delta\ Recovery_{(VC,TC,MH,CVH)} = Value_{y+i} - Value_y \quad (7)$$

and Δ Disturbance is defined as the difference in the forest structural variable value from the year before the fire and the year of the fire:

$$\Delta\ Disturbance_{(VC,TC,MH,CVH)} = Value_{y-1} - Value_y \quad (8)$$

Recovery Indicator (RI) was calculated at different successional stages to assess post-fire structural conditions immediately after fire (y+1, 1995), in the short term (y+6, 2000), mid-term (y+11 and y +16, -2005 and 2010-), and long-term (y+21 and y+26, -2015 and 2020-).

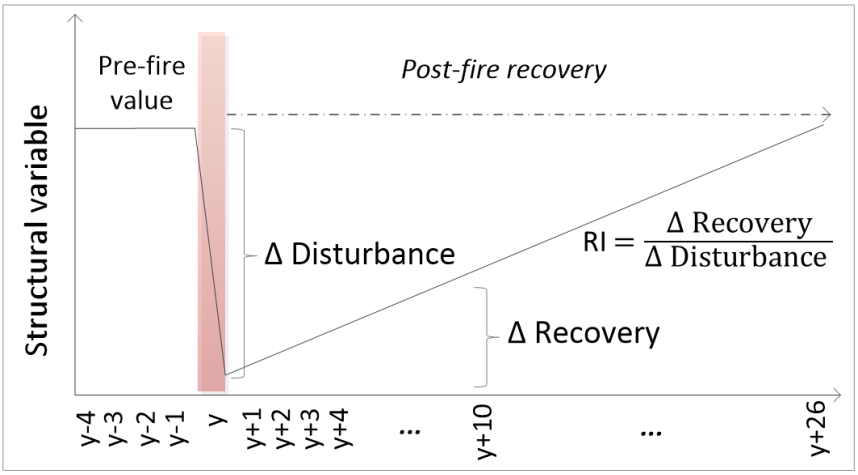

Figure 4.3. Schema of recovery metrics: Δ Recovery, Δ Disturbance, pre-fire value and Recovery Indicator (RI).

4.4. Results

4.4.1. Model assessment

Comparing forest structure variables estimated from Landsat to the reference dataset of LiDAR estimates, we found the overall best agreement for VC, followed by MH, TC and CVH (*Figure 4.4*). Models explain a good percentage of the variance, with model R^2 ranging from 0.63 to 0.78, and rRMSE below 30% for all variables except for the mean height (2016). Models from the temporal extrapolation (2009) maintain a good performance, although R^2 decreases (0.51 - 0.74) and the errors increase (rRMSE ranging from 31 to 44%). VC showed the highest agreement close to the 1:1 line with a MAE of 9.6% for 2016 and 11.1% for 2009. The agreement of TC estimates was lower (MAE of 11.3% for 2016 and 12.6% for 2009) displaying an over- and underestimation in the lowest and highest TC values, respectively. Mean height (MH) estimations showed moderate agreement with a MAE of 1.25 m (2016) and 1.5 m (2009) while Coefficient of Variation of height (CVH) estimations achieved a less strong correlation to the reference dataset. Positive bias in 2009 indicates that the model generally overestimated cover and height values, while we observed an underestimation of cover and height values in 2016.

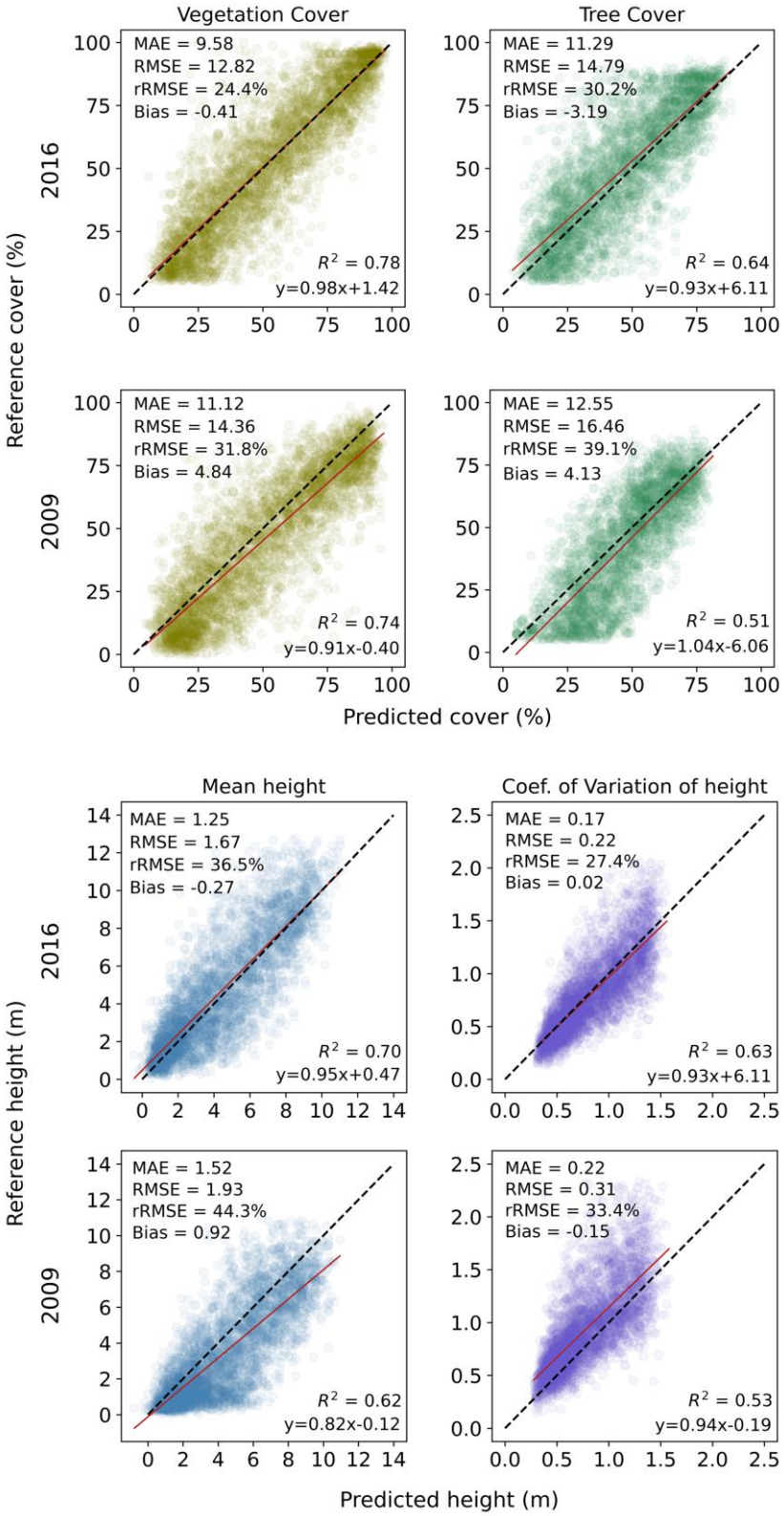

Figure 4.4. Scatterplots between predicted and observed values for canopy cover (VC and TC) and height (MH and CVH) response variables on the independent validation samples (2016 and 2009).

4.4.2. Estimations of annual forest cover and height

Figure 4.5 contains the time-series of VC, TC, MH and CVH variables for the burned pixels in 1994, burned pixels in both 1994 and 2017, and unburned forested pixels for the period 1990-2020. In those unburned areas, forest cover and height variables remained stable over the three decades, with a slight upward trend. Time-series of burned areas shows a loss of cover and height in the year of the fire that even extends into the following post-fire year. Most noticeable is that burned areas did not return to its pre-fire value in terms of Tree Cover and Mean Height within the temporal window of the time-series (26 years post-fire), although they remain close. Those patches with fire recurrence in 2017 were burned before reaching the previous conditions, returning to a starting point of the recovery process. Attending to the evolution of the CVH, the variability increases after the fire at the pixel level due to the presence of a mixture of soil, remnant vegetation and dead wood. In the following years after the fire, variability tends to be reduced by the regrowth of vegetation. Nonetheless, given the high heterogeneity of forests, even in unburned areas, the CVH remained above 0.5 m.

These temporal patterns are also observed in the detailed maps of the estimated variables for the years 1990, 1995, 2005 and 2020 (*Figure 4.6*). Vegetation cover, tree cover and mean height values are clearly more homogeneous throughout the area before the fire occurs (1990) with intermediate values of Coefficient of Variation of height. One year after fire (1995), vegetation cover, tree cover and mean height values drop sharply, increasing the CVH. The heterogeneity of the landscape in terms of cover and height is well visible in those burned areas in the mid-term and long-term (2005, 2020) while the unburned sector maintains stable values with a slight increase.

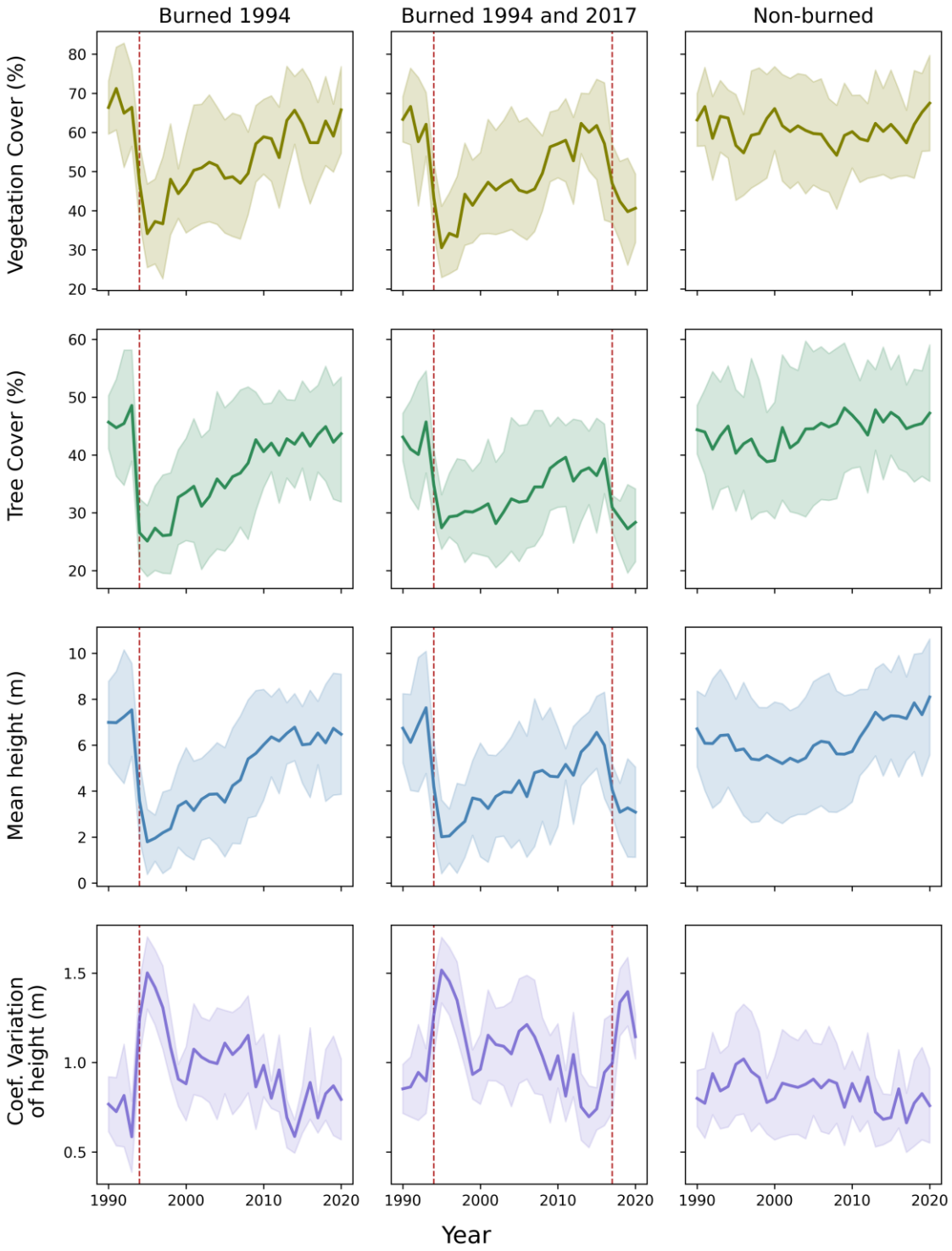

Figure 4.5. Time-series of mean values of forest structure variables for burned and unburned pixels. Shading around the mean values indicate the standard deviation. Vertical red lines indicate the year of the fire.

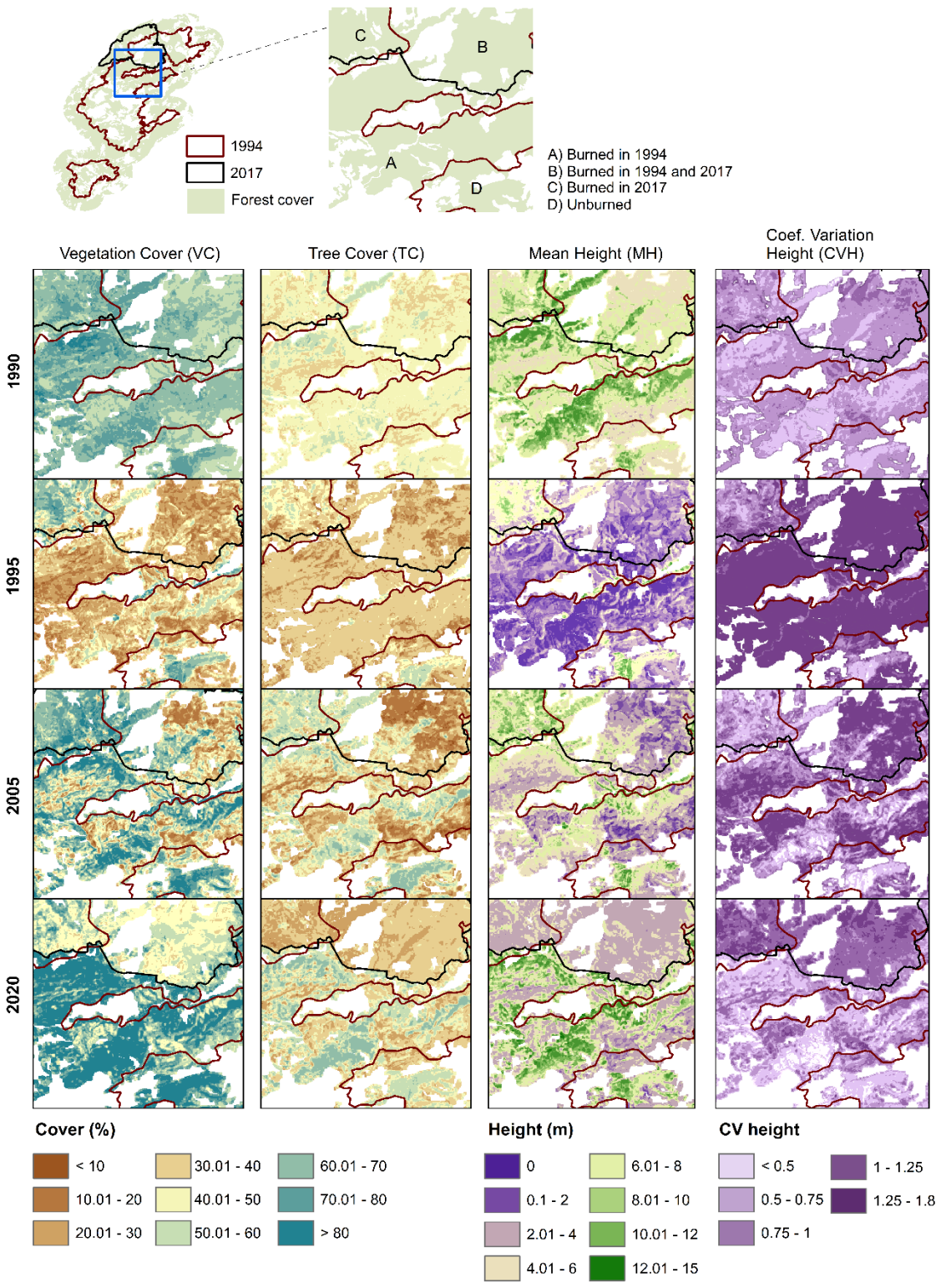

Figure 4.6. Maps of Vegetation Cover, Tree Cover, Mean Height and Coefficient of Variation of Height at four successional stages: 1990 (y-4), 1995 (y+1), 2005 (y+11) and 2020 (y+26). White spaces indicate masked areas.

4.4.3. Quantifying post-fire structural recovery

From a spatio-temporal perspective, we examined the annual maps to get a detailed wall-to wall analysis of the forest structure recovery from the fire occurrence until 2020. *Figure 4.7* shows the difference between 2020 and 1994 (immediately after fire) of the estimated forest structural attributes over burned and unburned forested areas. Vegetation cover, tree cover and mean height remained relatively stable in unburned forests with a slight increase over the period (10-20% in cover, 2-4 m in height). CVH also showed small changes in magnitude (-0.2), associated to the natural successional process of the forest.

Burned areas display different percentages of increases in vegetation cover but also patches with non-recovery in tree cover and mean height. Largest increases occur in terms of vegetation cover indicating a quick recovery of vegetation in the horizontal plane, whereas tree cover shows considerably lower values. Burned areas also show positive increases in mean height values throughout the study area, with higher regrowth along on north-facing valley slopes. Most negative values correspond to the area burned in 2017 that was not disturbed in 1994. The area subjected to fire-recurrence, meaning burned in 1994 and 2017, show low percentages of vegetation cover and mean height 3 years after the second fire. The variability of height decreased with respect to the year of the fire as the recovery process moves forward and vegetation starts to encroach the ground.

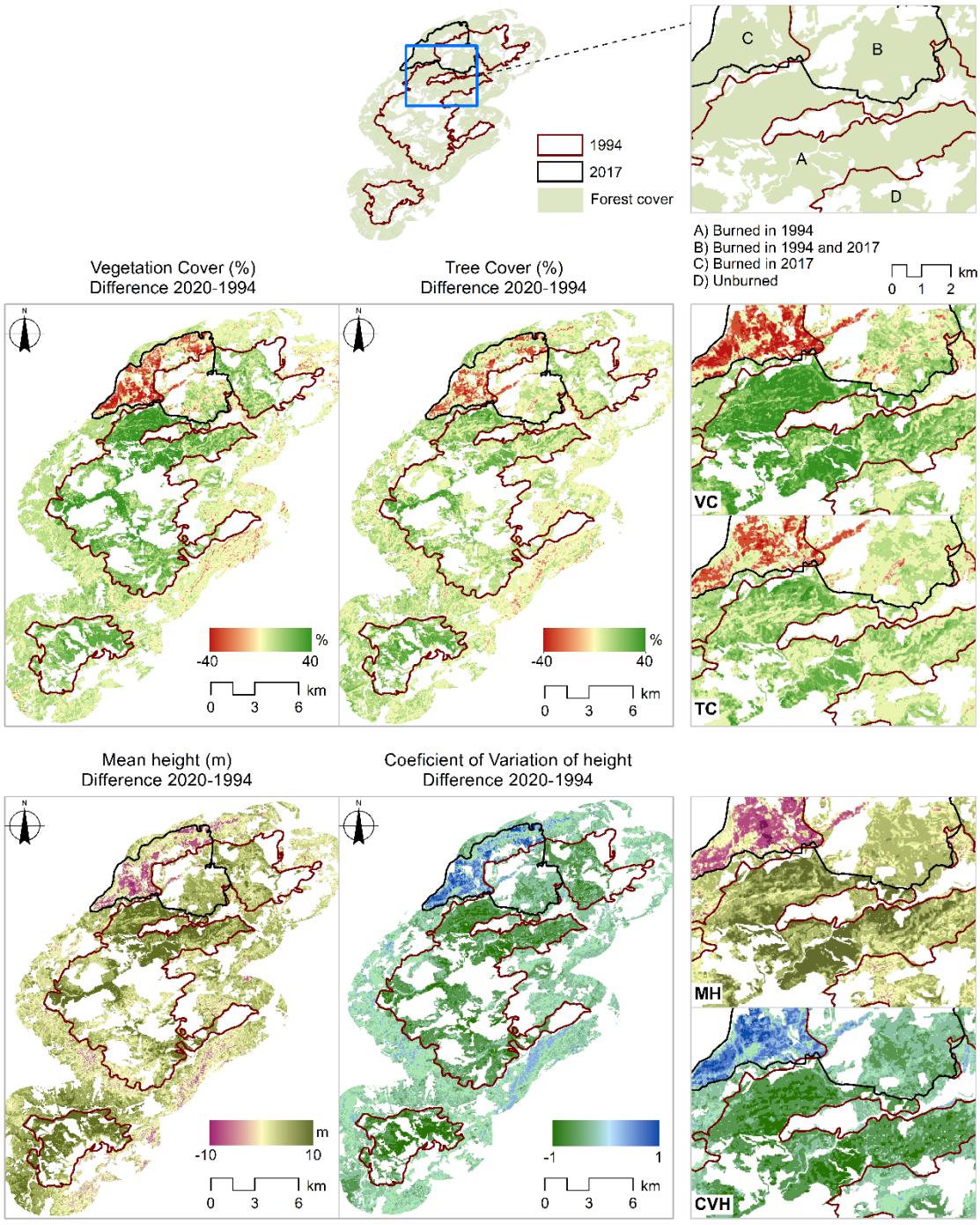

Figure 4.7. Difference (2020-1994) maps of post-fire Vegetation Cover, Tree Cover, Mean Height and Coefficient of Variation of Height. White spaces indicate masked areas.

Results from the Recovery Indicator (RI) of the forest structure variables at 5-yearly intervals (*Figure 4.8*) provide a measure of the immediately post-fire conditions (y+1, 1995) and the state of recovery in the short term (y+6, 2000), in

the mid-term (y+11-y+16, 2005-2010) and, in the long term (y+21-y+26, 2015-2020). The evolution of the RI shows a gradual recovery for all variables, although only vegetation cover reaches pre-fire values 26 years after fire. RI values reached the threshold of 0.5 (i.e. half of pre-fire state) in terms of vegetation cover in the short term, but remain below 0.5 according to the mean height, indicating an initial recovery of pioneer herbs and shrubs and an initial reestablishment of remnant trees. Over the mid-term to long-term (from 2010 onwards), tree cover almost recovered to pre-fire values, while mean height continues to increase at a slower pace. CVH shows the sharpest increase in the short-term and stabilises thereafter.

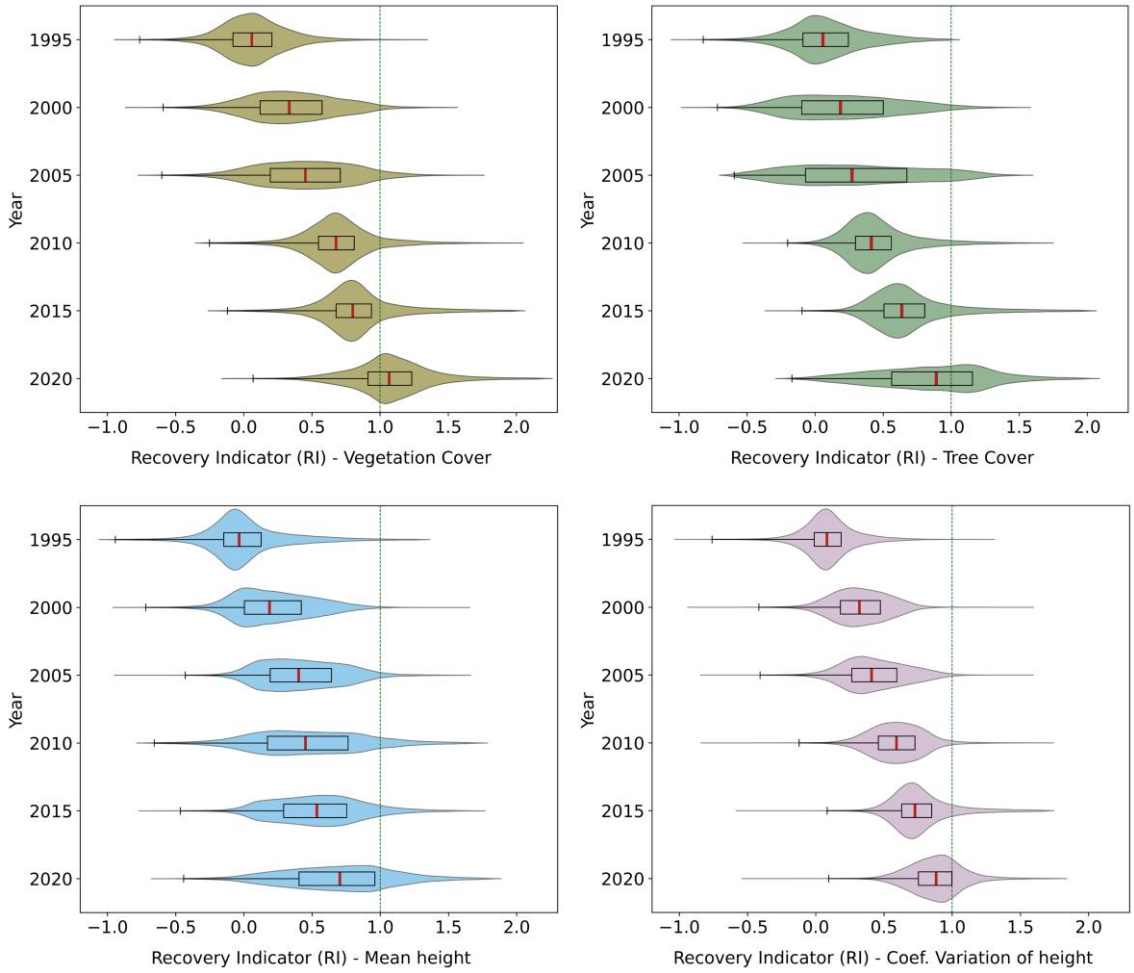

Figure 4.8. Violin plots and boxplots of the Recovery Indicator for each forest structure variable. Boxes indicate the 25, 50 and 75 percentiles, and the whiskers show confidence intervals (95%). Vertical line indicates a full recovery (RI = 1).

A quantitative overview of the recovery at the successional stages is provided by the percentage of pixels that recovered the pre-fire values regarding the four forest structure variables at 5-year intervals. We considered two scenarios to account for a completely recovery (threshold of 100%) (*Figure 4.9a*) and for an advanced state of the recovery (threshold of 80%) (*Figure 4.9b*). Considering a recovery threshold of 100%, less than 10% of the pixels completely recovered to its pre-fire structure before 6 years after fire and around 15-20% recovered in the mid-term (16 years post-fire). Approximately 40% of pixels recovered the pre-fire values in terms of tree cover 26 years after fire, while less than 30% of pixels were recovered attending to mean height. Nevertheless, considering a recovery threshold of 80% from the pre-fire values, the amount of recovered pixels increase to 73 % on vegetation cover, 58.6 % on tree cover, and 43.8% on mean height 26 years after fire, meaning a relatively advanced state of the recovery.

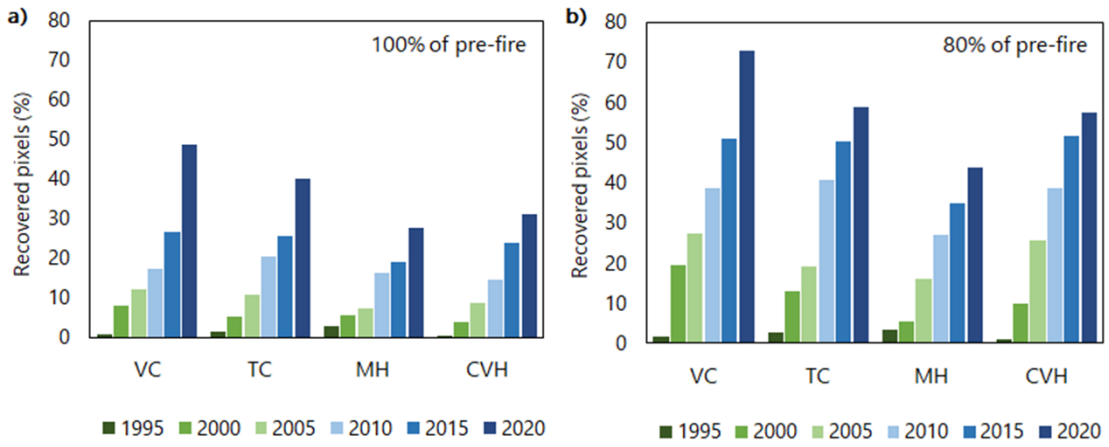

Figure 4.9. Statistics of recovered pixels from burned area in 1994 at a) 100% and b) 80% of recovery attending to the four structure variables in 1995 (y+1), 2000 (y+6), 2005 (y+11), 2010 (y+16), 2015 (y+21) and 2020 (y+26).

4.5. Discussion

4.5.1. Performance of Landsat-based forest structure extrapolation

Post-fire forest recovery dynamics are highly complex due to their high variability and processes undergone in changing environmental conditions. LiDAR data in combination with Landsat imagery provides a unique opportunity to extrapolate information on forest structure over time for a comprehensive evaluation of forest resilience to fire. Here we extrapolated LiDAR-derived cover and height variables over a 30-year window using Landsat imagery and topography variables through a SVR model. Our results confirm previous studies in boreal and temperate forests showing that Landsat data are well suited for mapping LiDAR-derived forest cover and height (Ahmed et al., 2015; Matasci et al., 2018; Senf et al., 2019; Zald et al., 2016). We assessed the performance of the models both spatially and temporally, thereby ensuring their capability to extrapolate LiDAR-based information on forest variables (Matasci et al., 2018; Zald et al., 2016).

The models performed better for the cover estimations, as cover metrics are assumed to be more directly related to the spectral response of the pixel (García et al., 2017; Zhao et al., 2011), resulting in RMSE of 12.8% (2016) and 14.3% (2009) for VC, and RMSE of 14.8% (2016) and 16.5% (2009) for TC. In this way, Matasci et al. (2018) better estimated annual forest cover than forest height by combining Landsat composites and LiDAR plots using a nearest neighbour imputation approach. Out of the cover variables, they also obtained higher errors for the cover above 2 m (RMSE ranging from 13.2% to 18.6%) than for the cover mean (9 to 11.7%). Limitations from optical data to characterise vertical structure are well-known in relation to the decrease of the sensor sensitivity in closed canopy conditions (Goetz and Dubayah, 2011; Pflugmacher et al., 2014). Even so, the models yielded a MAE below 1.5 m for mean height estimates in both spatial and temporal validation (RMSE of 1.67 and 1.93 m, respectively). Errors found here are in the same order of magnitude as those reported by Zald et al. (2016) (RMSE of 1.84 m in mean height) across taiga and boreal forests in

Central Canada. Compared to other research, our SVR model outperformed linear regression approaches according to the results obtained by Pascual et al. (2010) in central Spain (RMSE of 1.9-2.3 m) from a unique date of LiDAR data collected at higher point density (5pts/m^2). In the same line, Ahmed et al. (2015) reported varying errors in canopy height estimates according to forest maturity (RMSE ranging from 2.4 and 3.5 m) using Random Forests algorithm in boreal forests from West Canada. In accordance to our findings, the coefficient of variation of heights is the variable estimated with the lowest precision in both Zald et al. (2016) and Matasci et al. (2018) due to the limitations in capturing vertical structure variability from the spectral signal. Similarly, Senf et al. (2019) in a study carried out in temperate forest from Central Europe found better results for tree cover than for stand height estimations with a RMSE in tree cover of 15% and a RMSE in stand height estimates up to 3 m when comparing to an independent sample from the same LiDAR acquisition.

Limitations of Landsat indices related to saturation in closed canopies and the influence of soil and understory reflectance in open forests may explain the slight underestimations of forest attributes observed in the higher mean height ranges in contrast to the overestimations observed at the lower values (García et al., 2018; Potapov et al., 2021). A further potential source of error can be attributed to the dynamics of vegetation succession itself, implying that the spectral signal of vegetation at 2 metres in height (tree cover) within a pixel is a mixture of early-growing trees and shrubs in the initial stages of the recovery (Martín-Alcón et al., 2015). Although uncertainties may also arise due to the nature of the low-density LiDAR data itself, we can assume that LiDAR-derived cover and mean vegetation height display similar trends to the natural vegetation dynamics (Falkowski et al., 2009; Kane et al., 2010).

Another crucial factor is that the model accuracy relies on relationships between response variables and predictor variables. This means to assume that the dataset adequately contains the variables of interest and represents the range of variation in these forest variables. The models here obtained show high values

regarding the goodness of fit spatially achieving an R^2 from 0.63 to 0.78. Previous studies that also attempted to integrate LiDAR and Landsat to derive forest structure attributes confirmed that indices including SWIR bands (NBR, NDWI) but also TCT as TCA and TCW are closely related to LiDAR-derived structural variables in different ecosystems (Ahmed et al., 2015; García et al., 2018; Gómez et al., 2011; Pflugmacher et al., 2014).

Temporally, the models also showed to be consistent when calibrating the model in a different year (2016), although a wider variability was observed for the 2009 estimates, with model R^2 ranging between 0.51 to 0.74, and an increase in the errors (relative RMSE from 30 to 44%). Errors reported here are in the same order of magnitude as those found by Matasci et al. (2018) in the temporal assessment, with relative RMSE ranging from 38.3% to 46.6 % in mean height and 23% to 32% in cover mean. The relatively good temporal performance of the models is crucial for the generation of time series of structural variables that enable the assessment of vegetation recovery. Differences in the vegetative conditions of ecosystems require the model to adapt to these differences to accurately capture forest structure changes over the time-series (Matasci et al., 2018). Moreover, the temporal validation between two years of Landsat data from different sensors (TM in 2009 and OLI in 2016) ensures a temporal stability of the estimates despite the change in sensor, making it possible to extend the series in the future with the ongoing Landsat 8 data acquisitions and the recently launch of Landsat 9 with similar characteristics (Masek et al., 2020).

The possibility to validate models both temporally and spatially is crucial to obtain robust estimates (Matasci et al., 2018). Model performance could improve with the availability of more LiDAR datasets at different dates throughout the time series. This methodology is appropriate for regional and national analysis, using LiDAR coverages collected at low point densities. The annual maps of forest structure variables could be considered a starting point for the analysis of post-fire forest dynamics at larger scales. The recent accessibility to LiDAR acquisitions from the near-global mission GEDI (Dubayah et al., 2020) makes

possible the integration with Landsat imagery to generate information on forest attributes for larger area applications (Potapov et al., 2021).

4.5.2. Characterization of forest structure recovery dynamics

We examined the evolution of post-fire recovery attending to the LiDAR-derived forest cover, height and heterogeneity attributes to get a broad overview of forest structure dynamics after fire. Vegetation cover and mean height displayed a different rhythm of recovery. Vegetation cover reached pre-fire values within 26-years on average and tree cover remains close to pre-fire values, which can be attributed to tree regrowth and a higher density of stems per hectare (Bolton et al., 2015; Kane et al., 2014; Matasci et al., 2018). Although mean height showed a slower recovery, it reached values close to the pre-fire situation. Nonetheless, it should be mentioned that the recovery of forest height might also be underestimated, since small footprint LiDAR tend to underestimate the canopy height in coniferous forests, particularly when point density is low, because of the low probability of pulses hitting the tree tops (Magnussen and Boudewyn, 1998).

Studies addressing temporal extrapolation of LiDAR-derived forest attributes for recovery quantification are limited. Comparing our findings with those obtained by Matasci et al. (2018) in boreal forests, both agree on the marked differences in the evolution of cover with respect to height estimates, where tree cover reached pre-fire values earlier but canopy height did not recovered before 25 years after fire. Recovery estimates obtained from Landsat time-series in previous studies, were clearly overestimated, since estimations from spectral indices suggested that vegetation reached the pre-fire state in the short and mid-term in Mediterranean ecosystems (Hislop et al., 2018; Morresi et al., 2019; Viana-Soto et al., 2017). Although the results obtained here show that after 26 years we have a forest in an advanced state of recovery in terms of structure, our results evidenced that the variables used to characterise forest structure had not reached the pre-fire state. A temporal window of 26 years can give a clear picture

of whether there is a recovery process ongoing even if a longer period is needed to reach a mature forest (González-De Vega et al., 2016).

Many factors influence post-fire successional pathways (McLauchlan et al., 2020), depending not only on fire severity but also on the adaptations, surviving trees, canopy seed banks, changes in dominant species associated with inter-species competition processes (Calvo et al., 2008; Pausas and Keeley, 2014a) and post-fire climatic conditions (Mazza and Sarris, 2021). In these pine forests, the minimum interval commonly used for considering a forest as having recovered is above 15-20 years (Eugenio et al., 2006). This is connected to the fact that the juvenile reproductive phase is not reached until 20 years after fire in seed-species (Thanos and Daskalakou, 2000), meaning that pine trees take several years to establish from seed. Therefore, we expected a lower rhythm of recovery in mean height in the short-term that slightly increases after the first decade on average (*Figure 4.5*).

Using the Recovery Indicator (RI) for the four structure variables, we managed to monitor how the recovery has evolved at successive stages (*Figure 4.8*). Vegetation cover increased rapidly following fire indicating a quicker recovery of the canopy-filling gaps with the colonization of pioneer herbs and shrubs and an initial reestablishment of remnant trees (Bolton et al., 2015; González-De Vega et al., 2016). On the contrary, mean height remained further from reaching pre-fire values in the first decade, but values gradually increased according to the progress from a stage of stand initiation to the stem exclusion, in which shrub dominance is replaced by greater tree dominance (Martín-Alcón et al., 2015).

The recovery scenarios evidenced that percentage of pixels that completely recovered the pre-fire values of cover and height does not fulfil 50% within 26 years. Nevertheless, considering a recovery threshold of 80% of the pre-fire value (White et al., 2018), we observe higher percentages of recovered pixels (70% in vegetation cover and 44% in mean height). With these results, we can consider that resilience to fire of these Mediterranean pine forests is moderate. The challenge here is, as suggested by Moya et al. (2018) and Taboada et al. (2018),

the risk involved if the ecosystem remains in an immature state in the face of a likely recurrence of fire in shorter intervals than these pine species need to develop a productive seed bank. Combining the results of the time series (*Figure 4.5*) and the Recovery Indicator (*Figure 4.8*), these suggest the presence of patches that remain in ongoing recovery although they have not reached the pre-fire benchmark. In this way, a new fire may limit recovery by producing ecosystem degradation involving changes in ecosystem composition (Baudena et al., 2019). Analysing the forest structure values obtained for the first 3 years after the 2017 fire in the area with fire recurrence (*Figure 4.5*), signals of difficulty in initiating recovery after fire recurrence can be gathered from the time-series of cover and height estimates, whereas this initial recovery was observed in the 1994 fire.

Some methodological considerations should be considered when explaining ecological processes from the findings obtained here. Our approach provides an overview of the evolution of the forest structure after a large forest fire in concordance with the potential and limitations of the available low-resolution LiDAR data (Martín-Alcón et al., 2015). The use of Landsat data provides a unique opportunity to analyse the evolution through decades, but the 30-m pixel size may conceal a larger structural variability within. Even so, cover and height are important indicators of forest recovery that can be derived to larger areas, providing useful information to support post-fire restoration activities (De las Heras et al., 2012).

4.6. Conclusion

The feasibility of extrapolating LiDAR-derived structural variables using Landsat images over time has been demonstrated. The stability of the estimations both temporal and spatially enabled to analyse differences in post-fire forest structure recovery. Noticeable differences were found in terms of vegetation cover and mean height, as the cover values recovered to a pre-fire state but mean height did not reach this benchmark along the temporal window analysed. With less than 50% of burned pixels completely recovered to a pre-fire structure 26 years after

fire, we may conclude that the resilience to fire of these Mediterranean pine forests is moderate. Providing data on the dynamics of forest structure response is a valuable source of information to stakeholders and decision makers concerned with the assessment of post-fire forest recovery. Our work provides a first step in investigating the temporal evolution of the Mediterranean pine forests structure over three decades, which can support the design of mitigation and adaptation strategies that enhance fire resilience.

4.7. Acknowledgments

A.V.S. is supported by the Spanish Ministry of Science, Innovation and Universities through a FPU doctoral fellowship (FPU17/03260). Department support: Grant for Excellence in Teaching Staff of the Community of Madrid (EPU-DPTO/2020/008).

Author contribution

Alba Viana-Soto: Conceptualization, Methodology, Formal analysis, Writing – original draft. Mariano García: Conceptualization, Methodology, Writing – review & editing. Inmaculada Aguado: Conceptualization, Writing – review & editing. Javier Salas: Conceptualization, Writing – review & editing.

Chapter 5. Unravelling shifts in post-fire woody-vegetation cover from unmixing Landsat data

Based on:

Viana-Soto, A., Okujeni, A., Pflugmacher, D., García, M., Aguado, I., & Hostert, P. (2022). Quantifying post-fire shifts in woody-vegetation cover composition in Mediterranean pine forests using Landsat time series and regression-based unmixing. *Remote Sensing of Environment*, 281, 113239. https://doi.org/10.1016/j.rse.2022.113239

Abstract

Mediterranean forests are highly subjected to fire occurrence. Altered fire regimes resulting from changes in land use and climate may jeopardise their resilience to fire and induce changes in forest composition. Disentangling forest cover composition is therefore critical for understanding post-fire forest recovery dynamics. In this study, we demonstrate how fractional time series of different woody-vegetation types support the analysis of post-fire vegetation recovery in relation to the pre-fire situation for two burned areas in Mediterranean pine forests in Spain. We separately estimated tree, shrub and background (combining herbaceous, soil and rock) cover fractions on an annual basis (1990-2020) using Landsat Spectral-Temporal Metrics (STMs) and a regression-based unmixing approach. Our regression models effectively estimated fractions of the three cover types with Mean Absolute Errors ranging from 8.6% to 13.4% when comparing to a reference dataset derived from high-resolution orthophotos across 6 different years. Slightly overestimations of low cover fractions where found in tree and shrub cover fractions across the study sites. Despite these minor errors, time series of cover fractions revealed characteristic spatio-temporal patterns of different woody-vegetation types for burned and unburned areas. Based on the fractional cover estimates, we derived a Normalised Difference Tree-Shrub Fraction index (NDTSF) to contrast tree cover fraction relative to the shrub cover and map post-fire shifts in composition. Annual maps of NDTSF revealed a high spatial and temporal variability and a general dynamic towards the pre-fire cover composition in 79-80% of burned areas but a shift from tree to shrub dominance in 12.3-15.4% 26 years after fire. Our regression-based unmixing approach advances the analysis of post-fire recovery dynamics, unravelling shifts in forest composition that are of major concern to forest management.

Keywords: Post-fire recovery, Landsat, spectral unmixing, fractional cover, support vector regression (SVR), Mediterranean forest.

5.1. Introduction

Wildfires are a critical component in shaping the structure and composition of forest ecosystems worldwide (McLauchlan et al., 2020). In recent years, Mediterranean regions have suffered major fire disasters (Australia, California, Chile, Southern Europe), causing ecological, economic and human damage (Bowman et al., 2020; Keeley, 2012). In European Mediterranean areas, fire-prone ecosystems, such as those dominated by *Pinus* species (*Pinus halepensis* Mill. and *Pinus pinaster* Ait.), are highly subjected to fire occurrence (Fernández-García et al., 2019; Pausas and Vallejo, 1999). As an integral part of these ecosystems, pine species have long been adapted to fire activity by developing ecological strategies to naturally recover (i.e. resprouting from survival individuals and seedling recruitment) (Calvo et al., 2008; De las Heras et al., 2012; Pausas and Keeley, 2014a). Nevertheless, predictions of future fire regimes indicate an increased frequency of large forest fires under warmer conditions and more extended and severe droughts (Stephens et al., 2013; Turco et al., 2018). These changes in fire regimes induced by both climate and land use changes associated with rural abandonment may endanger their high resilience to fire (Moreno et al., 2014; Pausas and Fernández-Muñoz, 2012).

Mediterranean ecosystems are likely to face constraints in recovering after fire (Doblas-Miranda et al., 2017; Santana et al., 2014), depending on species adaptive traits (González-De Vega et al., 2016; Hernández-Serrano et al., 2013). The post-fire environments of Mediterranean forests are usually composed of a mixture of dead vegetation, remnant live trees, pioneer shrub and herbaceous species and bare soil (Quintano et al., 2013). In the stand initiation phase, seedling growth and competitive interactions between pine seedlings and sprouting shrubs occur (Calvo et al., 2008). Tree individuals surviving to competition tend to expand in a successional stage, leading to tree canopy dominance (De las Heras et al., 2012; Pausas et al., 2002). Nonetheless, recent studies suggest that fire recurrence and increased aridity may shift Mediterranean forests towards shrub-dominated ecosystems (Karavani et al.,

2018; Vasques et al., 2022), degrading forests to quickly regrowing low vegetation. Evaluating whether forests evolve towards their pre-fire state or whether vegetation transition is taking place requires meaningful information on how the composition of tree and shrub vegetation is shifting along the recovery process (Bartels et al., 2016).

Remote sensing offers powerful tools for monitoring forest recovery based on the spectral response of vegetation at multiple spatial and temporal scales. The Landsat archive, covering more than four decades of imagery, also enables the analysis of historical fire-recovery dynamics (Chuvieco et al., 2020; Wulder et al., 2019). Advances in data processing have increased the use of Landsat time series to estimate parameters related to vegetation recovery (Pérez-Cabello et al., 2021), taking advantage of trend analysis and change detection techniques (Zhu, 2017). Post-fire vegetation recovery is commonly measured by the time required for a burned pixel to return to the pre-fire spectral value (Pickell et al., 2016; White et al., 2022) or by the amount of pixels which reach the pre-fire threshold (Bright et al., 2019; Morresi et al., 2019; Viana-Soto et al., 2020). However, spectral bands or spectral indices represent reflectance, and respectively, unitless values that do not distinguish between different vegetation types within a pixel (Quintano et al., 2012). When post-fire vegetation recovery analysis aims at quantifying variations in forest composition within different successional stages or major compositional shifts relative to the pre-fire situation, the use of spectral bands or spectral indices alone is not sufficient to describe such cover type specific change processes (Kuemmerle et al., 2006; Suess et al., 2018).

Disentangling forest cover composition by means of cover fractions of different woody-vegetation types such as trees and shrubs through time provides a more comprehensive picture of post-fire forest recovery dynamics (Röder et al., 2008). Fractional cover mapping typically relies on spectral unmixing methods, including spectral mixture analysis (SMA) (Adams et al., 1986) or Multiple Endmember Spectral Mixture Analysis (MESMA) (Roberts et al., 1998). Previous studies

applied SMA to derive Landsat-based time series of green vegetation fraction for analysing vegetation dynamics (Hostert et al., 2003) and post-fire vegetation recovery (Röder et al., 2008; Solans Vila and Barbosa, 2010). As a variation of the SMA approach, MESMA has been commonly used for assessing burn severity (Quintano et al., 2017, 2013) and post-fire recovery in Mediterranean ecosystems (Fernández-Guisuraga et al., 2020; Fernández-Manso et al., 2016; Kibler et al., 2019; Veraverbeke et al., 2012) by means of photosynthetic vegetation (PV), non-photosynthetic vegetation (NPV) and soil. Other studies have used MESMA to quantify temporal changes in cover fractions for different vegetation growth forms (e.g. trees, shrubs, herbaceous) in fire-prone ecosystems from multi-temporal multispectral data (Lippitt et al., 2018; Sonnentag et al., 2007). Yet, the differentiation of tree and shrub fractions within the photosynthetic active vegetation remains challenging due to the spectral similarity of these vegetation types when represented by multispectral data (Baumann et al., 2018).

Regression-based unmixing has been demonstrated as an alternative approach for estimating fractions of different vegetation types within different ecosystems, including fire-prone Mediterranean forests and shrublands (Cooper et al., 2020; Montorio et al., 2020; Suess et al., 2018). Particularly, the generation of synthetic data from spectral libraries for regression model training (Okujeni et al., 2017, 2013) has been demonstrated as a useful strategy for deriving time series of vegetation-type fractions to be used for environmental change assessment from the Landsat archive. Following this method, Suess et al. (2018) derived annual fraction maps of shrub cover over three decades to characterise change intensity patterns in shrublands in Southern Portugal. Senf et al. (2020) demonstrated the value of the same approach to derive time series of forest cover fractions, thereby differentiating coniferous and broadleaved cover across temperate forests of Central Europe. However, both studies make use of annual Landsat images representative of a single date per year or a best observation composite for a specific period per year, and thus do not make use of the full spectral temporal variably within a year. Particularly when disentangling cover fractions of spectrally

similar vegetation types, the use of Spectral-Temporal Metrics (STM) in the unmixing procedure has been demonstrated as a better choice (Okujeni et al., 2021) because it incorporates not only the spectral-temporal variability of cover types, but also the variations caused by phenology or illumination and shading of the canopy (Pflugmacher et al., 2019). Moreover, none of these studies focused on the analysis of post-fire vegetation recovery and post-fire shifts in vegetation composition by separating different woody-vegetation types through time.

The overall objective of this paper is to analyse post-fire changes in tree-shrub dominance over large forest fires in the Mediterranean basin in Spain that occurred during the 1990s. We here considered recovery as an ongoing process, and therefore analyse if forest is trending toward its pre-fire composition of woody vegetation (i.e. tree versus shrubs). Therefore, fractional cover of two target classes, i.e. tree and shrub, and a background class representing all other relevant cover types were estimated on an annual basis using Landsat STM and a regression-based unmixing approach. We accordingly addressed the following research questions:

i) How accurate can time series of tree and shrub cover fractions be quantified based on annual Landsat STM and regression-based unmixing?

ii) What are the characteristic spatio-temporal patterns of cover fractions for burned and unburned areas?

iii) How does tree-shrub dominance shift over time and space after fire and with respect to the pre-fire situation?

5.2. Study sites

The study sites correspond to two areas that burned in the summer of 1994 in the southeast of the Iberian Peninsula (*Figure 5.1*): the Yeste Fire (Fig. 1A) (7th August, 11,685 ha of woody-vegetation burned), and the Requena Fire (Fig. 1B) (5th July, 16,373 ha of woody-vegetation burned). Fire perimeters were obtained

from previous work by using the Burned Area Algorithm Software (BAMS) (Bastarrika et al., 2014), selecting burned patches that were not recently burned, although neighbouring areas were affected by fires. These areas represent typical Mediterranean landscapes composed of a mosaic of coniferous trees (mainly *Pinus halepensis* Mill. and *Pinus pinaster* Ait.), shrubs (*Rosmarinus*, *Ulex*, *Juniperus*) and interspersed agricultural areas. The selected case studies represent regions highly subjected to fire recurrence (Pausas and Fernández-Muñoz, 2012), and based on pre-fire conditions ranged from higher shrub dominance in Requena to a higher proportion of tree cover in Yeste (affected by a recurrent fire in 2017). Both areas have a semi-arid Mediterranean climate, with hot dry summers (mean annual temperature around 15 °C) and mean annual rainfall around 600–700 mm, concentrated from October to March (Ninyerola et al., 2005). Heterogeneous topography characterises these areas, with elevations varying from 300 m to above 1500 m, and Calcisols and Calcari-lithic Leptosols as predominant soils (Jones et al., 2005).

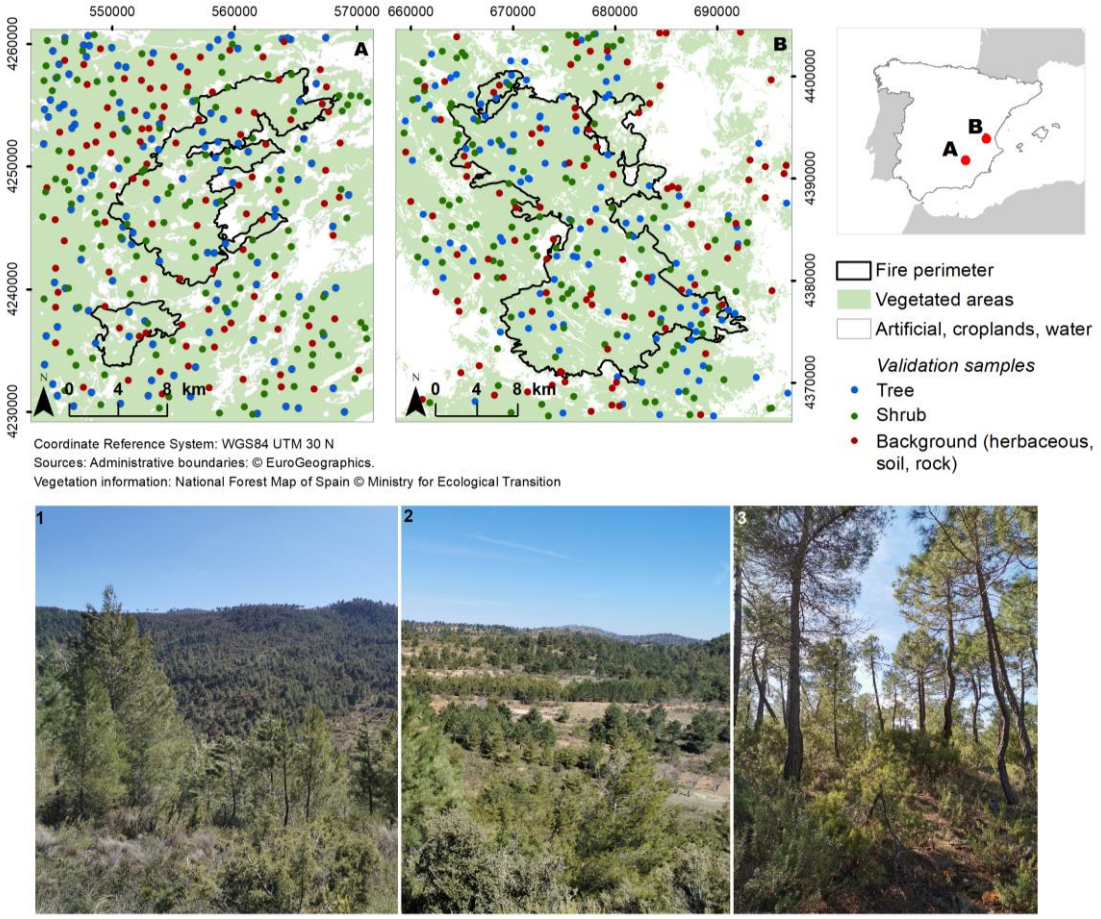

Figure 5.1. Location of burned area perimeters: A) Yeste Fire (August 7th 1994) and B) Requena Fire (July 5th1994), including validation samples (see section 3.4.). Bottom, photographs showing typical landscape patterns of the Mediterranean pine ecosystem in the SE of Spain: open-canopy pine forest with a high proportion of shrubs (1), mosaic of agricultural lands and forest patches (2), detail of an unburned Pinus halepensis plot (3) (Source: A. Viana-Soto March 2021). White: Masked areas correspond to water, croplands and artificial surfaces.

5.3. Materials and methods

The workflow of our study is presented in *Figure 5.2*. Each study site was processed separately as follows: First, we derived annual STM based on all available, cloud-free Landsat reflectance data for the period 1990-2020. Second, we developed an image spectral library from Landsat STM (in the following referred to as STM library). Third, regression based-unmixing with synthetic training data from the spectral library (Okujeni et al., 2017, 2013) was

implemented to derive annual fractional cover time series for the tree, shrub and background classes. We subsequently validated fractional cover estimates for six different years based on reference fractions from visually interpreted very high-resolution orthophotos. To quantify shifts in tree-shrub dominance over time and space, we finally calculated a normalised ratio based on the fraction estimates.

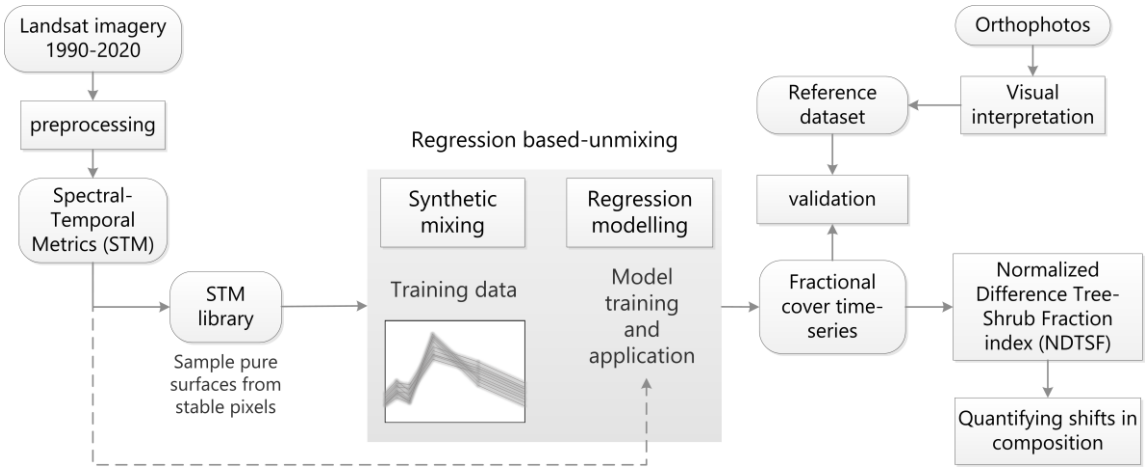

Figure 5.2. Workflow of the methodology for the estimation of cover fractions of tree, shrub and background using Landsat imagery and a regression-based unmixing approach.

5.3.1. Landsat data

We downloaded all available Landsat 5 TM, Landsat 7 ETM+ and Landsat 8 OLI collection 1 Level 1 Tier 1 images covering the study areas with cloud cover less than 75% for the period 1990-2020 from the United States Geological Survey (USGS). Clear observations (on average) per year ranged between 13 and 38 for the Yeste area and between 8 and 26 for Requena (*Figure S5.1*). Landsat images were processed to Level 2 Analysis Ready Data (ARD) using the Framework for Operational Radiometric Correction for Environmental Monitoring (FORCE version 3.6.5, Frantz, 2019). Atmospheric and topographic correction (Copernicus DEM GLO-30 dataset, Airbus Defence and Space, 2020), adjacency effect and bidirectional reflectance distribution function corrections as well as cloud and cloud shadow masking (Frantz et al., 2016; Roy et al., 2016; Zhu and Woodcock, 2012) were carried out. STM for each year were computed from six

reflectance bands to account for spectral variability of cover types using the Time Series Analysis submodule provided in FORCE to derive annual STMs aggregated over the year of the ARD. We calculated reflectance percentiles (Q10, Q25, Q50m Q75 and Q90) as well as Interquartile Range (IQR) and Range (RNG) representing reflectance variation (Schug et al., 2020). Water, urban and agricultural areas were masked using the National Forest maps of Spain (1:50.000).

5.3.2. Building the STM library

We developed an image-based STM library for each site. Each library contains STM for the two target classes, tree and shrub, as well as for the background class, which represents herbaceous, soil and rock surface cover types (*Figure 5.3*).

For STM library development, we extracted Landsat-based STM signatures for 2016 from temporally stable pixels of pure tree and shrub cover types as well as from pure and mixed herbaceous, soil and rock types. The use of such mixed cover types within the background class is feasible as long as the fraction of the tree or shrub components is 0% (Suess et al. 2018). In a first step, we preselected pixels that displayed a stable NDVI-trajectory (i.e. undisturbed pixels) throughout the 30-year observation period to ensure the temporal transferability of the STM library. NDVI-trajectories were derived in a previous study (Viana-Soto et al., 2020) using the LandTrendr algorithm (see Kennedy et al., 2010, for a detailed explanation of the trajectory-fitting process). Then, pixels with homogeneous cover were identified from the preselection based on visual interpretation of very high-resolution orthophotos (0.25-0.5-m spatial resolution) for 1983, 1998, 2002, 2006, 2008, 2009, 2012, 2015, and 2018 (National Geographic Institute of Spain - IGN) (*Figure S5.2*).

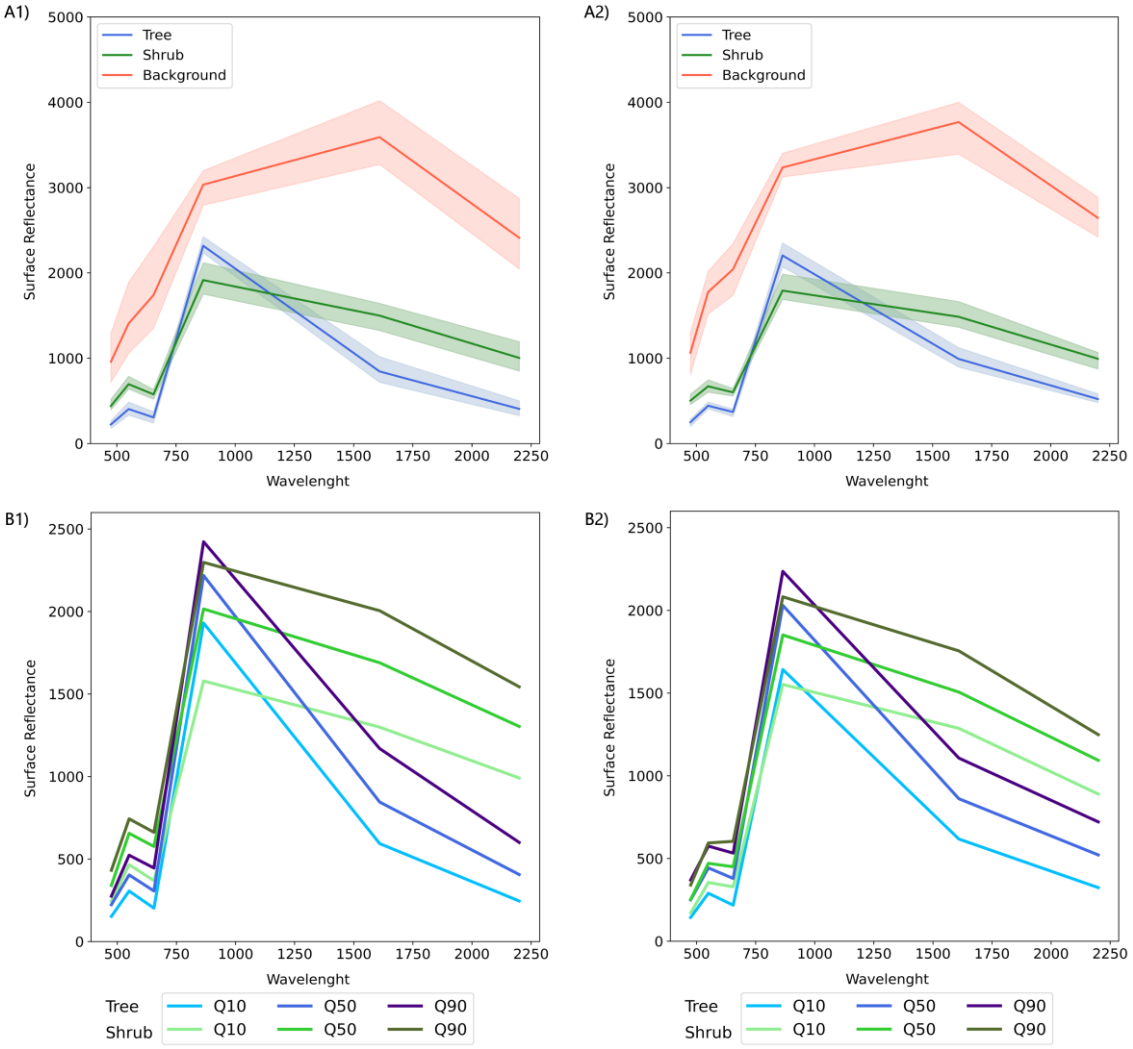

Figure 5.3. A) STM for tree, shrub and background (herbaceous, soil, rock) classes for Yeste (A1) and Requena (A2). Each class is represented by the mean Q50 STM and the variability (one standard deviation) of the Q50 STM is indicated by the shaded area. B) Example STM for tree and shrub classes for Yeste (B1) and Requena (B2). Q10 indicates 10% percentile of reflectance, Q50 medium reflectance and Q90 90% percentile of reflectance.

5.3.3. Regression-based unmixing

Synthetic training data

We followed the approach described in Cooper et al. (2020) and Okujeni et al. (2021) to generate synthetic training data from our STM libraries for subsequent regression-based unmixing using the Synthmix submodule provided in FORCE.

For each site, five synthetic training datasets were created for each class (tree, shrub and background). Each dataset contains 1,000 synthetic mixtures and related mixing proportions generated by mixing library STM with cover proportions between 0 and 1, thus ensuring that the regression model is capable of predicting the full potential range of cover proportions that may be present in the areas. Each synthetic mixture was randomly created as follows: First, we assigned the number of library STM contributing to the mixture such that there were chances of 60% for a mixture of two and 40% for a mixture of three STM. Second, a random library STM from the target class was drawn and assigned a random mixing fraction between 0 and 1. Third, the second and, if applicable, the third library STM was extracted randomly based on class-likelihoods and mixing fractions were assigned so that the sum of all mixing fractions was equal to one. Class-likelihoods were based on the proportional share of class entries in the library. Finally, the synthetic mixture was calculated as linear combination of the drawn STM weighted by the assigned mixing proportion.

Support vector regression modelling

We used SVR (Smola and Scholkopf, 2004) for cover fraction mapping. SVR is a state-of-the-art machine learning approach for predicting quantitative parameters from remote sensing data, including vegetation class fractions (Okujeni et al., 2021; Senf et al., 2020). We chose the standard version of SVR, which implements Vapnik's ε-insensitive loss function (Vapnik, 1995) and a Gaussian Radial Basis Function kernel. SVR model parameter tuning was performed based on a grid search using a 10-fold cross validation.

For each site, SVR models were trained for each class based on the synthetic training data. Instead of developing a single model per class, an ensemble of models for each class was trained based on the five randomly generated synthetic training datasets, and intermediate estimates were combined to a final class estimate based on averaging. This ensemble strategy enables the inclusion of a variety of different types of synthetic mixtures in small sample sizes (Okujeni

et al., 2017). The ensemble of SVR models were applied to each year to derive annual time series of tree, shrub and background cover fractions from 1990 to 2020.

5.3.4. Validation of fraction images

We validated our time series of tree, shrub and background cover fractions using reference cover fractions derived from visual interpretation of very high-resolution orthophotos across six years (2002, 2006, 2009, 2012, 2015 and 2018 –Yeste; 2002, 2006, 2008, 2012, 2015 and 2018 – Requena). Due to reduced quality, orthophotos from 1983 and 1998 were not considered for reference data generation.

Validation was based on separate sets of samples for each year and site. Validation samples, i.e. Landsat pixels to be validated, were selected by stratified random sampling (Stehman, 1996), thus ensuring that all variations of cover types were included. Estimated tree, shrub and background fractions were stratified from 0 to 100% in 20% steps (5 stratum). Then, four pixels were randomly sampled from each stratum, resulting in 60 samples per year and site. To avoid spatial correlation, we constrained the eligible pixels to a minimum distance of 90 m (3 pixels distance).

Reference cover fractions were estimated based on a grid method (Zhao et al., 2016). First, each pixel to be validated was divided into 36 cells of 5×5 m (*Figure S5.3*). Second, the dominant cover type, i.e., tree, shrub, or background, was assigned to each cell through visual interpretation. Third, the percentages of the cover types were calculated for the respective pixel. The final reference dataset was eventually reduced in 6.7% as some pixels could not be properly interpreted. For each cover type, year and site, estimated fractions were compared to reference values using the following goodness of fit measures: the coefficient of determination R^2, mean absolute error (MAE), root mean squared error (RMSE), and bias (i.e., average of estimated minus reference values).

5.3.5. Analysis of post-fire tree-shrub cover dynamics

In a post-fire scenario, tree and shrub cover are expected to decrease in the year of the fire. After this event, shrub cover is expected to quickly increase, followed by a period of both tree and shrub cover increase, related to competitive interactions between pine seedlings and sprouting shrubs. In those pre-fire tree dominated areas, tree cover is expected to also dominate again in the long-term as a result of the success of seedling growth, requiring a minimum of 15-20 years (De las Heras et al., 2012; Pausas and Keeley, 2014a). To contrast cover fractions Souza et al. (2005) proposed a ratio of cover fractions, the Normalised Difference Fraction Index (NDFI), to map canopy damage from forest fires. More recently, Bullock et al. (2020) used the NDFI to characterise tropical forest degradation from Landsat images and Kowalski et al. (2022) quantified drought effects in grasslands by contrasting NPV and soil to PV cover fractions from Sentinel 2 imagery. Following a similar approach we propose a normalised ratio to compare tree cover fraction relative to the shrub cover (NDTSF) to analyse how tree cover evolves with respect to shrub after fire:

$$NDTSF = \frac{(f_{tree} - f_{shrub})}{(f_{tree} + f_{shrub})}$$

If NDTSF is positive, the tree fraction is the predominant cover compared to the shrub. We used the NDTSF maps to quantify shifts in post-fire cover dominance. To evaluate the significance of the post-fire NDTSF trends we used the Mann-Kendall (MK) test (Kendall, 1955; Mann, 1945). MK is a non-parametric statistical test appropriate for identifying whether a time series exhibit a significant monotonic trend (*pvalue* < 0.05). The rate of the change was subsequently assessed by means of the Sen's slope (Sen, 1968), a non-parametric method for estimating the median slope. Non-significant trends were not considered for further analysis, although all pixels are still displayed in the maps of the NDTSF for completeness. Finally, we applied a rule set to the pre-fire (mean 1992-1993) and most recent (2020) NDTSF to classify areas characterised by shifts (i.e. tree

to shrub, shrub to tree) and areas without compositional shifts (i.e. tree-tree, shrub-shrub).

5.4. Results

5.4.1. Regression unmixing performance

Scatter plots with predicted and reference fraction values for the validation samples underline a high correspondence of estimated and observed fractions across all six years (*Figures 5.4* and *5.5*). Mean Absolute Errors (MAE) ranged between 9.6% and 13.4% (for tree), 8.9% and 12.2% (for shrub) and 8.6% and 11.6% (for background). Overall, R^2 values were consistent over successive years, ranging between 0.64 and 0.83. Estimation bias ranged between 1.1 and 6.9 (for tree), 1.2 and 9.6 (for shrub) and -7.8 and -2.5 (for background). Generally, there was a slight tendency towards underestimation for background fractions and overestimation for tree and shrub cover fractions, especially in low cover fractions.

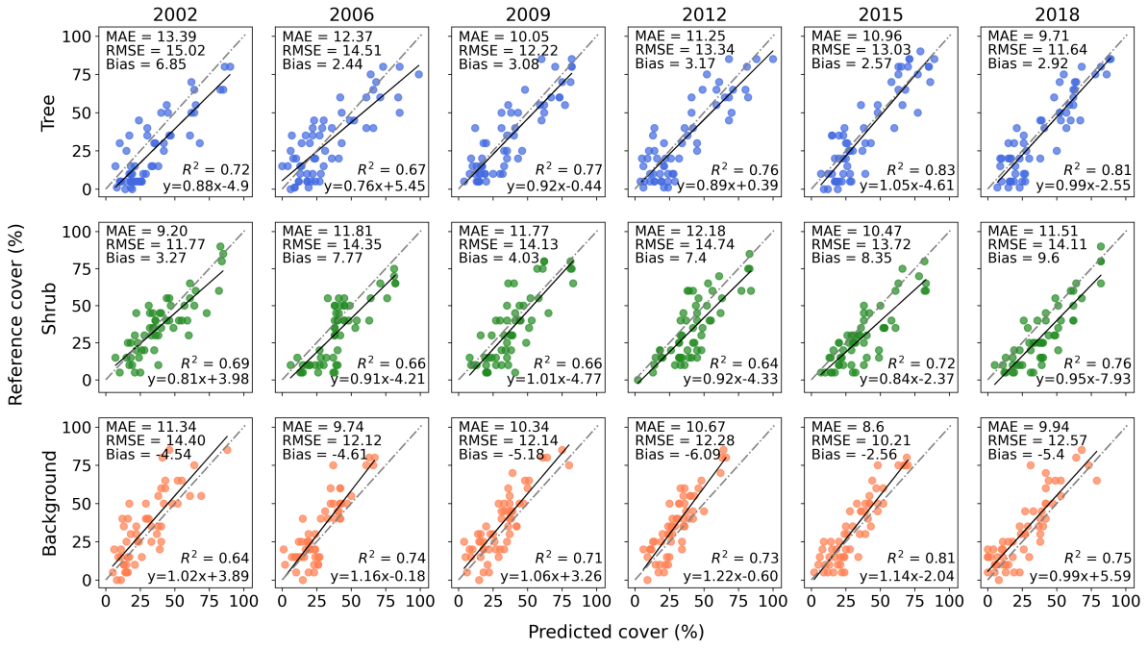

Figure 5.4. Comparison of tree, shrub and background fractional cover estimates from Landsat imagery and reference fractional cover from orthophotos from Yeste.

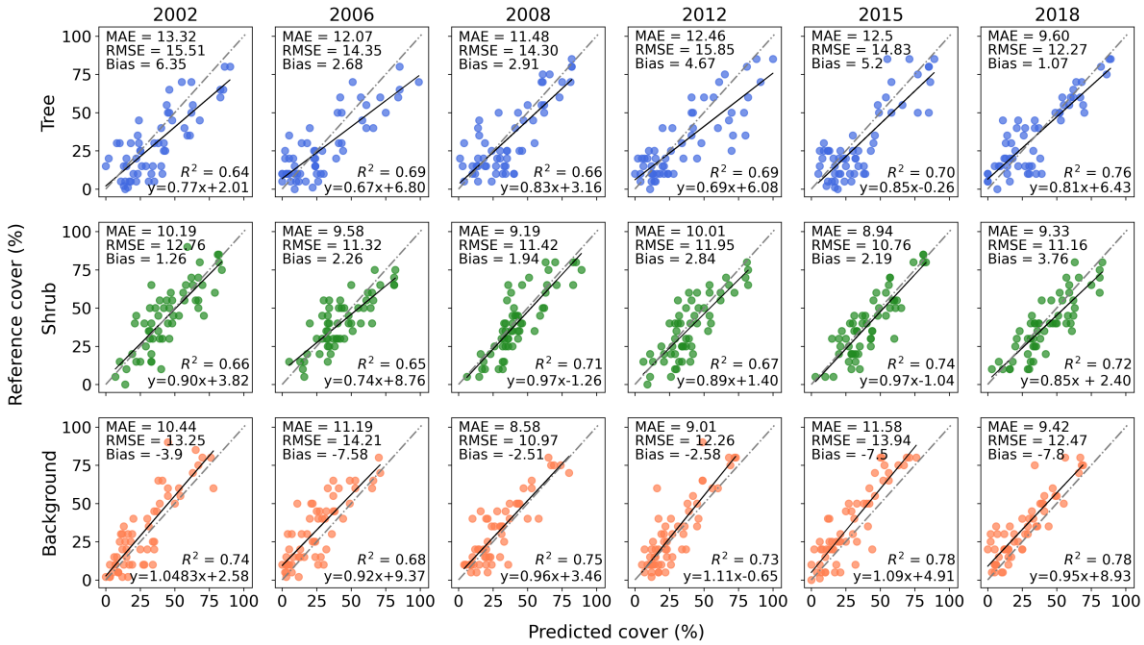

Figure 5.5. Comparison of tree, shrub and background fractional cover estimates from Landsat imagery and reference fractional cover from orthophotos from Requena.

5.4.2. Spatio-temporal patterns of tree and shrub cover

In 2020 the study areas are characterised by high spatial heterogeneity in tree and shrub cover due to their topographic complexity as well as the variability in land use (*Figure 5.6*). Most of the burned area is dominated by shrub cover 26 years after fire. In the northwestern part of the Yeste fire perimeter (*Figure 5.6, top*) a marked dominance of herbaceous-soil and shrub cover relates to a recent fire in 2017.

The annual fractional cover time series show common trends in vegetation recovery after fire in both study sites (*Figure 5.7*). Following the fire event in 1994, there is an abrupt increase of background fraction (early regrowing herbs and soil) to about 50% on average and a corresponding abrupt decrease in tree and shrub cover. Tree and shrub vegetation recovery strongly depended on pre-fire (1992-1993) and post-fire conditions. Areas dominated by shrubs prior to the fire (tree cover < 40%) recovered to the same shrub cover conditions about 5 years after the fire, whereas it took two and more decades to reach pre-fire tree cover.

After twenty-six years, tree cover in previously tree dominated (> 40%) areas was higher than previously shrub dominated areas. However, tree cover was slightly below pre-fire conditions, indicating that tree-cover dominated areas were not fully recovered within the time window analysed. Further, the time it took to shift from shrub dominance to tree dominance depended on pre-fire cover and varied by study region. In the Yeste area, a shift to tree cover dominance took on average about 23 years in areas with previous tree cover of 41-60% and 15 years in areas with previous tree cover above 61%, whereas in the Requena region, a shift to tree dominance occurred around 10 years earlier in areas with pre-fire tree cover above 61%.

As a reference, the fraction cover time series of unburned areas were generally stable. However, some areas also showed a slight but steady increase in tree cover at the expense of background and shrub cover related to natural succession. Moreover, a common pattern is also observed in the evolution of tree cover, with a clear slight decrease coinciding with severe droughts in 1994-1995, 2005 and 2012.

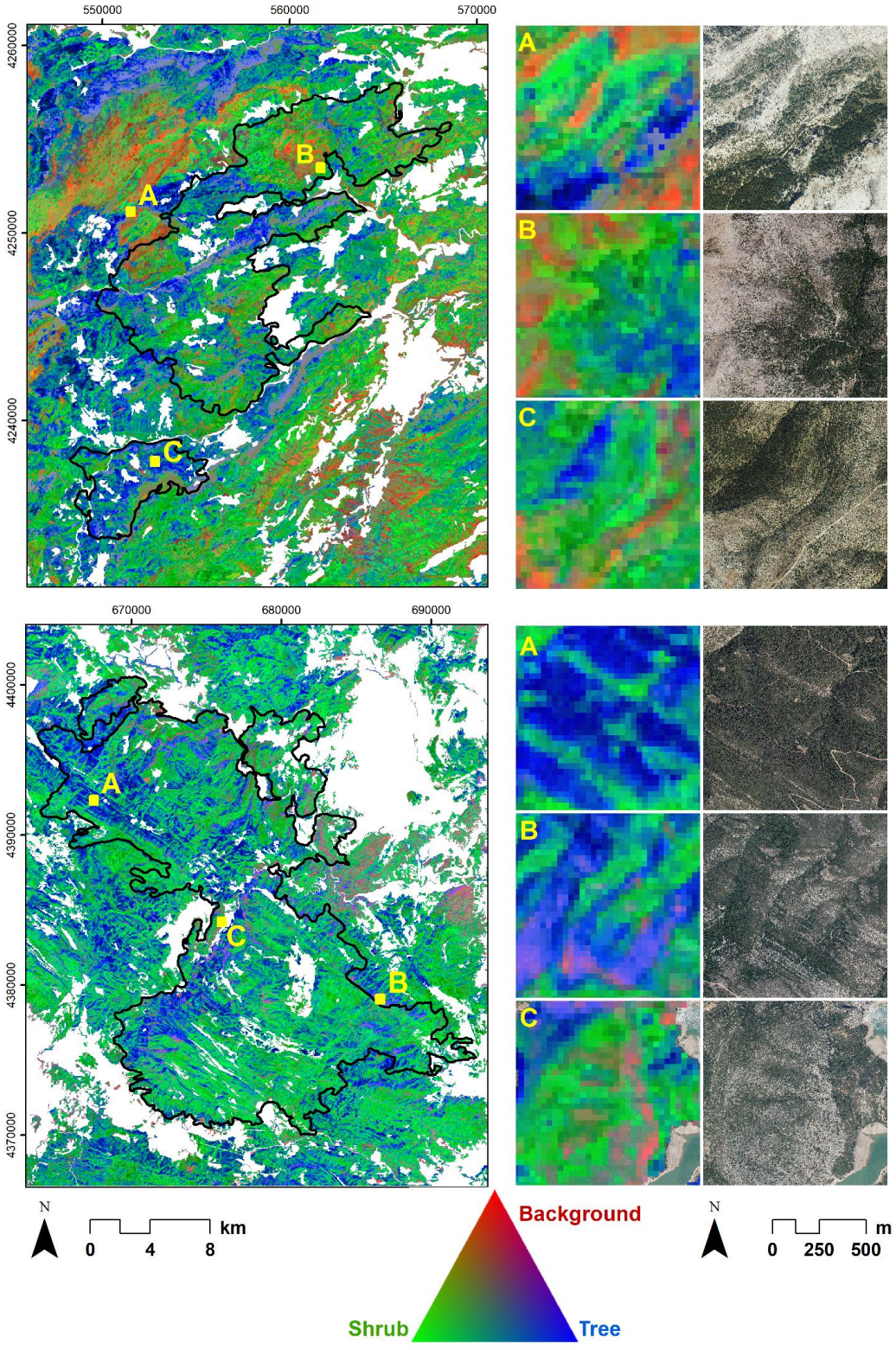

Figure 5.6. RGB composites illustrating cover fractions from 2020 for tree, shrub and background. Close-ups: high resolution orthophotos from National Plan of Orthophotography of Spain. White: Masked areas correspond to water, croplands and artificial surfaces.

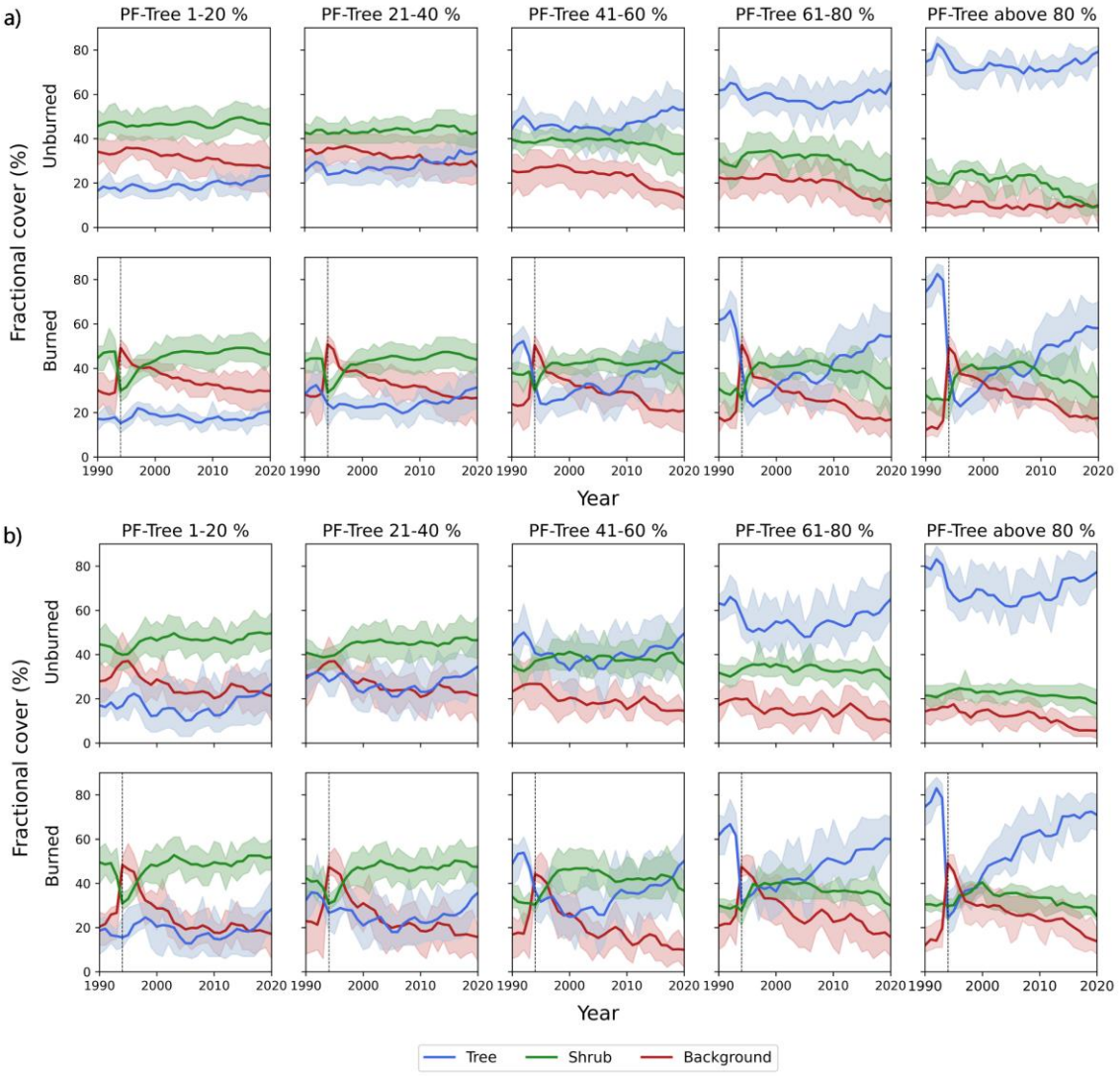

Figure 5.7. Annual time series of tree, shrub and background fractional cover from burned and unburned pixels for the Yeste area (a) and the Requena area (b). Shading indicates 25th and 75th percentiles. Vertical line indicates the year of the fire (1994). Time series are grouped according to pre-fire (PF) tree cover (mean tree cover fraction 1992-1993).

5.4.3. Quantifying shifts in tree and shrub cover in burned areas

Maps of the NDTSF for four selected years enhance the patterns of pre-fire and post-fire woody-vegetation cover proportions with regard to tree and shrub dominance (*Figure 5.8*). The composition of vegetation types was spatially heterogeneous before the fire showing a mixture of tree dominated areas (NDTSF > 0) and areas dominated by shrub (NDTSF < 0). In 1995, wildfires lead

to a relative homogenous composition with shrub dominance. Ten years after the fire (2004), the spatial recovery patterns start to resemble pre-fire conditions, whereas most of the tree dominated area has not reached pre-fire conditions, yet. The spatial patterns of the NDTSF in 2020 compare well to the pre-fire patterns in 1993, although there are also areas that still have less tree cover than before the fire.

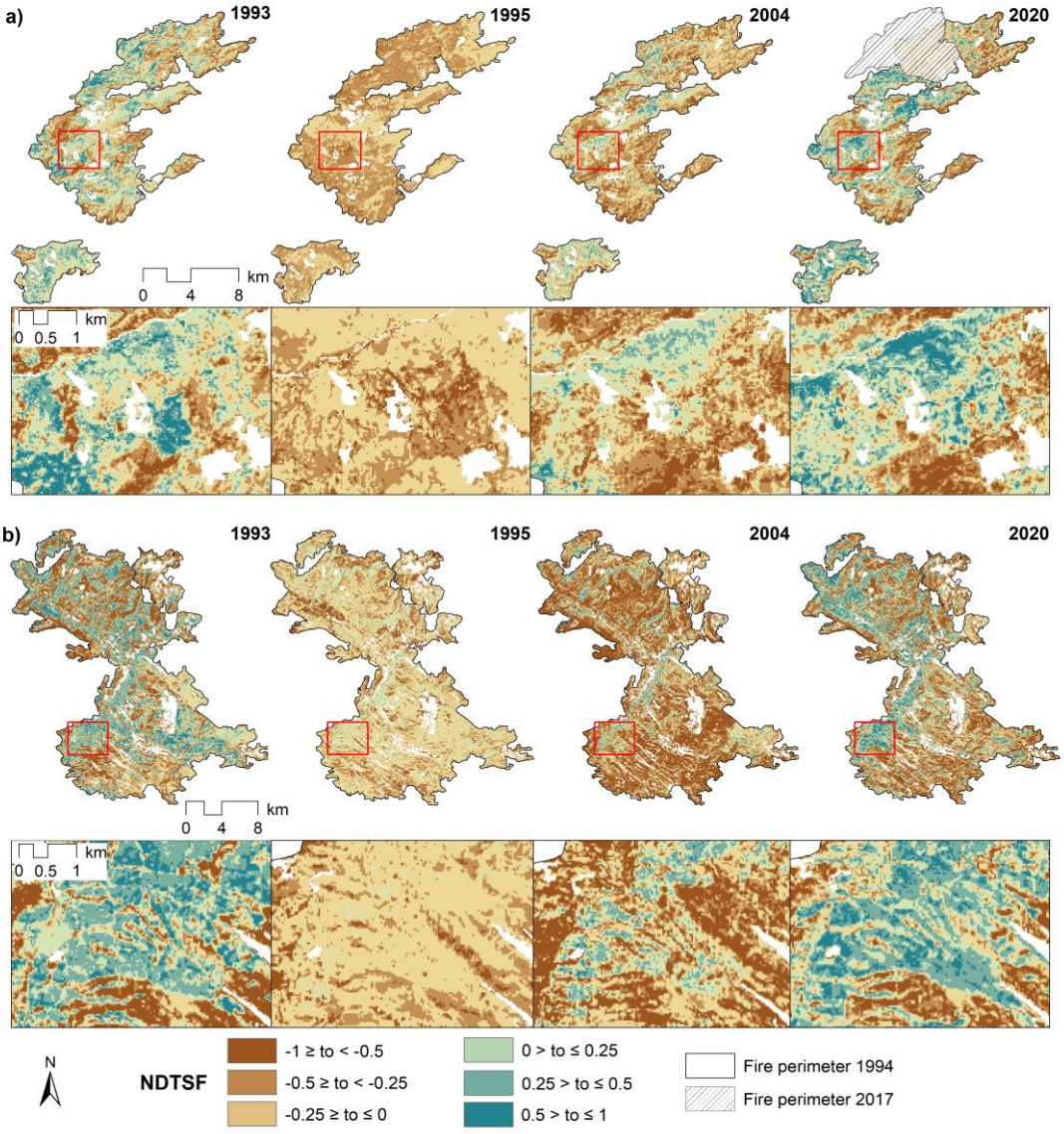

Figure 5.8. NDTSF for pre-fire (1993), 1 year post-fire (1995), 10 years post-fire (2004) and 2020 (26 years post-fire) for Yeste (a) and Requena (b). Masked areas correspond to water, croplands and artificial surfaces. Note that the area subjected to fire recurrence in Yeste in 2017 is masked in 2020.

Comparing the NDTSF maps from 2020 with the pre-fire situation, shifts in the cover dominance were found in 20% and 17.6% of the burned areas in Yeste and Requena, respectively (*Figure 5.9*). 12.3% and 15.4% of the pre-fire tree dominated areas shifted to shrub dominance 26 years after fire in Yeste and Requena, respectively, indicating a decline in the area of tree dominance (negative post-fire NDTSF trend, *Figure 5.10*). Shifts from shrub to tree dominance were 7.8% in Yeste and 4.2% in Requena, corresponding to mixed pixels with a similar proportion of trees and shrubs that display positive post-fire NDTSF trends (*Figure 5.10*). As a baseline, the rate of shift from tree to shrub dominance for unburned areas was 3.2% in Yeste and 5.5% in Requena, while areas shifting from shrub to tree dominance reached 20.1% and 19.4%, respectively. In contrast, 46.1% and 28% of the burned area maintain a dominance of tree cover (positive post-fire NDTSF trend) and 33.8% and 52.4% of the pre-fire shrub dominated areas remain with shrub dominance in the post-fire scenario, indicating a generalised tendency to the pre-fire composition throughout the burned areas in the long-term.

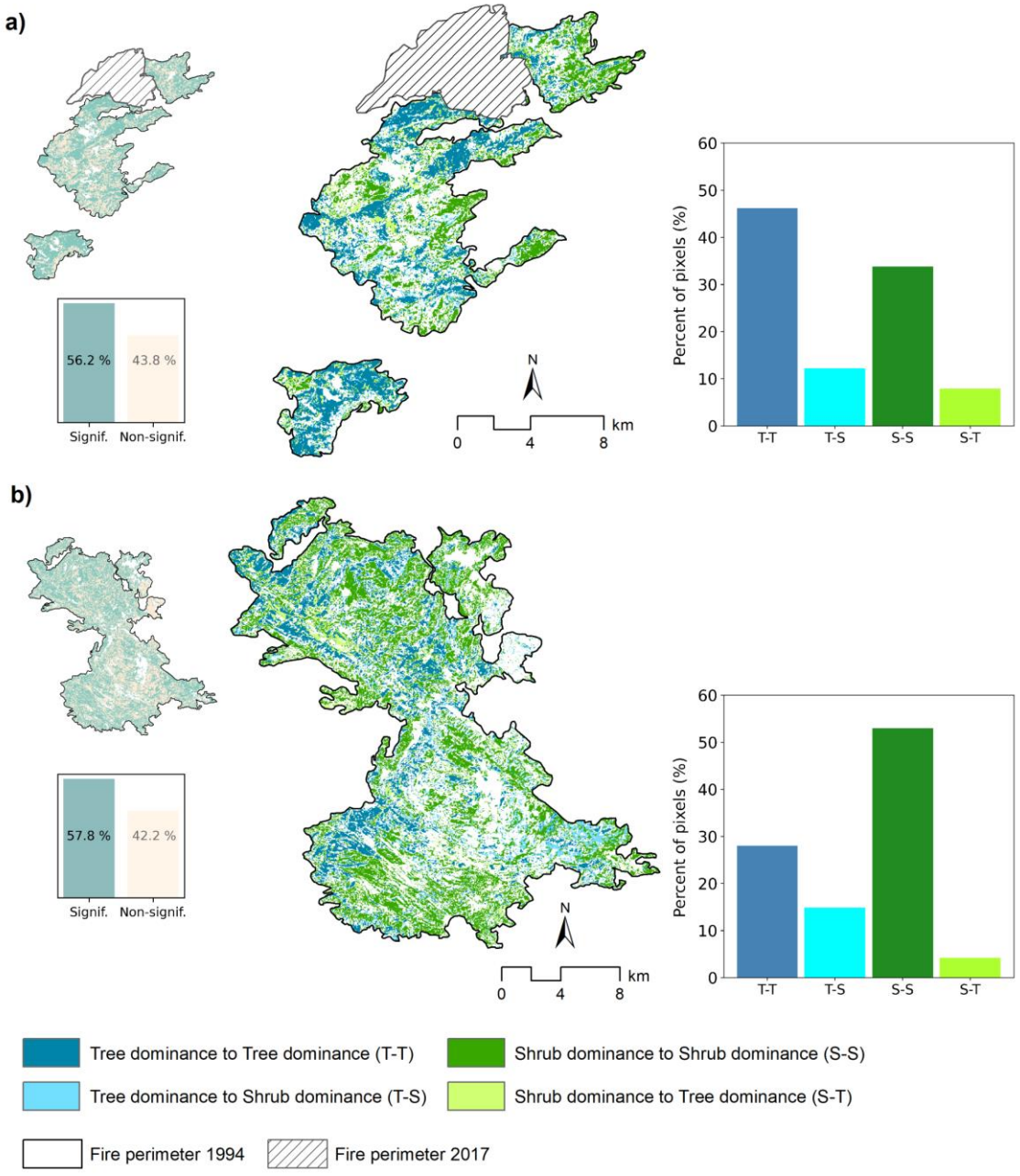

Figure 5.9. Shifts in tree and shrub cover dominance in 2020 compared to pre-fire for Yeste (a) and Requena (b). Only pixels exhibiting a significant trend are displayed on the maps and represented in the statistics.

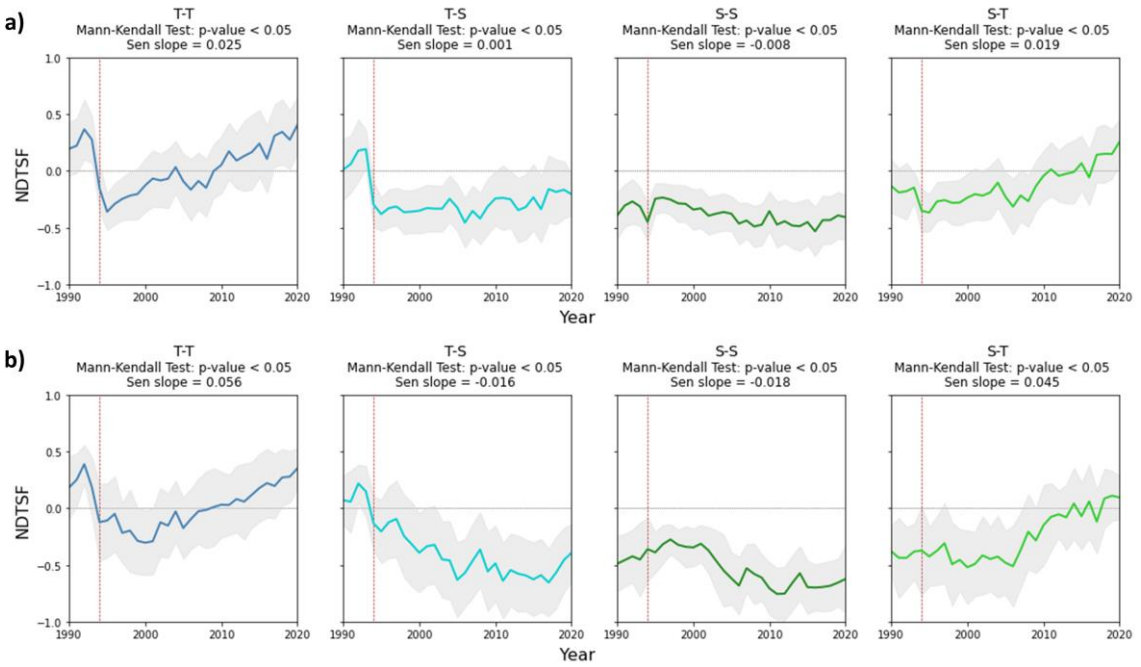

Figure 5.10. Annual time series of significant NDTSF according to Mann-Kendall test for the Yeste area (a) and the Requena area (b) grouped by category of change (T-T, T-S, S-S, and S-T). Shown are the mean and ± 1 standard deviation (grey ribbons). Vertical line indicates the year of the fire (1994). Horizontal line indicates the limit between tree dominance (NDTSF > 0) and shrub dominance (NDTSF < 0).

5.5. Discussion

5.5.1. Regression-based unmixing of annual Landsat STM

We retrieved a time series of tree, shrub and background (herbaceous-soil-rock) cover fractions for two burned areas from 30 years of annual Landsat STM. Model performances to predict cover fractions were overall high, as MAE remained stable and below 14% across the cover types and years, and for the two study sites. These results are in accordance with previous research showing that Landsat STM for a full year well suited for estimating different vegetation cover fractions (Okujeni et al., 2021). Visual inspection of fraction maps and validation plots indicated that the highest errors may stem from mixed pixels composed of young stands (recovering trees) and a well-developed shrub cover that are

difficult to distinguish in early recovery stages (Latifi et al., 2016; Martín-Alcón et al., 2015). Further errors such as the overestimations of tree and shrub indicated a confusion of these cover types due to the unsolvable spectral similarity among vegetation types even when incorporating the temporal information of multispectral data (Okujeni et al., 2021). This overestimation of shrub cover was also reported by previous studies in Mediterranean landscapes (Cooper et al., 2020) with MAE errors ranging from 8 to 20% that can be attributed to a confusion with background cover fractions (*Figure 5.6C*). Moreover, confusion in early regeneration stages may arise from changes in the spectral behaviour of tree stands in relation to age and crown shape (Nilson and Peterson, 1994; Rautiainen et al., 2004). Previous studies also suggested that there might be a tendency to overestimate cover fractions in pixels with low overall vegetation cover but this allocation remains unclear (Cooper et al., 2020; Senf et al., 2020). Despite these uncertainties, time-series of cover fractions well represented the temporal patterns of tree-shrub cover in our study sites. Although overall consistency was high, some slight declines in tree cover estimates were observed coinciding with dry years in the early 1990s, mid-2000s (2005, 2008) and 2012 in relation to the loss of water content leading to a higher reflectance in the SWIR and, therefore, higher similarity to shrub cover.

To our best knowledge, there are no studies focusing on regression-based unmixing approaches incorporating Landsat STM to differentiate annual tree and shrub cover fractions along the post-fire recovery process in Mediterranean forest ecosystems. SMA and MESMA methodologies were previously used to extract green vegetation together with non-photosynthetic, soil and ash cover types to assess burn severity (Fernández-Manso et al., 2016; Quintano et al., 2019) and short-term recovery of the green vegetation fraction (Fernández-Guisuraga et al., 2020; Kibler et al., 2019; Riaño et al., 2002; Veraverbeke et al., 2012). We here focused on differentiating woody-vegetation types, i.e. tree and shrub, from our background cover types, i.e. herbaceous, soil and rock, to provide a more detailed picture of the recovery process. Of the limited studies that used regression-based unmixing approaches in post-fire environments, Montorio et al.

(2020) demonstrated the value of a Random Forest Regression approach based on synthetic training data for quantifying fire severity by means of unitemporal fractional cover of green vegetation, non-photosynthetic vegetation, soil and ash. Our study should therefore be discussed in this context, providing an alternative approach that allows retrieving information on subpixel components of forest recovery attending to overstory evolution.

A crucial step in the unmixing procedure lies in the development of a representative spectral library (Somers et al., 2016). With regard to our strategy of developing an image STM library, finding suitable pure 30-m pixels with homogeneous cover for tree, shrub and background cover types was challenging. In highly heterogeneous landscapes such as Mediterranean forests, trees and shrubs are highly mixed (Guerschman et al., 2015; Hostert et al., 2003; Röder et al., 2008). We collected library STM from Landsat data with regard to homogeneity over time and in space, putting a lot of effort in representing pure cover. Incorporating LandTrendr-derived trajectory information prevented the high dependence on interpreting orthophotos alone by ensuring temporal stability of pure pixels based on a reproducible method. Still, in such open canopies the spectral signal of the purest pixels may still be laterally influenced by other cover types (Quintano et al., 2017; Suess et al., 2018). We consider this uncertainty as an acceptable limitation of our approach and acknowledge that may partially explain some of the observed errors. Further, temporally stable pixels for STM library development were spread all over each study site. Library STM for each class thus incorporate a wide range of spectral-temporal variability resulting from the intra-class spectral diversity, but also from the variations caused by phenology or illumination and shading of the canopy. Compared to other approaches (Fernández-Manso et al., 2016; Quintano et al., 2017), no explicit artificial shadow signature was therefore included into the library. In addition, it is important to mention that the synthetic training data created in this study was conceptualised to evaluate post-fire changes in tree-shrub cover over three decades, not to fire damage assessment. Thus, ash was also not included due to the short-lived nature of this cover (Quintano et al., 2017) and because its

signal can only be observed from days to a few months after a fire (Pérez-Cabello et al., 2012).

Our results show that the implementation of a workflow based on regression-based unmixing using synthetic mixing training data from annual Landsat STM enables the separation of spectrally similar woody-vegetation types, shrub and trees. Incorporating STM into unmixing has been previously shown to lead to accurate vegetation class fraction maps as they account for spectral-temporal variability from a full year that is not included using single-date imagery or best-available pixel composites (Okujeni et al., 2021). Based on a STM library with temporally stable spectral signatures, we here further demonstrate the great use of the same approach for retrieving annual time series of shrub, tree and background cover fractions from the Landsat archive for Mediterranean forest ecosystems, specifically related to post-fire ecosystem regeneration.

The potential of the regression-based unmixing with synthetic training datasets for mapping fractions at local, regional and national scales has been previously demonstrated (Okujeni et al., 2021; Schug et al., 2020; Senf et al., 2020; Suess et al., 2018). Particularly, large-scale mapping was made possible through the use of an image-based spectral library representative of the entire geographical area. Through embedding the unmixing approach into an ensemble framework, a high variability of different synthetic spectral mixtures from a large spectral library can be included using small-sized training sets (Okujeni et al., 2017). An extension of this work regarding large-area assessment of post-fire shifts in woody-vegetation cover using an extended image-based STM library therefore appears feasible. However, further research is required to better understand possibilities and limitations of model applications across larger areas and model transferability to other sites. Our study is based on a typical Mediterranean pine forest and we assume that our unmixing models will work in structurally and spectrally similar ecosystems. Extending the approach or transferring models to fire-prone ecosystems comprising different vegetation types and possibly also low numbers of clear sky observations, such as the tropical or boreal forests,

likely requires a further enhancement of the methodological approach. This particularly applies to the development of more generic spectral libraries representative of multiple biomes, and investigation on the possibilities and limitations to generalise unmixing models through space and time.

5.5.2. Post-fire recovery dynamics from fraction time-series

We evaluated forest recovery pertaining to the temporal evolution of tree and shrub cover fractions over three decades. We here considered recovery as an ongoing process, and therefore analyse if forest is trending toward its pre-fire composition of woody vegetation. Although measuring forest recovery is increasingly important to deal with the altered disturbance regimes caused by global change, assessing recovery is highly complex as it is an ongoing process that spans over decades (Bartels et al., 2016). Remote sensing-based studies commonly apply the engineering resilience definition, quantifying resilience as the time to return to the pre-fire state using a variety of indicators of forest characteristics (Nikinmaa et al., 2020). This study illustrates that time-series of different woody-vegetation cover fractions provides a means for an improved understanding of the post-fire forest recovery process.

Time-series of cover fractions well represented the spatial-temporal patterns of tree-shrub cover changes in our study sites (*Figures 5.6* and *5.7*). Pre-fire and post-fire cover proportions displayed common patterns over successional stages at both study sites. The increase in estimated background fractions immediately after the fire is related to the loss of woody vegetation and the emergence of soil and dead vegetation (De las Heras et al., 2012) followed by early-regrowing herbs (González-De Vega et al., 2018). Along the recovery process shifts in forest cover occurred at different times closely related to the pre-fire situation (*Figure 5.7*). Interactions between shrub species and pine establishment occur mostly during early recruitment processes (Calvo et al., 2008; Pausas and Keeley, 2014a). In those mixed pixels where shrubs intersperses with the tree (*Figure 5.7*), competition of cover dominance is well-visible during the first decade after fire

(Fernández-Guisuraga et al., 2022). Tree cover proportions gradually increase according to the progress from a stage of stand initiation to the stem exclusion (De las Heras et al., 2012), in which shrub dominance is replaced by greater tree dominance (in those pixels with pre-fire tree cover domain). However, tree cover was slightly below pre-fire conditions, indicating that tree-cover dominated areas were not yet fully recovered, as reported by Viana-Soto et al. (2022) from LiDAR estimations. In those pixels with pre-fire shrub cover dominance, shrubs also domain in the post-fire scenario, linked to their high resilience to fire by means of resprouting from fire-resistant structures and fire-protected seeds (Baudena et al., 2019; Santana et al., 2018).

Through the normalised ratio between tree and shrub (NDTSF) we emphasise how tree and shrub cover dominance evolve after fire. NDTSF well suited to capture those areas that remain treed-dominated or shrub-dominated in contrast to those areas that display a shift to more shrub dominance 26 years after fire (12.3-15.4%). Pre-fire composition explain the current situation (2020) since the same cover type prevails in 79-80% after 26 years (*Figure 5.9*). The Mann-Kendall test allowed us to extract significant trends over time for each type of change, illustrating positive trends in areas which recovered tree dominance and those which shifted from shrub to tree dominance. Negative trends in the NDTSF series correspond to areas that either lost the tree dominance, or those in which shrubs consolidates its dominance in the time series analysed (*Figure 5.10*).

Forest recovery hence depends on a combination of factors related to the fire severity (González-De Vega et al., 2016), pre-fire composition (Taboada et al., 2018), post-fire climatic conditions (Mazza and Sarris, 2021) and site characteristics (Rodríguez-García et al., 2022). According to our results, the spatial distribution of tree and shrub cover is highly controlled by topography, which may also be linked to soil conditions (Moya et al., 2018). Previous research also indicated that frequent fires and high fire severities can induce changes in woody vegetation composition, favouring the development of fast-growing resprouter shrubs (Fernández-García et al., 2019; Taboada et al., 2018) which

compete with pines for space (Pausas and Keeley, 2014a). Recovery patterns associated with tree and shrub cover show high spatial heterogeneity, requiring further analysis to better understand the factors driving recovery dynamics. Nonetheless, it is noticeable that 26 years after fire a considerable proportion of the burned area is undergoing recovery towards its pre-fire state and some sectors show signs of vegetation transition as the dominant cover is shifting from tree to shrub 26 years after the fire (*Figure 5.9*). In line with these findings, Baeza et al. (2007) reported a low pine resilience 23 years after fire and a clear domain of successional shrublands in the Mediterranean basin in Spain. Recent studies from other Mediterranean regions around the world also investigated this transition from tree dominance to fire-prone shrubs, e.g., California (Tubbesing et al., 2020), Patagonia (Paritsis et al., 2015) and Australia (Nolan et al., 2021), suggesting that resprouting species are likely to be more resilient under changing fire regimes (Karavani et al., 2018). However, considering the time period analysed here we cannot determine whether the shrub dominance found constitutes a successional stage or will prevail and consolidate in a mature stage. Therefore, a broadening of the timeframe and expanding this analysis to other areas will be required to get a clearer picture of the recovery process in later successional stages.

In areas undergoing recovery, recurrent fires may jeopardise the recovery process affecting the success of pine re-establishment (González-De Vega et al., 2016; Taboada et al., 2018). Fire may induce changes in vegetation composition and structure since maturity (structurally and functionally) is estimated to require at least 20–30 years in pine forests (Trabaud, 1994; Vega et al., 2011). In line with this, ecosystem diversity can be negatively affected as a result of the immaturity risk of species under recovery processes (González-De Vega et al., 2018). We did not attempt here to differentiate tree species, which may also occur, e.g. regarding fire-induced change in relation to oak thriving (*Quercus ilex* L.), a shade-tolerant that resprouts vigorously after fire (Zavala et al., 2000). Further research may address estimating of tree species-related cover fractions,

for example by combining LiDAR data and unmixing from multispectral imagery to help in determining the composition of post-fire communities.

5.6. Conclusion

Mapping changes in vegetation cover types after fire is crucial to better understand forest resilience to fire. In this study, we addressed the characterization of changes in tree and shrub cover in large burned areas in Spain using Landsat imagery and a regression-based unmixing approach. Our study thereby contributes to the research on post-fire forest recovery using remote sensing data. This approach includes (i) the retrieval of woody-vegetation cover fractions over three decades using synthetically mixed training data from Landsat STMs, and (ii) the quantification of post-fire shifts in cover dominance through the NDTSF. According to our findings, the combination of synthetically mixed training data from Landsat-based STM as input for an SVR model was very well-suited to disentangling tree and shrub cover dynamics in Mediterranean forests. For the first time, we provide spatio-temporally explicit, multi-decadal information on forest composition recovery in a post-fire environment, ultimately allowing to identify shifts in cover dominance. Maps and time series of cover fractions revealed different succession dynamics in relation to pre-fire conditions. Annual maps of NDTSF highlighted areas that shifted from tree to shrub cover dominance after 26 years whereas the majority of the burned areas tend to the pre-fire composition. Our results emphasise the utility of regression-based unmixing from Landsat to provide meaningful information on post-fire forest composition to design forest management that enhance fire resilience under environmental changing conditions.

5.7. Acknowledgments

A.V.S. is supported by the Spanish Ministry of Science, Innovation and Universities through a FPU doctoral fellowship (FPU17/03260) and a research stay fellowship (EST19/00215). This research contributes to the Landsat Science

Team 2018-2023 (https://www.usgs.gov/landsat-missions/2018-2023-landsat-science-team). We thank four anonymous reviewers for their constructive comments to improve the manuscript. We thank David Frantz for his inputs on FORCE processing.

Author contribution

Alba Viana-Soto: Conceptualization, Methodology, Validation, Formal analysis, Investigation, Data curation, Writing - original draft. Akpona Okujeni: Conceptualization, Methodology, Investigation, Writing – review & editing. Dirk Pflugmacher: Methodology, Investigation, Data curation, Writing - review & editing. Mariano García: Validation, Investigation, Writing – review & editing. Inmaculada Aguado: Investigation, Writing – review & editing. Patrick Hostert: Conceptualization, Methodology, Investigation, Writing – review & editing.

Chapter 6. Synthesis

6.1. Summary of key findings

This thesis advances in the understanding of post-fire forest recovery dynamics using remotely sensed data from active and passive sensors. Firstly, Paper I (Chapter 3) disentangles post-fire recovery trajectories from Landsat time series and provides insights on the influence of environmental and contextual factors on the recovery rates. Then, Paper II (Chapter 4) addresses the integration of LiDAR data and Landsat imagery to characterise changes in forest structure along the recovery process. Lastly, Paper III (Chapter 5) presents a novel approach to unravel shifts in post-fire forest cover composition from unmixing Landsat data. Therefore, this thesis investigates forest recovery from three perspectives: spectral (Paper I), structural (Paper II) and compositional (Paper III). Below, the main results are summarised in reference to the hypothesis and objectives presented in Chapter 2.

First, **Paper I** identified post-fire recovery trajectories from Landsat time series using the LandTrendr segmentation algorithm, thereby accounting for **spectral recovery**. Different categories of recovery trajectories were distinguished underlying slow but more stable recovery processes (continuous recovery) compared to other faster but interrupted recovery processes (continuous recovery with slope changes, continuous recovery stabilised, and non-continuous recovery). Our findings showed that recovery rates vary not only in space and time, but also depending on the Tasseled Cap component used. Trajectories derived from the Wetness component, which is related to forest structure, were much more gradual, whereas trajectories extracted from the Angle metric, which is more linked to vegetation cover, tended to saturate quickly after fire. As fire-prone ecosystems, vegetation quickly colonised the space after fire by displaying higher recovery rates in the short-term, but this does not imply the recovery to the pre-fire forests conditions two decades after fire.

Second, the appraisal of **factors driving the recovery** at successional stages revealed that fire severity strongly influenced short-term recovery rates, but post-fire climate in relation to drought further explained recovery rates in the medium

and long term. Pre-fire conditions mainly contributed to explain the recovery rates in the first stage. Despite showing less influence, site conditions represented by topographic variables such as elevation or aspect also contributed to explain the recovery rates. Although we found that post-fire climate was the most important variable in explaining post-fir recovery in the mid and long-term, other variables related to forest management, disturbance legacies or soil conditions may be affecting the recovery rates.

Third, the integration of LiDAR data and Landsat imagery in **Paper II** enabled an accurate quantification of forest **structural recovery** over three decades. Model performances to estimate LiDAR-derived structural variables (Vegetation Cover, Tree Cover, Mean Height and heterogeneity) using Landsat images was high, showing stability of the estimations both temporal and spatially. Time-series of structural metrics revealed differences in cover and height recovery. Although vegetation cover recovered pre-fire conditions within the 26 years post-fire, Mean height and Tree cover did not reach the pre-fire benchmark. Overall, less than 50% of burned pixels completely recovered to a pre-fire structure 26 years after fire, suggesting an ongoing recovery process and moderate resilience of the analysed Mediterranean pine forests.

Finally, **Paper III** provided insights on how woody-vegetation (tree and shrub) cover composition shift over time using a regression-based unmixing approach from Landsat Spectral Temporal Metrics (STM). Encouraged by recent studies on fire ecology suggesting possible shifts from Mediterranean pine forests to shrub-dominated ecosystems, we yielded spatio-temporally explicit information on post-fire forest **compositional recovery** in Mediterranean burned areas. Our findings suggest that successional dynamics of tree and shrub strongly depended on pre-fire conditions since the majority of the burned areas tended to the pre-fire composition. However, areas shifting from tree to shrub dominance were found 26 years after fire, indicating ongoing transitions that may constitute a successional stage or would prevail in a mature stage. Our results emphasise the utility of combining synthetically mixed data from Landsat STM as input for SVR

models to disentangling tree and shrub cover dynamics, which is of major concern for supporting management strategies that aim to leading fire-prone Mediterranean forests toward more resilient ecosystems.

6.2. Limitations and outlook

Forest recovery is a dynamic process that span different spatial and temporal scales. Forest recovery after a fire event takes several decades, and therefore requires a temporal perspective for a comprehensive evaluation of the recovery at successional stages (Bartels et al., 2016). One of the limitations for analysing recovery is the time period for which data are available. This limitation can be partially overcome using long time series of Landsat imagery to provide spatially-explicit baseline information concerning spectral recovery (Kennedy et al., 2014), as we demonstrated in **Paper I**. We analysed post-fire forest recovery at Mediterranean areas burned in the 1990s, thus obtaining retrospective information on the pre-fire forest conditions and almost 25 years of data after fire. Spectral trajectories derived from temporal segmentation of Landsat time series are a good proxy to monitor multiple aspects of forest recovery, such as the impact of fire disturbance and the return of vegetation (Frazier et al., 2015; Hislop et al., 2019; Pickell et al., 2016; Röder et al., 2008; Shvetsov et al., 2019). However, limitations of spectral recovery measures in relation to signal saturation at closed canopies mean that spectral recovery rates are frequently faster than the actual recovery of ecosystem structure and composition (Pérez-Cabello et al., 2021).

Beyond the analysis of the spectral recovery, we advanced in the study of post-fire structural recovery (**Paper II**). Data fusion of LiDAR and Landsat imagery provided a means to estimate changes on forest structure along the recovery process. The major challenge in this regard lies in adequately calibrate a model that enables the extrapolation of LiDAR-derived metrics in space and time (Coops et al., 2021). LiDAR data used herein from two different dates allowed to calibrate and independently validate estimations of forest structure, ensuring the good

performance of the extrapolation procedure. However, LiDAR data were acquired at low densities (< 1pt/m^2), therefore a higher density as well as a third coverage would allow developing more robust models. In addition to the aforementioned limitations for predicting forest structure regarding optical data saturation in closed canopies (García et al., 2018), difficulties arise when attempting to map forest attributes at large scales (Matasci et al., 2018; Potapov et al., 2021; White et al., 2022). Achieving stability of estimates between Landsat sensors and under different environmental conditions is crucial to further extend the estimations presented in this thesis. Future efforts would investigate scaling-up methods for large scale estimation of recovery rates in Mediterranean ecosystems.

Recovery assessment in terms of forest compositional changes has been limited primarily to studies based on plot-based measurements collected at specific times and spatially limited (González-De Vega et al., 2018; Santana et al., 2014; Tubbesing et al., 2020). As presented in **Paper III**, this limitation can be partially overcome with the implementation of a regression-based unmixing approach using spectral-temporal information from Landsat imagery. We further explored changes in woody-vegetation cover composition at the sub-pixel level over three decades, thus opening the opportunity for larger area characterization. As a first attempt of application, we addressed the estimation of fire-induced changes in cover dominance between tree and shrub that intensely compete and strongly determine long-term forest composition (De las Heras et al., 2012). We acknowledge that fire-induced changes in tree species composition may also occur in Mediterranean ecosystems, such as oak thriving in post-fire plant communities (Vasques et al., 2022). Therefore, forthcoming research should delve into the estimation of species composition while keeping the broad scope of application in larger areas.

In addition to the mentioned challenges arising from each research paper in this thesis, open questions and opportunities for the future also remain to bridge the remote sensing, ecology and forest management fields. Recovery processes depend on several factors that span from pre-fire conditions, e.g. legacy effects

of land use, impacts of fire disturbance and recurrence effects, ecosystem adaptive traits, environmental and site conditions to post-fire interventions. Bringing together the influence of all these factors with the spatial driving factors analysed in this thesis is an outstanding future challenge.

6.3. Relevance and impact for post-fire recovery management

With increasing awareness about forest resilience under changing fire regimes and climate conditions (Anderson-Teixeira et al., 2013; Forzieri et al., 2022), remote sensing has come into the spotlight as a powerful source of information that is well suited to monitoring forest recovery. Although the research in this thesis is focused on the post-fire recovery of Mediterranean forests in Spain, it has a broader relevance to the scientific community with its contribution to advancing the analysis of the recovery from three perspectives using both open and free available data and software.

In this thesis we developed remote sensing-based methods for estimating post-fire recovery rates. This baseline enables to assess the evolution of post-fire recovery and can be used to highlight areas where recovery may be slower or faster than expected. This information is crucial for an efficient planning of post-fire interventions, considering that areas undergoing slower recovery are likely to be more vulnerable (Keeley and Pausas, 2022; Nolan et al., 2021) in the face of fire recurrence and the outbreak of other disturbances (Doblas-Miranda et al., 2017).

Post-fire restoration strategies mainly focus on immediate management actions, e.g. mulching, salvage logging, erosion barriers, and planting (Castro, 2021). Yet these actions might also undermine natural regeneration by negatively affecting seedlings and sprout processes and nutrient cycling (Fernández et al., 2019; Leverkus et al., 2020). There is no simple solution to decide on the best post-fire management option (Coll et al., 2021), but restoration should focus on enhancing the ecosystem elements that accelerate forest recovery, considering not only

costs and benefits, but also socio-ecological implications in the context of ecosystem services.

Expected changes in environmental conditions (IPCC, 2018) would have serious impacts upon Mediterranean ecosystems (Pausas and Fernández-Muñoz, 2012; Turco et al., 2018) and their resilience capacity (Keeley and Pausas, 2022; Nolan et al., 2021). Measurable definitions of recovery should be provided for adapting forest management to better cope with climate change and facilitate decision-makers the selection of management alternatives (Vallejo et al., 2012). Nevertheless, to date there is no common agreement on how resilience should be defined (Nikinmaa et al., 2020) or applied in the context of forestry and remote sensing, which is an important gap for defining policy interventions. Further, accurate and spatially explicit information on past post-fire management across burned areas is either lacking or constrained to research sites. Nonetheless, the possibility to systematically assess post-fire recovery over large areas, as illustrated in this thesis, constitutes a first step toward designing mitigation and adaptation strategies to enhance forest recovery.

Chapter 7. References

Adams, J.B., Smith, M.O., Johnson, P.E., 1986. Correction [to “Spectral mixture modeling: A new analysis of rock and soil types at the Viking Lander 1 site” by John B. Adams, Milton O. Smith, and Paul E. Johnson]. J. Geophys. Res. 91, 10513. https://doi.org/10.1029/jb091ib10p10513

Ahmed, O.S., Franklin, S.E., Wulder, M.A., 2014. Integration of lidar and Landsat data to estimate forest canopy cover in coastal British Columbia. Photogramm. Eng. Remote Sensing 80, 953–962. https://doi.org/10.14358/PERS.80.10.953

Ahmed, O.S., Franklin, S.E., Wulder, M.A., White, J.C., 2015. Characterizing stand-level forest canopy cover and height using Landsat time series, samples of airborne LiDAR, and the Random Forest algorithm. ISPRS J. Photogramm. Remote Sens. 101, 89–101. https://doi.org/10.1016/j.isprsjprs.2014.11.007

Airbus Defence and Space, 2020. Copernicus DEM (Digital Elevation Model) Product Handbook.

Anderson-Teixeira, K.J., Miller, A.D., Mohan, J.E., Hudiburg, T.W., Duval, B.D., DeLucia, E.H., 2013. Altered dynamics of forest recovery under a changing climate. Glob. Chang. Biol. 19, 2001–2021. https://doi.org/10.1111/gcb.12194

Aponte, C., de Groot, W.J., Wotton, M., 2016. Forest fires and climate change: causes, consequences and management options. Int. J. Wildl. Fire 25, 861–875. https://doi.org/10.1071/WFv25n8_FO

Archibald, S., Lehmann, C.E.R., Belcher, C.M., Bond, W.J., Bradstock, R.A., Daniau, A.L., Dexter, K.G., Forrestel, E.J., Greve, M., He, T., Higgins, S.I., Hoffmann, W.A., Lamont, B.B., McGlinn, D.J., Moncrieff, G.R., Osborne, C.P., Pausas, J.G., Price, O., Ripley, B.S., Rogers, B.M., Schwilk, D.W., Simon, M.F., Turetsky, M.R., Van Der Werf, G.R., Zanne, A.E., 2018. Biological and geophysical feedbacks with fire in the Earth system. Environ. Res. Lett. 13. https://doi.org/10.1088/1748-9326/aa9ead

Awad, M., Khanna, R., 2015. Support Vector Regression, in: Efficient Learning Machines. Apress, Berkeley, CA, pp. 67–80. https://doi.org/https://doi.org/10.1007/978-1-4302-5990-9_4

Baeza, M.J., Valdecantos, A., Alloza, J.A., Vallejo, V.R., 2007. Human disturbance and environmental factors as drivers of long-term post-fire regeneration patterns in Mediterranean forests. J. Veg. Sci. 18, 243–252. https://doi.org/10.1111/j.1654-1103.2007.tb02535.x

Baig, M.H.A., Zhang, L., Shuai, T., Tong, Q., 2014. Derivation of a tasselled cap transformation based on Landsat 8 at-satellite reflectance. Remote Sens. Lett. 5, 423–431. https://doi.org/10.1080/2150704X.2014.915434

Banskota, A., Kayastha, N., Falkowski, M.J., Wulder, M.A., Froese, R.E., White, J.C., 2014. Forest monitoring using Landsat time series data: a review. Can. J. Remote Sens. 40. https://doi.org/10.1080/07038992.2014.987376.

Bartels, S.F., Chen, H.Y.H., Wulder, M.A., White, J.C., 2016. Trends in post-disturbance recovery rates of Canada’s forests following wildfire and harvest. For. Ecol. Manage. 361, 194–207. https://doi.org/10.1016/j.foreco.2015.11.015

Bastarrika, A., Alvarado, M., Artano, K., Martinez, M.P., Mesanza, A., Torre, L., Ramo, R., Chuvieco, E., 2014. BAMS: A tool for supervised burned area mapping using landsat data. Remote Sens. 6, 12360–12380. https://doi.org/10.3390/rs61212360

Baudena, M., Santana, V.M., Baeza, M.J., Bautista, S., Eppinga, M.B., Hemerik, L., Garcia Mayor, A., Rodriguez, F., Valdecantos, A., Vallejo, V.R., Vasques, A., Rietkerk, M., 2019. Increased aridity drives post- fire recovery of Mediterranean forests towards open shrublands, New Phytologist. https://doi.org/10.1111/nph.16252

Baumann, M., Levers, C., Macchi, L., Bluhm, H., Waske, B., Gasparri, N.I., Kuemmerle, T., 2018. Mapping continuous fields of tree and shrub cover across the Gran Chaco using Landsat 8 and Sentinel-1 data. Remote Sens. Environ. 216, 201–211. https://doi.org/10.1016/j.rse.2018.06.044

Berger, M., Moreno, J., Johannessen, J.A., Levelt, P.F., Hanssen, R.F., 2012. ESA's sentinel missions in support of Earth system science. Remote Sens. Environ. 120, 84–90. https://doi.org/10.1016/j.rse.2011.07.023

Bolton, D.K., Coops, N.C., Wulder, M.A., 2015. Characterizing residual structure and forest recovery following high-severity fire in the western boreal of Canada using Landsat time-series and airborne lidar data. Remote Sens. Environ. 163, 48–60. https://doi.org/10.1016/j.rse.2015.03.004

Bottalico, F., Chirici, G., Giannini, R., Mele, S., Mura, M., Puxeddu, M., McRoberts, R.E., Valbuena, R., Travaglini, D., 2017. Modeling Mediterranean forest structure using airborne laser scanning data. Int. J. Appl. Earth Obs. Geoinf. 57, 145–153. https://doi.org/10.1016/j.jag.2016.12.013

Bowman, D.M.J.S., Balch, J.K., Artaxo, P., Bond, W.J., Carlson, J.M., Cochrane, M.A., D'Antonio, C.M., DeFries, R.S., Doyle, J.C., Harrison, S.P., Johnston, F.H., Keeley, J.E., Krawchuk, M.A., Kull, C.A., Marston, J.B., Moritz, M.A., Prentice, I.C., Roos, C.I., Scott, A.C., Swetnam, T.W., Van Der Werf, G.R., Pyne, S.J., 2009. Fire in the earth system. Science (80-.). 324, 481–484. https://doi.org/10.1126/science.1163886

Bowman, D.M.J.S., Kolden, C.A., Abatzoglou, J.T., Johnston, F.H., van der Werf, G.R., Flannigan, M., 2020. Vegetation fires in the Anthropocene. Nat. Rev. Earth Environ. 1, 500–515. https://doi.org/10.1038/s43017-020-0085-3

Bowman, D.M.J.S., Williamson, G.J., Abatzoglou, J.T., Kolden, C.A., Cochrane, M.A., Smith, A.M.S., 2017. Human exposure and sensitivity to globally extreme wildfire events. Nat. Ecol. Evol. 1, 1–6. https://doi.org/10.1038/s41559-016-0058

Braaten, J.D., Cohen, W.B., Yang, Z., 2017. LandsatLinkr. Zenodo. https://doi.org/10.5281/zenodo.807733

Bright, B.C., Hudak, A.T., Kennedy, R.E., Braaten, J.D., Henareh Khalyani, A., 2019. Examining post-fire vegetation recovery with Landsat time series analysis in three western North American forest types. Fire Ecol. 15. https://doi.org/10.1186/s42408-018-0021-9

Brunsdon, C., Fotheringham, A.S., Charlton, M.E., 2010. Geographically Weighted Regression: A Method for Exploring Spatial Nonstationarity. Geogr. Anal. 28, 281–298. https://doi.org/10.1111/j.1538-4632.1996.tb00936.x

Bullock, E.L., Woodcock, C.E., Olofsson, P., 2020. Monitoring tropical forest degradation using spectral unmixing and Landsat time series analysis. Remote Sens. Environ. 238, 0–1. https://doi.org/10.1016/j.rse.2018.11.011

Calvo, L., Santalla, S., Valbuena, L., Marcos, E., Tárrega, R., Luis-Calabuig, E., 2008. Post-fire natural regeneration of a Pinus pinaster forest in NW Spain. Plant Ecol.

197, 81–90. https://doi.org/10.1007/s11258-007-9362-1

Castro, J., 2021. Post-fire Restoration of Mediterranean Pine Forests BT - Pines and Their Mixed Forest Ecosystems in the Mediterranean Basin, in: Ne'eman, G., Osem, Y. (Eds.), . Springer International Publishing, Cham, pp. 537–565. https://doi.org/10.1007/978-3-030-63625-8_25

Chance, C.M., Hermosilla, T., Coops, N.C., Wulder, M.A., White, J.C., 2016. Effect of topographic correction on forest change detection using spectral trend analysis of Landsat pixel-based composites. Int. J. Appl. Earth Obs. Geoinf. 44, 186–194. https://doi.org/10.1016/j.jag.2015.09.003

Chu, T., Guo, X., 2013. Remote sensing techniques in monitoring post-fire effects and patterns of forest recovery in boreal forest regions: A review. Remote Sens. 6, 470–520. https://doi.org/10.3390/rs6010470

Chu, T., Guo, X., Takeda, K., 2017. Effects of burn severity and environmental conditions on post-fire regeneration in Siberian Larch forest. Forests 8, 1–27. https://doi.org/10.3390/f8030076

Chuvieco, E., 2016. Fundamentals of Satellite Remote Sensing. An Environmental Approach, Second Edition. CRC Press. https://doi.org/https://doi.org/10.1201/b19478

Chuvieco, E., 2009. Global Impacts of Fire, in: Chuvieco, E. (Ed.), Earth Observation of Wildland Fires in Mediterranean Ecosystems. Springer Berlin Heidelberg, pp. 1–10. https://doi.org/10.1007/978-3-642-01754-4

Chuvieco, E., Aguado, I., Salas, J., García, M., Yebra, M., Oliva, P., 2020. Satellite Remote Sensing Contributions to Wildland Fire Science and Management. Curr. For. Reports 6, 81–96. https://doi.org/10.1007/s40725-020-00116-5

Cohen, W.B., Yang, Z., Kennedy, R., 2010. Detecting trends in forest disturbance and recovery using yearly Landsat time series: 2. TimeSync - Tools for calibration and validation. Remote Sens. Environ. 114, 2911–2924. https://doi.org/10.1016/j.rse.2010.07.010

Coll, L., Ameztegui, A., Calama, R., Lucas-Borja, M.E., 2021. Dynamics and Management of Western Mediterranean Pinewoods 659–677. https://doi.org/10.1007/978-3-030-63625-8_31

Congalton, R.G., Green, K., 1999. Assessing the Accuracy of Remotely Sensed Data: Principles and Practices. Boca Raton: Lewis Publishers.

Cooper, S., Okujeni, A., Jänicke, C., Clark, M., van der Linden, S., Hostert, P., 2020. Disentangling fractional vegetation cover: Regression-based unmixing of simulated spaceborne imaging spectroscopy data. Remote Sens. Environ. 246, 111856. https://doi.org/10.1016/j.rse.2020.111856

Coops, N.C., Tompalski, P., Goodbody, T.R.H., Queinnec, M., Luther, J.E., Bolton, D.K., White, J.C., Wulder, M.A., van Lier, O.R., Hermosilla, T., 2021. Modelling lidar-derived estimates of forest attributes over space and time: A review of approaches and future trends. Remote Sens. Environ. 260, 112477. https://doi.org/10.1016/j.rse.2021.112477

Crist, E.P., 1985. A TM Tasseled Cap equivalent transformation for reflectance factor data. Remote Sens. Environ. 17, 301–306. https://doi.org/10.1016/0034-4257(85)90102-6

Crotteau, J.S., Morgan Varner, J., Ritchie, M.W., 2013. Post-fire regeneration across a fire severity gradient in the southern Cascades. For. Ecol. Manage. 287, 103–112. https://doi.org/10.1016/j.foreco.2012.09.022

De las Heras, J., Moya, D., Vega, J.A., Daskalakou, E., Vallejo, R., Grigoriadis, N., Tsitsoni, T., Baeza, J., Valdecantos, A., Fernández, C., Espelta, J., Fernandes, P., 2012. Post-Fire Management of Serotinous Pine Forests, in: Moreira, F., Arianoutsou, M., Corona, P., de las Heras, J. (Eds.), Post-Fire Management and Restoration of Southern European Forests. Springer, pp. 121–149. https://doi.org/10.1007/978-94-007-2208-8_6

DeVries, B., Decuyper, M., Verbesselt, J., Zeileis, A., Herold, M., Joseph, S., 2015. Tracking disturbance-regrowth dynamics in tropical forests using structural change detection and Landsat time series. Remote Sens. Environ. 169, 320–334. https://doi.org/10.1016/j.rse.2015.08.020

Doblas-Miranda, E., Alonso, R., Arnan, X., Bermejo, V., Brotons, L., de las Heras, J., Estiarte, M., Hódar, J.A., Llorens, P., Lloret, F., López-Serrano, F.R., Martínez-Vilalta, J., Moya, D., Peñuelas, J., Pino, J., Rodrigo, A., Roura-Pascual, N., Valladares, F., Vilà, M., Zamora, R., Retana, J., 2017. A review of the combination among global change factors in forests, shrublands and pastures of the Mediterranean Region: Beyond drought effects. Glob. Planet. Change 148, 42–54. https://doi.org/10.1016/j.gloplacha.2016.11.012

Duane, M. V., Cohen, W.B., Campbell, J.L., Hudiburg, T., Turner, D.P., Weyermann, D.L., 2010. Implications of alternative field-sampling designs on landsat-based mapping of stand age and carbon stocks in Oregon forests. For. Sci. 56, 405–416. https://doi.org/10.1093/forestscience/56.4.405

Dubayah, R., Blair, J.B., Goetz, S., Fatoyinbo, L., Hansen, M., Healey, S., Hofton, M., Hurtt, G., Kellner, J., Luthcke, S., Armston, J., Tang, H., Duncanson, L., Hancock, S., Jantz, P., Marselis, S., Patterson, P.L., Qi, W., Silva, C., 2020. The Global Ecosystem Dynamics Investigation: High-resolution laser ranging of the Earth's forests and topography. Sci. Remote Sens. 1, 100002. https://doi.org/10.1016/j.srs.2020.100002

Escuin, S., Navarro, R., Fernández, P., 2008. Fire severity assessment by using NBR (Normalized Burn Ratio) and NDVI (Normalized Difference Vegetation Index) derived from LANDSAT TM/ETM images. Int. J. Remote Sens. 29, 1053–1073. https://doi.org/10.1080/01431160701281072

Eugenio, M., Verkaik, I., Lloret, F., Espelta, J.M., 2006. Recruitment and growth decline in Pinus halepensis populations after recurrent wildfires in Catalonia (NE Iberian Peninsula). For. Ecol. Manage. 231, 47–54. https://doi.org/10.1016/j.foreco.2006.05.007

Fahey, T.J., Woodbury, P.B., Battles, J.J., Goodale, C.L., Hamburg, S.P., Ollinger, S. V., Woodall, C.W., 2010. Forest carbon storage: Ecology, management, and policy. Front. Ecol. Environ. 8, 245–252. https://doi.org/10.1890/080169

Falkowski, M.J., Evans, J.S., Martinuzzi, S., Gessler, P.E., Hudak, A.T., 2009. Characterizing forest succession with lidar data: An evaluation for the Inland Northwest, USA. Remote Sens. Environ. 113, 946–956. https://doi.org/10.1016/j.rse.2009.01.003

FAO, 2020. Global Forest Resources Assessment 2020. Main report. FAO, Rome. https://doi.org/10.4060/ca9825en

Fernandes, P.M., Vega, J.A., Jiménez, E., Rigolot, E., 2008. Fire resistance of European pines. For. Ecol. Manage. 256, 246–255. https://doi.org/10.1016/j.foreco.2008.04.032

Fernández-García, V., Fulé, P.Z., Marcos, E., Calvo, L., 2019. The role of fire frequency and severity on the regeneration of Mediterranean serotinous pines under different environmental conditions. For. Ecol. Manage. 444, 59–68. https://doi.org/10.1016/j.foreco.2019.04.040

Fernández-Guisuraga, J.M., Calvo, L., Suárez-Seoane, S., 2022. Monitoring post-fire neighborhood competition effects on pine saplings under different environmental conditions by means of UAV multispectral data and structure-from-motion photogrammetry. J. Environ. Manage. 305. https://doi.org/10.1016/j.jenvman.2021.114373

Fernández-Guisuraga, J.M., Calvo, L., Suárez-Seoane, S., 2020. Comparison of pixel unmixing models in the evaluation of post-fire forest resilience based on temporal series of satellite imagery at moderate and very high spatial resolution. ISPRS J. Photogramm. Remote Sens. 164, 217–228. https://doi.org/10.1016/j.isprsjprs.2020.05.004

Fernández-Manso, A., Quintano, C., Roberts, D.A., 2016. Burn severity influence on post-fire vegetation cover resilience from Landsat MESMA fraction images time series in Mediterranean forest ecosystems. Remote Sens. Environ. 184, 112–123. https://doi.org/10.1016/j.rse.2016.06.015

Fernández, C., Fontúrbel, T., Vega, J.A., 2019. Effects of pre-fire site preparation and post-fire erosion barriers on soil erosion after a wildfire in NW Spain. Catena 172, 691–698. https://doi.org/10.1016/j.catena.2018.09.038

Flannigan, M.D., Krawchuk, M.A., De Groot, W.J., Wotton, B.M., Gowman, L.M., 2009. Implications of changing climate for global wildland fire. Int. J. Wildl. Fire 18, 483–507. https://doi.org/10.1071/WF08187

Flood, N., 2013. Seasonal composite landsat TM/ETM+ Images using the medoid (a multi-dimensional median). Remote Sens. 5, 6481–6500. https://doi.org/10.3390/rs5126481

FOREST EUROPE, 2020. State of Europe's Forests 2020.

Forzieri, G., Dakos, V., McDowell, N.G., Ramdane, A., Cescatti, A., 2022. Emerging signals of declining forest resilience under climate change. Nature 608, 534–539. https://doi.org/10.1038/s41586-022-04959-9

Fotheringham, A.S., Brunsdon, C., Charlton, M., 2003. Geographically weighted regression: the analysis of spatially varying relationships. John Wiley & Sons.

Frantz, D., 2019. FORCE-Landsat + Sentinel-2 analysis ready data and beyond. Remote Sens. 11. https://doi.org/10.3390/rs11091124

Frantz, D., Röder, A., Stellmes, M., Hill, J., 2016. An operational radiometric landsat preprocessing framework for large-area time series applications. IEEE Trans. Geosci. Remote Sens. 54, 3928–3943. https://doi.org/10.1109/TGRS.2016.2530856

Frazier, R.J., .Coops, N.C., Wulder, M.A., Hermosilla, T., White, J.C., 2018. Analyzing spatial and temporal variability in short-term rates of post-fire vegetation return from Landsat time series. Remote Sens. Environ. 205.

https://doi.org/10.1016/j.rse.2017.11.007

Frazier, R.J., Coops, N.C., Wulder, M.A., 2015. Boreal Shield forest disturbance and recovery trends using Landsat time series. Remote Sens. Environ. 170. https://doi.org/10.1016/j.rse.2015.09.015

Frolking, S., Palace, M.W., Clark, D.B., Chambers, J.Q., Shugart, H.H., Hurtt, G.C., 2009. Forest disturbance and recovery: A general review in the context of spaceborne remote sensing of impacts on aboveground biomass and canopy structure. J. Geophys. Res. Biogeosciences 114. https://doi.org/10.1029/2008JG000911

Gao, B.-C., 1996. NDWI A Normalized Difference Water Index for Remote Sensing of Vegetation Liquid Water From Space. Remote Sens. Environ. 58, 257–266. https://doi.org/https://doi.org/10.1016/S0034-4257(96)00067-3

García, M., North, P., Viana-Soto, A., Stavros, N.E., Rosette, J., Martín, M.P., Franquesa, M., González-Cascón, R., Riaño, D., Becerra, J., Zhao, K., 2020. Evaluating the potential of LiDAR data for fire damage assessment: A radiative transfer model approach. Remote Sens. Environ. 247, 111893. https://doi.org/10.1016/j.rse.2020.111893

García, M., Riaño, D., Chuvieco, E., Salas, J., Danson, F.M., 2011. Multispectral and LiDAR data fusion for fuel type mapping using Support Vector Machine and decision rules. Remote Sens. Environ. 115, 1369–1379. https://doi.org/10.1016/j.rse.2011.01.017

García, M., Saatchi, S., Casas, A., Koltunov, A., Ustin, S.L., Ramirez, C., Balzter, H., 2017. Extrapolating forest canopy fuel properties in the California Rim fire by combining airborne LiDAR and landsat OLI data. Remote Sens. 9, 1–18. https://doi.org/10.3390/rs9040394

García, M., Saatchi, S., Ustin, S., Balzter, H., 2018. Modelling forest canopy height by integrating airborne LiDAR samples with satellite Radar and multispectral imagery. Int. J. Appl. Earth Obs. Geoinf. 66, 159–173. https://doi.org/10.1016/j.jag.2017.11.017

Gelabert, P.J., Montealegre, A.L., Lamelas, M.T., Domingo, D., 2020. Forest structural diversity characterization in Mediterranean landscapes affected by fires using Airborne Laser Scanning data. GIScience Remote Sens. 57, 497–509. https://doi.org/10.1080/15481603.2020.1738060

Gitas, I., Mitri, G., Veraverbeke, S., Polychronaki, A., 2012. Advances in Remote Sensing of Post-Fire Vegetation Recovery Monitoring - A Review, in: Remote Sensing of Biomass - Principles and Applications. IntechOpen. https://doi.org/10.5772/20571

Goetz, S., Dubayah, R., 2011. Advances in remote sensing technology and implications for measuring and monitoring forest carbon stocks and change. Carbon Manag. 2, 231–244. https://doi.org/10.4155/cmt.11.18

Gómez, C., Alejandro, P., Hermosilla, T., Montes, F., Pascual, C., Ruiz, L.A., Álvarez-Taboada, F., Tanase, M., Valbuena, R., 2019. Remote sensing for the Spanish forests in the 21st century: a review of advances, needs, and opportunities. For. Syst. 28, eR001. https://doi.org/10.5424/fs/2019281-14221

Gómez, C., White, J.C., Wulder, M.A., 2011. Characterizing the state and processes of change in a dynamic forest environment using hierarchical spatio-temporal segmentation. Remote Sens. Environ. 115, 1665–1679.

https://doi.org/10.1016/j.rse.2011.02.025

Gómez, C., Wulder, M.A., White, J.C., Montes, F., Delgado, J.A., 2012. Characterizing 25 years of change in the area, distribution, and carbon stock of Mediterranean pines in Central Spain. Int. J. Remote Sens. 33, 5546–5573. https://doi.org/10.1080/01431161.2012.663115

González-De Vega, S., de las Heras, J., Moya, D., 2018. Post-fire regeneration and diversity response to burn severity in Pinus halepensis Mill. Forests. Forests 9. https://doi.org/10.3390/f9060299

González-De Vega, S., De las Heras, J., Moya, D., 2016. Resilience of Mediterranean terrestrial ecosystems and fire severity in semiarid areas: Responses of Aleppo pine forests in the short, mid and long term. Sci. Total Environ. 573, 1171–1177. https://doi.org/10.1016/j.scitotenv.2016.03.115

Gordon, C.E., Price, O.F., Tasker, E.M., 2017. Mapping and exploring variation in post-fire vegetation recovery following mixed severity wildfire using airborne LiDAR: Ecol. Appl. 27, 1618–1632. https://doi.org/10.1002/eap.1555

Gorelick, N., Hancher, M., Dixon, M., Ilyushchenko, S., Thau, D., Moore, R., 2017. Google Earth Engine: planetary-scale geospatial analysis for everyone. Remote Sens. Environ. 202. https://doi.org/10.1016/j.rse.2017.06.031

Gouveia, C., DaCamara, C.C., Trigo, R.M., 2010. Post-fire vegetation recovery in Portugal based on spot/vegetation data. Nat. Hazards Earth Syst. Sci. 10. https://doi.org/10.5194/nhess-10-673-2010

Griffiths, P., Kuemmerle, T., Baumann, M., Radeloff, V.C., Abrudan, I. V., Lieskovsky, J., Munteanu, C., Ostapowicz, K., Hostert, P., 2014. Forest disturbances, forest recovery, and changes in forest types across the carpathian ecoregion from 1985 to 2010 based on landsat image composites. Remote Sens. Environ. 151, 72–88. https://doi.org/10.1016/j.rse.2013.04.022

Gu, D., Gillespie, A., 1998. Topographic normalization of Landsat TM images of forest based on subpixel Sun-canopy-sensor geometry. Remote Sens. Environ. 64, 166–175. https://doi.org/10.1016/S0034-4257(97)00177-6

Guerschman, J.P., Scarth, P.F., McVicar, T.R., Renzullo, L.J., Malthus, T.J., Stewart, J.B., Rickards, J.E., Trevithick, R., 2015. Assessing the effects of site heterogeneity and soil properties when unmixing photosynthetic vegetation, non-photosynthetic vegetation and bare soil fractions from Landsat and MODIS data. Remote Sens. Environ. 161, 12–26. https://doi.org/10.1016/j.rse.2015.01.021

Hansen, M.J., Franklin, S.E., Woudsma, C., Peterson, M., 2001. Forest structure classification in the North Columbia mountains using the Landsat TM Tasseled Cap wetness component. Can. J. Remote Sens. 27, 20–32. https://doi.org/10.1080/07038992.2001.10854916

Hartigan, J.. A.., Wong, M.. A.., 1979. Algorithm AS 136 : A K-Means Clustering Algorithm. J. R. Stat. Soc. Ser. C (Applied Stat. 28, 100–108.

Hernández-Blanco, M., Costanza, R., Chen, H., deGroot, D., Jarvis, D., Kubiszewski, I., Montoya, J., Sangha, K., Stoeckl, N., Turner, K., van 't Hoff, V., 2022. Ecosystem health, ecosystem services, and the well-being of humans and the rest of nature. Glob. Chang. Biol. 5027–5040. https://doi.org/10.1111/gcb.16281

Hernández-Serrano, A., Verdú, M., González-Martínez, S.C., Pausas, J.G., 2013. Fire

structures pine Serotiny at different scales. Am. J. Bot. 100, 2349–2356. https://doi.org/10.3732/ajb.1300182

Hirschmugl, M., Gallaun, H., Dees, M., Datta, P., Deutscher, J., Koutsias, N., Schardt, M., 2017. Methods for Mapping Forest Disturbance and Degradation from Optical Earth Observation Data: a Review. Curr. For. Reports 3, 32–45. https://doi.org/10.1007/s40725-017-0047-2

Hislop, S., Jones, S., Soto-Berelov, M., Skidmore, A., Haywood, A., Nguyen, T.H., 2019. High fire disturbance in forests leads to longer recovery, but varies by forest type. Remote Sens. Ecol. Conserv. 1–13. https://doi.org/10.1002/rse2.113

Hislop, S., Jones, S., Soto-Berelov, M., Skidmore, A., Haywood, A., Nguyen, T.H., 2018. Using landsat spectral indices in time-series to assess wildfire disturbance and recovery. Remote Sens. 10, 1–17. https://doi.org/10.3390/rs10030460

Hope, A., Tague, C., Clark, R., 2007. Characterizing post-fire vegetation recovery of California chaparral using TM/ETM+ time-series data. Int. J. Remote Sens. 28. https://doi.org/10.1080/01431160600908924

Hostert, P., Röder, A., Hill, J., 2003. Coupling spectral unmixing and trend analysis for monitoring of long-term vegetation dynamics in Mediterranean rangelands. Remote Sens. Environ. 87, 183–197. https://doi.org/10.1016/s0034-4257(03)00145-7

Huang, C., Goward, S.N., Masek, J.G., Thomas, N., Zhu, Z., Vogelmann, J.E., 2010. An automated approach for reconstructing recent forest disturbance history using dense Landsat time series stacks. Remote Sens. Environ. 114. https://doi.org/10.1016/j.rse.2009.08.017

Huete, A., Didan, K., Miura, T., Rodriguez, E.P., Gao, X., Ferreira, L.G., 2002. Overview of the radiometric and biophysical performance of the MODIS vegetation indices. Remote Sens. Environ. 83, 195–213. https://doi.org/https://doi.org/10.1016/S0034-4257(02)00096-2

Hurvich, C.M., Simonoff, J.S., Tsai, C.-L., 1998. Smoothing parameter selection in nonparametric regression using an improved Akaike information criterion. J. R. Stat. Soc. Ser. B (Statistical Methodol. 60, 271–293.

Ibáñez, I., Acharya, K., Juno, E., Karounos, C., Lee, B.R., Mccollum, C., Schaffer-Morrison, S., Tourville, J., 2019. Forest resilience under global environmental change : Do we have the information we need ? A systematic review. PLoS One 14 (9), 1–17. https://doi.org/https://doi.org/ 10.1371/journal.pone.0222207

IPCC, 2018. Global Warming of 1.5°C. An IPCC Special Report on the impacts of global warming of 1.5°C above pre-industrial levels and related global greenhouse gas emission pathways, in the context of strengthening the global response to the threat of climate change. (V. Masson-Delmotte, P. Zhai, H.-O. Pörtner, D. Roberts, J. Skea, P. R. Shukla, et al., Eds.).

Ireland, G., Petropoulos, G.P., 2015. Exploring the relationships between post-fire vegetation regeneration dynamics, topography and burn severity: A case study from the Montane Cordillera Ecozones of Western Canada. Appl. Geogr. 56, 232–248. https://doi.org/10.1016/j.apgeog.2014.11.016

Jennings, S.B., Brown, N.D., Sheil, D., 1999. Assessing forest canopies and understorey illumination: Canopy closure, canopy cover and other measures. Forestry 72, 59–73. https://doi.org/10.1093/forestry/72.1.59

Johnstone, J.F., Allen, C.D., Franklin, J.F., Frelich, L.E., Harvey, B.J., Higuera, P.E., Mack, M.C., Meentemeyer, R.K., Metz, M.R., Perry, G.L.W., Schoennagel, T., Turner, M.G., 2016. Changing disturbance regimes, ecological memory, and forest resilience. Front. Ecol. Environ. 14, 369–378. https://doi.org/10.1002/fee.1311

Jones, A., Montanarella, L., Jones, R., 2005. Soil atlas of Europe. European Commission, Luxembourg.

Jones, M.W., Abatzoglou, J.T., Veraverbeke, S., Andela, N., Lasslop, G., Forkel, M., Smith, A.J.P., Burton, C., Betts, R.A., Werf, G.R., Sitch, S., Canadell, J.G., Santín, C., Kolden, C., Doerr, S.H., Le Quéré, C., 2022. Global and regional trends and drivers of fire under climate change. Rev. Geophys. 1–76. https://doi.org/10.1029/2020rg000726

Kane, van R., McGaughey, R.J., Bakker, J.D., Gersonde, R.F., Lutz, J.A., Franklin, J.F., 2010. Comparisons between field- and LiDAR-based measures of stand structural complexity. Can. J. For. Res. 40, 761–773. https://doi.org/10.1139/X10-024

Kane, V.R., North, M.P., Lutz, J.A., Churchill, D.J., Roberts, S.L., Smith, D.F., McGaughey, R.J., Kane, J.T., Brooks, M.L., 2014. Assessing fire effects on forest spatial structure using a fusion of landsat and airborne LiDAR data in Yosemite national park. Remote Sens. Environ. 151, 89–101. https://doi.org/10.1016/j.rse.2013.07.041

Karavani, A., Boer, M.M., Baudena, M., Colinas, C., Díaz-Sierra, R., Pemán, J., de Luis, M., Enríquez-de-Salamanca, Á., Resco de Dios, V., 2018. Fire-induced deforestation in drought-prone Mediterranean forests: drivers and unknowns from leaves to communities. Ecol. Monogr. 88, 141–169. https://doi.org/10.1002/ecm.1285

Keeley, J.E., 2012. Fire in Mediterranean Climate Ecosystems—A Comparative Overview. Isr. J. Ecol. Evol. 58, 123–135. https://doi.org/10.1560/IJEE.58.2-3.123

Keeley, J.E., Bond, W.J., Bradstock, R.A., Pausas, J.G., Rundel, P.W., 2011. Fire in Mediterranean Ecosystems: Ecology, Evolution and Management. Cambridge University Press, Cambridge. https://doi.org/DOI: 10.1017/CBO9781139033091

Keeley, J.E., Pausas, J.G., 2022. Evolutionary Ecology of Fire. Annu. Rev. ofEcology, Evol. Syst. 1–23. https://doi.org/10.3390/books978-3-0365-4052-8

Keenan, R.J., 2015. Climate change impacts and adaptation in forest management: a review. Ann. For. Sci. 72, 145–167. https://doi.org/10.1007/s13595-014-0446-5

Kendall, M.G., 1955. Rank correlation methods., Rank correlation methods. Griffin, Oxford, England.

Kennedy, R.E., Andréfouët, S., Cohen, W.B., Gómez, C., Griffiths, P., Hais, M., Healey, S.P., Helmer, E.H., Hostert, P., Lyons, M.B., Meigs, G.W., Pflugmacher, D., Phinn, S.R., Powell, S.L., Scarth, P., Sen, S., Schroeder, T.A., Schneider, A., Sonnenschein, R., Vogelmann, J.E., Wulder, M.A., Zhu, Z., 2014. Bringing an ecological view of change to landsat-based remote sensing. Front. Ecol. Environ. 12, 339–346. https://doi.org/10.1890/130066

Kennedy, R.E., Yang, Z., Cohen, W.B., Pfaff, E., Braaten, J., Nelson, P., 2012. Spatial and temporal patterns of forest disturbance and regrowth within the area of the Northwest Forest Plan. Remote Sens. Environ. 122. https://doi.org/10.1016/j.rse.2011.09.024

Kennedy, R.E., Yang, Z.G., Cohen, W.B., 2010. Detecting trends in forest disturbance and recovery using yearly Landsat time series: 1. LandTrendr- temporal segmentation algorithms. Remote Sens. Environ. 114. https://doi.org/10.1016/j.rse.2010.07.008

Key, C.H., Benson, N.C., 2006. Landscape assessment: Remote sensing of severity, the Normalized Burn Ratio. FIREMON Fire Eff. Monit. Invent. Syst. Gen. Tech. Report, RMRS-GTR-164-CD 305–325. https://doi.org/10.1002/app.1994.070541203

Kibler, C.L., Parkinson, A.M.L., Peterson, S.H., Roberts, D.A., D'Antonio, C.M., Meerdink, S.K., Sweeney, S.H., 2019. Monitoring post-fire recovery of chaparral and conifer species using field surveys and landsat time series. Remote Sens. 11. https://doi.org/10.3390/rs11242963

Kowalski, K., Okujeni, A., Brell, M., Hostert, P., 2022. Quantifying drought effects in Central European grasslands through regression-based unmixing of intra-annual Sentinel-2 time series. Remote Sens. Environ. 268, 112781. https://doi.org/10.1016/j.rse.2021.112781

Kuemmerle, T., Röder, A., Hill, J., 2006. Separating grassland and shrub vegetation by multidate pixel-adaptive spectral mixture analysis. Int. J. Remote Sens. 27, 3251–3271. https://doi.org/10.1080/01431160500488944

Lary, D.J., Alavi, A.H., Gandomi, A.H., Walker, A.L., 2016. Machine learning in geosciences and remote sensing. Geosci. Front. 7, 3–10. https://doi.org/10.1016/j.gsf.2015.07.003

Latifi, H., Heurich, M., Hartig, F., Müller, J., Krzystek, P., Jehl, H., Dech, S., 2016. Estimating over- and understorey canopy density of temperate mixed stands by airborne LiDAR data. Forestry 89, 69–81. https://doi.org/10.1093/forestry/cpv032

Lechner, A.M., Foody, G.M., Boyd, D.S., 2020. Applications in Remote Sensing to Forest Ecology and Management. One Earth 2, 405–412. https://doi.org/10.1016/j.oneear.2020.05.001

Lefsky, M.A., Cohen, W.B., Parker, G.G., Harding, D.J., 2002. Lidar remote sensing for ecosystem studies. Bioscience 52, 19–30. https://doi.org/10.1641/0006-3568(2002)052[0019:LRSFES]2.0.CO;2

Lentile, L.B., Holden, Z.A., Smith, A.M.S., Falkowski, M.J., Hudak, A.T., Morgan, P., Lewis, S.A., Gessler, P.E., Benson, N.C., 2006. Remote sensing techniques to assess active fire characteristics and post-fire effects. Int. J. Wildl. Fire 15, 319–345. https://doi.org/10.1071/WF05097

Leverkus, A.B., Gustafsson, L., Lindenmayer, D.B., Castro, J., Rey Benayas, J.M., Ranius, T., Thorn, S., 2020. Salvage logging effects on regulating ecosystem services and fuel loads. Front. Ecol. Environ. 18, 391–400. https://doi.org/10.1002/fee.2219

Lhermitte, S., Verbesselt, J., Verstraeten, W.W., Veraverbeke, S., Coppin, P., 2011. Assessing intra-annual vegetation regrowth after fire using the pixel based regeneration index. ISPRS J. Photogramm. Remote Sens. 66, 17–27. https://doi.org/10.1016/j.isprsjprs.2010.08.004

Lindner, M., Fitzgerald, J.B., Zimmermann, N.E., Reyer, C., Delzon, S., van der Maaten, E., Schelhaas, M.J., Lasch, P., Eggers, J., van der Maaten-Theunissen, M., Suckow, F., Psomas, A., Poulter, B., Hanewinkel, M., 2014. Climate change and European forests: What do we know, what are the uncertainties, and what are the

implications for forest management? J. Environ. Manage. 146, 69–83. https://doi.org/10.1016/j.jenvman.2014.07.030

Lindner, M., Maroschek, M., Netherer, S., Kremer, A., Barbati, A., Garcia-Gonzalo, J., Seidl, R., Delzon, S., Corona, P., Kolström, M., Lexer, M.J., Marchetti, M., 2010. Climate change impacts, adaptive capacity, and vulnerability of European forest ecosystems. For. Ecol. Manage. 259, 698–709. https://doi.org/10.1016/j.foreco.2009.09.023

Lippitt, C.L., Stow, D.A., Roberts, D.A., Coulter, L.L., 2018. Multidate MESMA for monitoring vegetation growth forms in southern California shrublands. Int. J. Remote Sens. 39, 655–683. https://doi.org/10.1080/01431161.2017.1388936

Liu, Z., 2016. Effects of climate and fire on short-term vegetation recovery in the boreal larch forests of northeastern China. Sci. Rep. 6. https://doi.org/10.1038/srep37572

Magnussen, S., Boudewyn, P., 1998. Derivations of stand heights from airborne laser scanner data with canopy-based quantile estimators. Can. J. For. Res. 28, 1016–1031. https://doi.org/10.1139/x98-078

Maltamo, M., Næsset, E., Vauhkonen, J., 2014. Forestry Applications of Airborne Laser Scanning: Concepts and Case Studies. Springer, Dordrecht, New York. https://doi.org/10.1007/978-94-017-8663-8

Mann, H.B., 1945. Nonparametric Tests Against Trend. Econometrica 13, 245–259.

Martín-Alcón, S., Coll, L., 2016. Unraveling the relative importance of factors driving post-fire regeneration trajectories in non-serotinous Pinus nigra forests. For. Ecol. Manage. 361, 13–22. https://doi.org/10.1016/j.foreco.2015.11.006

Martín-Alcón, S., Coll, L., De Cáceres, M., Guitart, L., Cabré, M., Just, A., González-Olabarría, J.R., 2015. Combining aerial LiDAR and multispectral imagery to assess postfire regeneration types in a Mediterranean forest. Can. J. For. Res. 45, 856–866. https://doi.org/10.1139/cjfr-2014-0430

Masek, J.G., Vermote, E.F., Saleous, N.E., Wolfe, R., Hall, F.G., Huemmrich, K.F., Gao, F., Kutler, J., Lim, T.-. K., 2006. A Landsat surface reflectance dataset for North America, 1990-2000. IEEE Geosci. Remote Sens. Lett. 3. https://doi.org/10.1109/LGRS.2005.857030

Masek, J.G., Wulder, M.A., Markham, B., McCorkel, J., Crawford, C.J., Storey, J., Jenstrom, D.T., 2020. Landsat 9: Empowering open science and applications through continuity. Remote Sens. Environ. 248, 111968. https://doi.org/10.1016/j.rse.2020.111968

Matasci, G., Hermosilla, T., Wulder, M.A., White, J.C., Coops, N.C., Hobart, G.W., Bolton, D.K., Tompalski, P., Bater, C.W., 2018. Three decades of forest structural dynamics over Canada's forested ecosystems using Landsat time-series and lidar plots. Remote Sens. Environ. 216, 697–714. https://doi.org/10.1016/j.rse.2018.07.024

Mazza, G., Sarris, D., 2021. Identifying the full spectrum of climatic signals controlling a tree species' growth and adaptation to climate change. Ecol. Indic. 130, 108109. https://doi.org/10.1016/j.ecolind.2021.108109

McCarley, T.R., Kolden, C.A., Vaillant, N.M., Hudak, A.T., Smith, A.M.S., Wing, B.M., Kellogg, B.S., Kreitler, J., 2017. Multi-temporal LiDAR and Landsat quantification of fire-induced changes to forest structure. Remote Sens. Environ. 191, 419–432.

https://doi.org/10.1016/j.rse.2016.12.022

McDowell, N.G., Allen, C.D., Anderson-Teixeira, K., Aukema, B.H., Bond-Lamberty, B., Chini, L., Clark, J.S., Dietze, M., Grossiord, C., Hanbury-Brown, A., Hurtt, G.C., Jackson, R.B., Johnson, D.J., Kueppers, L., Lichstein, J.W., Ogle, K., Poulter, B., Pugh, T.A.M., Seidl, R., Turner, M.G., Uriarte, M., Walker, A.P., Xu, C., 2020. Pervasive shifts in forest dynamics in a changing world. Science (80-.). 368. https://doi.org/10.1126/science.aaz9463

McGaughey, R.J., 2018. FUSION/LDV: Software for LIDAR Data Analysis and Visualization - V3.80. U.S. Department of Agriculture, Forest Service, Pacific Northwest Research Station, Seattle.

McLauchlan, K.K., Higuera, P.E., Miesel, J., Rogers, B.M., Schweitzer, J., Shuman, J.K., Tepley, A.J., Varner, J.M., Veblen, T.T., Adalsteinsson, S.A., Balch, J.K., Baker, P., Batllori, E., Bigio, E., Brando, P., Cattau, M., Chipman, M.L., Coen, J., Crandall, R., Daniels, L., Enright, N., Gross, W.S., Harvey, B.J., Hatten, J.A., Hermann, S., Hewitt, R.E., Kobziar, L.N., Landesmann, J.B., Loranty, M.M., Maezumi, S.Y., Mearns, L., Moritz, M., Myers, J.A., Pausas, J.G., Pellegrini, A.F.A., Platt, W.J., Roozeboom, J., Safford, H., Santos, F., Scheller, R.M., Sherriff, R.L., Smith, K.G., Smith, M.D., Watts, A.C., 2020. Fire as a fundamental ecological process: Research advances and frontiers. J. Ecol. 108, 2047–2069. https://doi.org/10.1111/1365-2745.13403

Meng, R., Dennison, P.E., Huang, C., Moritz, M.A., D'Antonio, C., 2015. Effects of fire severity and post-fire climate on short-term vegetation recovery of mixed-conifer and red fir forests in the Sierra Nevada Mountains of California. Remote Sens. Environ. 171, 311–325. https://doi.org/10.1016/j.rse.2015.10.024

Miller, J.D., Thode, A.E., 2007. Quantifying burn severity in a heterogeneous landscape with a relative version of the delta Normalized Burn Ratio (dNBR). Remote Sens. Environ. 109, 66–80. https://doi.org/10.1016/j.rse.2006.12.006

Ministerio de Agricultura Pesca y Alimentación. Second National Forest Inventory of Spain. URL: https://www.miteco.gob.es/es/biodiversidad/servicios/banco-datos-naturaleza/informacion-disponible/ifn2.aspx (accessed 1.27.20).

Ministerio de Agricultura Pesca y Alimentación. Forest Map of Spain. URL: https://www.miteco.gob.es/es/biodiversidad/servicios/banco-datos-naturaleza/informacion-disponible/mfe200.aspx (accessed 1.27.20).

Montealegre, A.L., 2017. Aplicaciones forestales de los datos LiDAR-PNOA en ambiente mediterráneo: su filtrado e interpolación y el modelado de parámetros estructurales con apoyo en trabajo de campo. PhD thesis. Geography and Territorial Planning Dep., Zaragoza University (Spain).

Montealegre, A.L., Lamelas, M.T., De La Riva, J., García-Martín, A., Escribano, F., 2016. Use of low point density ALS data to estimate stand-level structural variables in Mediterranean Aleppo pine forest. Forestry 89, 373–382. https://doi.org/10.1093/forestry/cpw008

Montealegre, A.L., Lamelas, M.T., Tanase, M.A., De la Riva, J., 2014. Forest fire severity assessment using ALS data in a mediterranean environment. Remote Sens. 6, 4240–4265. https://doi.org/10.3390/rs6054240

Montorio, R., Pérez-Cabello, F., Borini Alves, D., García-Martín, A., 2020. Unitemporal approach to fire severity mapping using multispectral synthetic databases and

Random Forests. Remote Sens. Environ. 249, 112025. https://doi.org/10.1016/j.rse.2020.112025

Moreira, F., Ascoli, D., Safford, H., Adams, M.A., Moreno, J.M., Pereira, J.M.C., Catry, F.X., Armesto, J., Bond, W., González, M.E., Curt, T., Koutsias, N., McCaw, L., Price, O., Pausas, J.G., Rigolot, E., Stephens, S., Tavsanoglu, C., Vallejo, V.R., Van Wilgen, B.W., Xanthopoulos, G., Fernandes, P.M., 2020. Wildfire management in Mediterranean-type regions: Paradigm change needed. Environ. Res. Lett. 15. https://doi.org/10.1088/1748-9326/ab541e

Moreno, M.V., Conedera, M., Chuvieco, E., Pezzatti, G.B., 2014. Fire regime changes and major driving forces in Spain from 1968 to 2010. Environ. Sci. Policy 37, 11–22. https://doi.org/10.1016/j.envsci.2013.08.005

Morresi, D., Vitali, A., Urbinati, C., Garbarino, M., 2019. Forest spectral recovery and regeneration dynamics in stand-replacing wildfires of central Apennines derived from Landsat time series. Remote Sens. 11. https://doi.org/10.3390/rs11030308

Morsdorf, F., Kötz, B., Meier, E., Itten, K.I., Allgöwer, B., 2006. Estimation of LAI and fractional cover from small footprint airborne laser scanning data based on gap fraction. Remote Sens. Environ. 104, 50–61. https://doi.org/10.1016/j.rse.2006.04.019

Moya, D., Espelta, J.M., López-Serrano, F.R., Eugenio, M., Heras, J.D. Las, 2008. Natural post-fire dynamics and serotiny in 10-year-old Pinus halepensis Mill. stands along a geographic gradient. Int. J. Wildl. Fire 17, 287–292. https://doi.org/10.1071/WF06121

Moya, D., González-De Vega, S., García-Orenes, F., Morugán-Coronado, A., Arcenegui, V., Mataix-Solera, J., Lucas-Borja, M.E., De las Heras, J., 2018. Temporal characterisation of soil-plant natural recovery related to fire severity in burned Pinus halepensis Mill. forests. Sci. Total Environ. 640–641, 42–51. https://doi.org/10.1016/j.scitotenv.2018.05.212

Mulverhill, C., Coops, N.C., Hermosilla, T., White, J.C., Wulder, M.A., 2022. Evaluating ICESat-2 for monitoring, modeling, and update of large area forest canopy height products. Remote Sens. Environ. 271, 112919. https://doi.org/10.1016/j.rse.2022.112919

National Geographic Institute of Spain (IGN). National Plan of Aerial Orthophotography of Spain (PNOA). URL: http://centrodedescargas.cnig.es/CentroDescargas/index.jsp (accessed 3.2.22).

Ne'eman, G., Osem, Y. (Eds.), 2021. Pines and Their Mixed Forest Ecosystems in the Mediterranean Basin. Springer International Publishing.

Neumann, T.A., Martino, A.J., Markus, T., Bae, S., Bock, M.R., Brenner, A.C., Brunt, K.M., Cavanaugh, J., Fernandes, S.T., Hancock, D.W., Harbeck, K., Lee, J., Kurtz, N.T., Luers, P.J., Luthcke, S.B., Magruder, L., Pennington, T.A., Ramos-Izquierdo, L., Rebold, T., Skoog, J., Thomas, T.C., 2019. The Ice, Cloud, and Land Elevation Satellite – 2 mission: A global geolocated photon product derived from the Aadvanced Ttopographic Llaser Aaltimeter Ssystem. Remote Sens. Environ. 233, 111325. https://doi.org/10.1016/j.rse.2019.111325

Nguyen, T.H., Jones, S.D., Soto-Berelov, M., Haywood, A., Hislop, S., 2018. A spatial and temporal analysis of forest dynamics using Landsat time-series. Remote Sens. Environ. 217, 461–475. https://doi.org/10.1016/j.rse.2018.08.028

Nikinmaa, L., Lindner, M., Cantarello, E., Jump, A.S., Seidl, R., Winkel, G., Muys, B., 2020. Reviewing the Use of Resilience Concepts in Forest Sciences. Curr. For. Reports 6, 61–80. https://doi.org/10.1007/s40725-020-00110-x

Nilson, T., Peterson, U., 1994. Age dependence of forest reflectance: Analysis of main driving factors. Remote Sens. Environ. https://doi.org/10.1016/0034-4257(94)90006-X

Ninyerola, M., Fernàndez, X.P., i Nolla, J.M.R., 2005. Atlas climático digital de la Península Ibérica: metodología y aplicaciones en bioclimatología y geobotánica. Universitat Autònoma de Barcelona.

Nolan, R.H., Collins, L., Leigh, A., Ooi, M.K.J., Curran, T.J., Fairman, T.A., Resco de Dios, V., Bradstock, R., 2021. Limits to post-fire vegetation recovery under climate change. Plant Cell Environ. 44, 3471–3489. https://doi.org/10.1111/pce.14176

Okujeni, A., Jänicke, C., Cooper, S., Frantz, D., Hostert, P., Clark, M., Segl, K., van der Linden, S., 2021. Multi-season unmixing of vegetation class fractions across diverse Californian ecoregions using simulated spaceborne imaging spectroscopy data. Remote Sens. Environ. 264. https://doi.org/10.1016/j.rse.2021.112558

Okujeni, A., Van Der Linden, S., Suess, S., Hostert, P., 2017. Ensemble Learning from Synthetically Mixed Training Data for Quantifying Urban Land Cover with Support Vector Regression. IEEE J. Sel. Top. Appl. Earth Obs. Remote Sens. 10, 1640–1650. https://doi.org/10.1109/JSTARS.2016.2634859

Okujeni, A., van der Linden, S., Tits, L., Somers, B., Hostert, P., 2013. Support vector regression and synthetically mixed training data for quantifying urban land cover. Remote Sens. Environ. 137, 184–197. https://doi.org/10.1016/j.rse.2013.06.007

Oliver, C., Larson, B., 1996. Forest Stand Dynamics (Update Edition), Forest Science. FES Other Publications. https://doi.org/10.1093/forestscience/42.3.397

Paritsis, J., Veblen, T.T., Holz, A., 2015. Positive fire feedbacks contribute to shifts from Nothofagus pumilio forests to fire-prone shrublands in Patagonia. J. Veg. Sci. 26, 89–101. https://doi.org/10.1111/jvs.12225

Pascual, C., García-Abril, A., Cohen, W.B., Martín-Fernández, S., 2010. Relationship between LiDAR-derived forest canopy height and Landsat images. Int. J. Remote Sens. 31, 1261–1280. https://doi.org/10.1080/01431160903380656

Pausas, J.G., Bladé, C., Valdecantos, A., Seva, J.P., Fuentes, D., Alloza, J.A., Vilagrosa, A., Bautista, S., Cortina, J., Vallejo, R., 2004. Pines and oaks in the restoration of Mediterranean landscapes of Spain: New perspectives for an old practice - A review. Plant Ecol. 171, 209–220. https://doi.org/10.1023/B:VEGE.0000029381.63336.20

Pausas, J.G., Fernández-Muñoz, S., 2012. Fire regime changes in the Western Mediterranean Basin: From fuel-limited to drought-driven fire regime. Clim. Change 110, 215–226. https://doi.org/10.1007/s10584-011-0060-6

Pausas, J.G., Keeley, J.E., 2014a. Evolutionary ecology of resprouting and seeding in fire-prone ecosystems. New Phytol. 204, 55–65. https://doi.org/10.1111/nph.12921

Pausas, J.G., Keeley, J.E., 2014b. Abrupt Climate-Independent Fire Regime Changes. Ecosystems 17, 1109–1120. https://doi.org/10.1007/s10021-014-9773-5

Pausas, J.G., Keeley, J.E., 2009. A Burning Story: The Role of Fire in the History of Life. Bioscience 59, 593–601. https://doi.org/10.1525/bio.2009.59.7.10

Pausas, J.G., Ouadah, N., Ferran, A., Gimeno, T., Vallejo, R., 2002. Fire severity and seedling establishment in Pinus halepensis woodlands, eastern Iberian Peninsula. Plant Ecol. 169, 205–213. https://doi.org/10.1023/A:1026019528443

Pausas, J.G., Ribeiro, E., 2017. Fire and plant diversity at the global scale. Glob. Ecol. Biogeogr. 26, 889–897. https://doi.org/10.1111/geb.12596

Pausas, J.G., Vallejo, V.R., 1999. The role of fire in European Mediterranean ecosystems. Remote Sens. Large Wildfires 3–16. https://doi.org/10.1007/978-3-642-60164-4_2

Pedregosa, F., Varoquaux, G., Gramfort, A., Michel, V., Thirion, B., Grisel, O., Blondel, M., Prettenhofer, P., Weiss, R., Dubourg, V., Vanderplas, J., Passos, A., Cournapeu, D., 2011. Scikit-learn. J. ofMachine Learn. Res. 12, 2825–2830. https://doi.org/10.1145/2786984.2786995

Pérez-Cabello, F., Cerdà, A., de la Riva, J., Echeverría, M.T., García-Martín, A., Ibarra, P., Lasanta, T., Montorio, R., Palacios, V., 2012. Micro-scale post-fire surface cover changes monitored using high spatial resolution photography in a semiarid environment: A useful tool in the study of post-fire soil erosion processes. J. Arid Environ. 76, 88–96. https://doi.org/10.1016/j.jaridenv.2011.08.007

Pérez-Cabello, F., Montorio, R., Alves, D.B., 2021. Remote Sensing Techniques to assess Post-Fire Vegetation Recovery. Curr. Opin. Environ. Sci. Heal. 100251. https://doi.org/10.1016/j.coesh.2021.100251

Peterson, D.L., 2014. Fire in Mediterranean Ecosystems: Ecology, Evolution and Management. 2012. By J.E. Keeley, W.J. Bond, R.A. Bradstock, J.G. Pausas, and P.W. Rundel. Cambridge University Press, United Kingdom. 515 pages. Hardback. US$127. ISBN 978-0-521-82491-0, Fire Ecology. Cambridge University Press. https://doi.org/10.4996/fireecology.1001086

Pflugmacher, D., Cohen, W.B., Kennedy, R.E., Yang, Z., 2014. Using Landsat-derived disturbance and recovery history and lidar to map forest biomass dynamics. Remote Sens. Environ. 151, 124–137. https://doi.org/10.1016/j.rse.2013.05.033

Pflugmacher, D., Rabe, A., Peters, M., Hostert, P., 2019. Mapping pan-European land cover using Landsat spectral-temporal metrics and the European LUCAS survey. Remote Sens. Environ. 221, 583–595. https://doi.org/10.1016/j.rse.2018.12.001

Pickell, P.D., Hermosilla, T., Frazier, R.J., Coops, N.C., Wulder, M.A., 2016. Forest recovery trends derived from Landsat time series for North American boreal forests. Int. J. Remote Sens. 37, 138–149. https://doi.org/10.1080/2150704X.2015.1126375

Potapov, P., Li, X., Hernandez-Serna, A., Tyukavina, A., Hansen, M.C., Kommareddy, A., Pickens, A., Turubanova, S., Tang, H., Silva, C.E., Armston, J., Dubayah, R., Blair, J.B., Hofton, M., 2021. Mapping global forest canopy height through integration of GEDI and Landsat data. Remote Sens. Environ. 253, 112165. https://doi.org/10.1016/j.rse.2020.112165

Pourshamsi, M., Xia, J., Yokoya, N., Garcia, M., Lavalle, M., Pottier, E., Balzter, H., 2021. Tropical forest canopy height estimation from combined polarimetric SAR and LiDAR using machine-learning. ISPRS J. Photogramm. Remote Sens. 172, 79–94. https://doi.org/10.1016/j.isprsjprs.2020.11.008

Powell, S.L., Cohen, W.B., Healey, S.P., Kennedy, R.E., Moisen, G.G., Pierce, K.B., Ohmann, J.L., 2010. Quantification of live aboveground forest biomass dynamics

with Landsat time-series and field inventory data: A comparison of empirical modeling approaches. Remote Sens. Environ. 114, 1053–1068. https://doi.org/10.1016/j.rse.2009.12.018

Purnima, B., Arvind, K., 2014. EBK-Means: A Clustering Technique based on Elbow Method and K-Means in WSN. Int. J. Comput. Appl. 105, 17–24.

Qiu, T., Andrus, R., Aravena, M.C., Ascoli, D., Bergeron, Y., Berretti, R., Berveiller, D., Bogdziewicz, M., Boivin, T., Bonal, R., Bragg, D.C., Caignard, T., Calama, R., Camarero, J.J., Chang-Yang, C.H., Cleavitt, N.L., Courbaud, B., Courbet, F., Curt, T., Das, A.J., Daskalakou, E., Davi, H., Delpierre, N., Delzon, S., Dietze, M., Calderon, S.D., Dormont, L., Espelta, J., Fahey, T.J., Farfan-Rios, W., Gehring, C.A., Gilbert, G.S., Gratzer, G., Greenberg, C.H., Guo, Q., Hacket-Pain, A., Hampe, A., Han, Q., Hille Ris Lambers, J., Hoshizaki, K., Ibanez, I., Johnstone, J.F., Journé, V., Kabeya, D., Kilner, C.L., Kitzberger, T., Knops, J.M.H., Kobe, R.K., Kunstler, G., Lageard, J.G.A., LaMontagne, J.M., Ledwon, M., Lefevre, F., Leininger, T., Limousin, J.M., Lutz, J.A., Macias, D., McIntire, E.J.B., Moore, C.M., Moran, E., Motta, R., Myers, J.A., Nagel, T.A., Noguchi, K., Ourcival, J.M., Parmenter, R., Pearse, I.S., Perez-Ramos, I.M., Piechnik, L., Poulsen, J., Poulton-Kamakura, R., Redmond, M.D., Reid, C.D., Rodman, K.C., Rodriguez-Sanchez, F., Sanguinetti, J.D., Scher, C.L., Schlesinger, W.H., Schmidt Van Marle, H., Seget, B., Sharma, S., Silman, M., Steele, M.A., Stephenson, N.L., Straub, J.N., Sun, I.F., Sutton, S., Swenson, J.J., Swift, M., Thomas, P.A., Uriarte, M., Vacchiano, G., Veblen, T.T., Whipple, A. V., Whitham, T.G., Wion, A.P., Wright, B., Wright, S.J., Zhu, K., Zimmerman, J.K., Zlotin, R., Zywiec, M., Clark, J.S., 2022. Limits to reproduction and seed size-number trade-offs that shape forest dominance and future recovery. Nat. Commun. 13, 1–12. https://doi.org/10.1038/s41467-022-30037-9

Quintano, C., Fernández-Manso, A., Calvo, L., Roberts, D.A., 2019. Vegetation and soil fire damage analysis based on species distribution modeling trained with multispectral satellite data. Remote Sens. 11. https://doi.org/10.3390/rs11151832

Quintano, C., Fernandez-Manso, A., Roberts, D.A., 2017. Burn severity mapping from Landsat MESMA fraction images and Land Surface Temperature. Remote Sens. Environ. 190, 83–95. https://doi.org/10.1016/j.rse.2016.12.009

Quintano, C., Fernández-Manso, A., Roberts, D.A., 2013. Multiple Endmember Spectral Mixture Analysis (MESMA) to map burn severity levels from Landsat images in Mediterranean countries. Remote Sens. Environ. 136, 76–88. https://doi.org/10.1016/j.rse.2013.04.017

Quintano, C., Fernández-Manso, A., Shimabukuro, Y.E., Pereira, G., 2012. Spectral unmixing. Int. J. Remote Sens. 33, 5307–5340. https://doi.org/10.1080/01431161.2012.661095

Rautiainen, M., Stenberg, P., Nilson, T., Kuusk, A., 2004. The effect of crown shape on the reflectance of coniferous stands. Remote Sens. Environ. 89, 41–52. https://doi.org/10.1016/j.rse.2003.10.001

Reynolds, C.H., 1975. The NAD-linked α-glycerophosphate dehydrogenase of trypanosomes. Biochem. Biophys. Res. Commun. 67, 538–543. https://doi.org/10.1016/0006-291X(75)90845-1

Riaño, D., Chuvieco, E., Ustin, S., Zomer, R., Dennison, P., Roberts, D., Salas, J., 2002. Assessment of vegetation regeneration after fire through multitemporal analysis of AVIRIS images in the Santa Monica Mountains. Remote Sens. Environ. 79.

https://doi.org/10.1016/S0034-4257(01)00239-5

Rigo, D. De, Libertà, G., Durrant, T.H., Artés, T., San-Miguel-, J., 2017. Forest fire danger extremes in Europe under climate change: variability and uncertainty. Publications Office of the European Union, Luxembourg. https://doi.org/10.2760/13180

Rivas-Martínez, S., 1981. Etages bioclimatiques, secteurs chorologiques et séries de végétation de l'Espagne méditerranéenne. An. del Jardín Botánico Madrid 37, 251–268.

Roberts, D.A., Gardner, M., Church, R., Ustin, S., Scheer, G., Green, R.O., 1998. Mapping chaparral in the Santa Monica Mountains using multiple endmember spectral mixture models. Remote Sens. Environ. 65, 267–279. https://doi.org/10.1016/S0034-4257(98)00037-6

Roberts, D.W., Cooper, S. V, 1989. Concepts and techniques of vegetation mapping. Pages 90–96 BT - compilers. Proceedings of a symposium—land classifications based on vegetation: applications for resource management. USDA Forest Service General Technical Report INT-257, in: Ferguson, D.E., Morgan, P., Johnson, F.D. (Eds.), . Intermountain Research Station, Ogden.

Röder, A., Hill, J., Duguy, B., Alloza, J.A., Vallejo, R., 2008. Using long time series of Landsat data to monitor fire events and post-fire dynamics and identify driving factors. A case study in the Ayora region (eastern Spain). Remote Sens. Environ. 112. https://doi.org/10.1016/j.rse.2007.05.001

Rodríguez-García, E., Santana, V.M., Alloza, J.A., Ramón Vallejo, V., 2022. Predicting natural hyperdense regeneration after wildfires in Pinus halepensis (Mill.) forests using prefire site factors, forest structure and fire severity. For. Ecol. Manage. 512, 120164. https://doi.org/10.1016/j.foreco.2022.120164

Roy, D.P., Kovalskyy, V., Zhang, H.K., Vermote, E.F., Yan, L., Kumar, S.S., Egorov, A., 2016. Characterization of Landsat-7 to Landsat-8 reflective wavelength and normalized difference vegetation index continuity. Remote Sens. Environ. 185, 57–70. https://doi.org/10.1016/j.rse.2015.12.024

Ruiz-Benito, P., Gómez-Aparicio, L., Zavala, M.A., 2012. Large-scale assessment of regeneration and diversity in Mediterranean planted pine forests along ecological gradients. Divers. Distrib. 18, 1092–1106. https://doi.org/10.1111/j.1472-4642.2012.00901.x

Salomonson, V. V., Barnes, W., Xiong, J., Kempler, S., Masuoka, E., 2002. An overview of the earth observing system MODIS instrument and associated data systems performance. Int. Geosci. Remote Sens. Symp. 2, 1174–1176. https://doi.org/10.1109/igarss.2002.1025812

San-Miguel-Ayanz, J., Durrant, T., Boca, R., Liberta`, G., Branco, A., De Rigo, D., Ferrari, D., Maianti, P., Artes Vivancos, T., Pfeiffer, H., Loffler, P., Nuijten, D., Leray, T., Jacome Felix Oom, D., 2019. Forest Fires in Europe, Middle East and North Africa 2018. Publications Office of the European Union, Luxembourg. https://doi.org/10.2760/1128

San-Miguel-Ayanz, J., Durrant, T., Boca, R., Maianti, P., Liberta', P., Artes Vivancos, T., Jacome Felix Oom, D.P., Branco, A., De Rigo, D., Ferrari, D., Pfeiffer, H., Grecchi, R., Nuijten, D., Onida, M., Loffler, P., 2021. Forest Fires in Europe, Middle East and North Africa 2020.

San-Miguel-Ayanz, J., Moreno, J.M., Camia, A., 2013. Analysis of large fires in European

Mediterranean landscapes: Lessons learned and perspectives. For. Ecol. Manage. 294, 11–22. https://doi.org/10.1016/j.foreco.2012.10.050

Santana, V.M., Alday, J.G., Baeza, M.J., 2014. Effects of fire regime shift in Mediterranean Basin ecosystems: Changes in soil seed bank composition among functional types. Plant Ecol. 215, 555–566. https://doi.org/10.1007/s11258-014-0323-1

Santana, V.M., Baeza, M.J., Valdecantos, A., Vallejo, V.R., 2018. Redirecting fire-prone Mediterranean ecosystems toward more resilient and less flammable communities. J. Environ. Manage. 215, 108–115. https://doi.org/10.1016/j.jenvman.2018.03.063

Schroeder, T.A., Wulder, M.A., Healey, S.P., Moisen, G.G., 2011. Mapping wildfire and clearcut harvest disturbances in boreal forests with Landsat time series data. Remote Sens. Environ. 115, 1421–1433. https://doi.org/10.1016/j.rse.2011.01.022

Schug, F., Frantz, D., Okujeni, A., van der Linden, S., Hostert, P., 2020. Mapping urban-rural gradients of settlements and vegetation at national scale using Sentinel-2 spectral-temporal metrics and regression-based unmixing with synthetic training data. Remote Sens. Environ. 246, 111810. https://doi.org/10.1016/j.rse.2020.111810

Scott, A.C., Glasspool, I.J., 2006. The diversification of Paleozoic fire systems and fluctuations in atmospheric oxygen concentration. Proc. Natl. Acad. Sci. U. S. A. 103, 10861–10865. https://doi.org/10.1073/pnas.0604090103

Seidl, R., Schelhaas, M.J., Lexer, M.J., 2011. Unraveling the drivers of intensifying forest disturbance regimes in Europe. Glob. Chang. Biol. 17, 2842–2852. https://doi.org/10.1111/j.1365-2486.2011.02452.x

Seidl, R., Thom, D., Kautz, M., Martin-Benito, D., Peltoniemi, M., Vacchiano, G., Wild, J., Ascoli, D., Petr, M., Honkaniemi, J., Lexer, M.J., Trotsiuk, V., Mairota, P., Svoboda, M., Fabrika, M., Nagel, T.A., Reyer, C.P.O., 2017. Forest disturbances under climate change. Nat. Clim. Chang. 7, 395–402. https://doi.org/10.1038/nclimate3303

Sen, P.K., 1968. Estimates of the Regression Coefficient Based on Kendall's Tau. J. Am. Stat. Assoc. 63, 1379–1389. https://doi.org/10.1080/01621459.1968.10480934

Senande-Rivera, M., Insua-Costa, D., Miguez-Macho, G., 2022. Spatial and temporal expansion of global wildland fire activity in response to climate change. Nat. Commun. 13, 1–9. https://doi.org/10.1038/s41467-022-28835-2

Senf, C., Laštovička, J., Okujeni, A., Heurich, M., van der Linden, S., 2020. A generalized regression-based unmixing model for mapping forest cover fractions throughout three decades of Landsat data. Remote Sens. Environ. 240. https://doi.org/10.1016/j.rse.2020.111691

Senf, C., Müller, J., Seidl, R., 2019. Post-disturbance recovery of forest cover and tree height differ with management in Central Europe. Landsc. Ecol. 34, 2837–2850. https://doi.org/10.1007/s10980-019-00921-9

Senf, C., Seidl, R., 2021. Mapping the forest disturbance regimes of Europe. Nat. Sustain. 4, 63–70. https://doi.org/10.1038/s41893-020-00609-y

Shi, Y., Wang, T., Skidmore, A.K., Heurich, M., 2018. Important LiDAR metrics for discriminating forest tree species in Central Europe. ISPRS J. Photogramm. Remote Sens. 137, 163–174. https://doi.org/10.1016/j.isprsjprs.2018.02.002

Shvetsov, E.G., Kukavskaya, E.A., Buryak, L. V., Barrett, K., 2019. Assessment of post-fire vegetation recovery in Southern Siberia using remote sensing observations. Environ. Res. Lett. 14. https://doi.org/10.1088/1748-9326/ab083d

Smola, A.J., Scholkopf, B., 2004. A tutorial on support vector regression. Stat. Comput. 14, 199–222.

Soenen, S.A., Peddle, D.R., Coburn, C.A., 2005. SCS+C: A modified sun-canopy-sensor topographic correction in forested terrain. IEEE Trans. Geosci. Remote Sens. 43, 2148–2159. https://doi.org/10.1109/TGRS.2005.852480

Solans Vila, J.P., Barbosa, P., 2010. Post-fire vegetation regrowth detection in the Deiva Marina region (Liguria-Italy) using Landsat TM and ETM+ data. Ecol. Modell. 221. https://doi.org/10.1016/j.ecolmodel.2009.03.011

Somers, B., Tits, L., Roberts, D., Wetherley, E., 2016. Endmember Library Approaches to Resolve Spectral Mixing Problems in Remotely Sensed Data: Potential, Challenges, and Applications, 1st ed, Data Handling in Science and Technology. Elsevier B.V. https://doi.org/10.1016/B978-0-444-63638-6.00017-6

Sonnentag, O., Chen, J.M., Roberts, D.A., Talbot, J., Halligan, K.Q., Govind, A., 2007. Mapping tree and shrub leaf area indices in an ombrotrophic peatland through multiple endmember spectral unmixing. Remote Sens. Environ. 109, 342–360. https://doi.org/10.1016/j.rse.2007.01.010

Souza, C.M., Roberts, D.A., Cochrane, M.A., 2005. Combining spectral and spatial information to map canopy damage from selective logging and forest fires. Remote Sens. Environ. 98, 329–343. https://doi.org/10.1016/j.rse.2005.07.013

Stehman, S. V., 1996. Estimating the kappa coefficient and its variance under stratified random sampling. Photogramm. Eng. Remote Sensing 62, 401–407.

Stephens, S.L., Agee, J.K., Fulé, P.Z., North, M.P., Romme, W.H., Swetnam, T.W., Turner, M.G., 2013. Managing forests and fire in changing climates. Science (80-.). 342, 41–42. https://doi.org/10.1126/science.1240294

Storey, E.A., Stow, D.A., Roberts, D.A., 2020. Evaluating uncertainty in Landsat-derived postfire recovery metrics due to terrain, soil, and shrub type variations in southern California. GIScience Remote Sens. 57, 352–368. https://doi.org/10.1080/15481603.2019.1703287

Suess, S., van der Linden, S., Okujeni, A., Griffiths, P., Leitão, P.J., Schwieder, M., Hostert, P., 2018. Characterizing 32 years of shrub cover dynamics in southern Portugal using annual Landsat composites and machine learning regression modeling. Remote Sens. Environ. 219, 353–364. https://doi.org/10.1016/j.rse.2018.10.004

Taboada, A., Fernández-García, V., Marcos, E., Calvo, L., 2018. Interactions between large high-severity fires and salvage logging on a short return interval reduce the regrowth of fire-prone serotinous forests. For. Ecol. Manage. 414, 54–63. https://doi.org/10.1016/j.foreco.2018.02.013

Taboada, A., Tárrega, R., Marcos, E., Valbuena, L., Suárez-Seoane, S., Calvo, L., 2017. Fire recurrence and emergency post-fire management influence seedling recruitment and growth by altering plant interactions in fire-prone ecosystems. For. Ecol. Manage. 402, 63–75. https://doi.org/10.1016/j.foreco.2017.07.029

Tanase, M., de la Riva, J., Santoro, M., Pérez-Cabello, F., Kasischke, E., 2011.

Sensitivity of SAR data to post-fire forest regrowth in Mediterranean and boreal forests. Remote Sens. Environ. 115, 2075–2085. https://doi.org/10.1016/j.rse.2011.04.009

Tapias, R., Gil, L., Fuentes-Utrilla, P., Pardos, J.A., 2001. Canopy seed banks in Mediterranean pines of southeastern Spain: A comparison between Pinus halepensis Mill., P. pinaster Ait., P. nigra Arn. and P. pinea L. J. Ecol. 89, 629–638. https://doi.org/10.1046/j.1365-2745.2001.00575.x

Thanos, C.A., Daskalakou, E.N., 2000. Reproduction in Pinus halepensis and P. brutia, in: Ecology, Biogeography and Management of Pinus Halepensis and P. Brutia. Forest Ecosystems in the Mediterranean Basin. Backhuys Publishers, Leiden, The Netherlands, pp. 79–90.

Tijerín, J., Moreno-Fernández, D., Zavala, M.A., Astigarraga, J., García, M., 2022. Identifying Forest Structural Types along an Aridity Gradient in Peninsular Spain: Integrating Low-Density LiDAR , Forest Inventory , and Aridity Index. Remote Sens. 14, 235. https://doi.org/https://doi.org/10.3390/rs14010235

Trabaud, L., 1994. Postfire Plant Community Dynamics in the Mediterranean Basin 1–15. https://doi.org/10.1007/978-1-4613-8395-6_1

Tubbesing, C.L., York, R.A., Stephens, S.L., Battles, J.J., 2020. Rethinking fire-adapted species in an altered fire regime. Ecosphere 11. https://doi.org/10.1002/ecs2.3091

Tucker, C.J., 1979. Red and photographic infrared linear combinations for monitoring vegetation. Remote Sens. Environ. 8, 127–150. https://doi.org/https://doi.org/10.1016/0034-4257(79)90013-0

Turco, M., Rosa-Cánovas, J.J., Bedia, J., Jerez, S., Montávez, J.P., Llasat, M.C., Provenzale, A., 2018. Exacerbated fires in Mediterranean Europe due to anthropogenic warming projected with non-stationary climate-fire models. Nat. Commun. 9, 1–9. https://doi.org/10.1038/s41467-018-06358-z

United States Geological Survey (USGS). Earth Explorer Server. URL: https://earthexplorer.usgs.gov/ (accessed 1.27.20).

Vadell, E., de-Miguel, S., Pemán, J., 2016. Large-scale reforestation and afforestation policy in Spain: A historical review of its underlying ecological, socioeconomic and political dynamics. Land use policy 55, 37–48. https://doi.org/10.1016/j.landusepol.2016.03.017

Vallejo, V.R., Arianoutsou, M., Moreira, F., 2012. Post-Fire Management and Restoration of Southern European Forests. Post-fire For. Manag. South. Eur. a COST action Gather. disseminating Sci. Knowl. 24, 93–119. https://doi.org/10.1007/978-94-007-2208-8

Vapnik, V.N., 1995. The nature of statistical learning theory. 1995. Springer, New York.

Vasques, A., Baudena, M., Vallejo, V.R., Kéfi, S., Bautista, S., Santana, V.M., Baeza, M.J., Maia, P., Keizer, J.J., Rietkerk, M., 2022. Post-fire Regeneration Traits of Understorey Shrub Species Modulate Successional Responses to High Severity Fire in Mediterranean Pine Forests. Ecosystems. https://doi.org/10.1007/s10021-022-00750-z

Vega, J., Jimenez, E., Vega, D., Ortiz, L., Pérez, J.R., 2011. Pinus pinaster Ait. tree mortality following wildfire in Spain. For. Ecol. Manage. 261, 2232–2242. https://doi.org/10.1016/j.foreco.2010.10.019

Veraverbeke, S., Somers, B., Gitas, I., Katagis, T., Polychronaki, A., Goossens, R., 2012. Spectral mixture analysis to assess post-fire vegetation regeneration using Landsat Thematic Mapper imagery: Accounting for soil brightness variation. Int. J. Appl. Earth Obs. Geoinf. 14, 1–11. https://doi.org/10.1016/j.jag.2011.08.004

Verbesselt, J., Hyndman, R., Newnham, G., Culvenor, D., 2010. Detecting trend and seasonal changes in satellite image time series. Remote Sens. Environ. 114, 106–115. https://doi.org/10.1016/j.rse.2009.08.014

Vermote, E., Justice, C., Claverie, M., Franch, B., 2016. Preliminary analysis of the performance of the Landsat 8/OLI land surface reflectance product. Remote Sens. Environ. 185, 46–56. https://doi.org/10.1016/j.rse.2016.04.008

Viana-Soto, A., Aguado, I., Martínez, S., 2017. Assessment of Post-Fire Vegetation Recovery Using Fire Severity and Geographical Data in the Mediterranean Region (Spain). Environments 4, 90. https://doi.org/10.3390/environments4040090

Viana-Soto, A., Aguado, I., Salas, J., García, M., 2020. Identifying post-fire recovery trajectories and driving factors using landsat time series in fire-prone mediterranean pine forests. Remote Sens. 12. https://doi.org/10.3390/RS12091499

Viana-Soto, A., García, M., Aguado, I., Salas, J., 2022. Assessing post-fire forest structure recovery by combining LiDAR data and Landsat time series in Mediterranean pine forests. Int. J. Appl. Earth Obs. Geoinf. 108, 102754. https://doi.org/10.1016/j.jag.2022.102754

Viana Soto, A., Aguado, I., Salas, J., García, M., 2019. Classification of post-fire recovery trajectories using Landsat time series in the Mediterranean region: Spain, in: Earth Resources and Environmental Remote Sensing/GIS Applications. International Society for Optics and Photonics, Strasbourg, p. 6. https://doi.org/10.1117/12.2532247

Vicente-Serrano, S.M., Beguería, S., López-Moreno, J.I., 2010. A multiscalar drought index sensitive to global warming: The standardized precipitation evapotranspiration index. J. Clim. 23, 1696–1718. https://doi.org/10.1175/2009JCLI2909.1

Vicente-Serrano, S.M., Gouveia, C., Camarero, J.J., Beguería, S., Trigo, R., López-Moreno, J.I., Azorín-Molina, C., Pasho, E., Lorenzo-Lacruz, J., Revuelto, J., Morán-Tejeda, E., Sanchez-Lorenzo, A., 2013. Response of vegetation to drought time-scales across global land biomes. Proc. Natl. Acad. Sci. U. S. A. 110, 52–57. https://doi.org/10.1073/pnas.1207068110

Vicente-Serrano, S.M., Tomas-Burguera, M., Beguería, S., Reig, F., Latorre, B., Peña-Gallardo, M., Luna, M.Y., Morata, A., González-Hidalgo, J.C., 2017. A high resolution dataset of drought indices for Spain. Data 2, 1–10. https://doi.org/10.3390/data2030022

Vogeler, J.C., Braaten, J.D., Slesak, R.A., Falkowski, M.J., 2018. Extracting the full value of the Landsat archive: Inter-sensor harmonization for the mapping of Minnesota forest canopy cover (1973–2015). Remote Sens. Environ. 209, 363–374. https://doi.org/10.1016/j.rse.2018.02.046

White, J.C., Hermosilla, T., Wulder, M.A., Coops, N.C., 2022. Mapping, validating, and interpreting spatio-temporal trends in post-disturbance forest recovery. Remote Sens. Environ. 271, 112904. https://doi.org/10.1016/j.rse.2022.112904

White, J.C., Saarinen, N., Kankare, V., Wulder, M.A., Hermosilla, T., Coops, N.C.,

Pickell, P.D., Holopainen, M., Hyyppä, J., Vastaranta, M., 2018. Confirmation of post-harvest spectral recovery from Landsat time series using measures of forest cover and height derived from airborne laser scanning data. Remote Sens. Environ. 216, 262–275. https://doi.org/10.1016/j.rse.2018.07.004

White, J.C., Wulder, M.A., Hermosilla, T., Coops, N.C., Hobart, G.W., 2017. A nationwide annual characterization of 25 years of forest disturbance and recovery for Canada using Landsat time series. Remote Sens. Environ. 194, 303–321. https://doi.org/10.1016/j.rse.2017.03.035

White, P.S., Pickett, S.T.A., 1985. Natural disturbance and patch dynamics: an introduction., The ecology of natural disturbance and patch dynamics. ACADEMIC PRESS, INC. https://doi.org/10.1016/b978-0-08-050495-7.50006-5

Wittenberg, L., Malkinson, D., Beeri, O., Halutzy, A., Tesler, N., 2007. Spatial and temporal patterns of vegetation recovery following sequences of forest fires in a Mediterranean landscape, Mt. Carmel Israel. Catena 71. https://doi.org/10.1016/j.catena.2006.10.007

Wulder, M.A., Loveland, T.R., Roy, D.P., Crawford, C.J., Masek, J.G., Woodcock, C.E., Allen, R.G., Anderson, M.C., Belward, A.S., Cohen, W.B., Dwyer, J., Erb, A., Gao, F., Griffiths, P., Helder, D., Hermosilla, T., Hipple, J.D., Hostert, P., Hughes, M.J., Huntington, J., Johnson, D.M., Kennedy, R., Kilic, A., Li, Z., Lymburner, L., McCorkel, J., Pahlevan, N., Scambos, T.A., Schaaf, C., Schott, J.R., Sheng, Y., Storey, J., Vermote, E., Vogelmann, J., White, J.C., Wynne, R.H., Zhu, Z., 2019. Current status of Landsat program, science, and applications. Remote Sens. Environ. 225, 127–147. https://doi.org/10.1016/j.rse.2019.02.015

Wulder, M.A., Masek, J.G., Cohen, W.B., Loveland, T.R., Woodcock, C.E., 2012a. Opening the archive: How free data has enabled the science and monitoring promise of Landsat. Remote Sens. Environ. 122, 2–10. https://doi.org/10.1016/j.rse.2012.01.010

Wulder, M.A., Roy, D.P., Radeloff, V.C., Loveland, T.R., Anderson, M.C., Johnson, D.M., Healey, S., Zhu, Z., Scambos, T.A., Pahlevan, N., Hansen, M., Gorelick, N., Crawford, C.J., Masek, J.G., Hermosilla, T., White, J.C., Belward, A.S., Schaaf, C., Woodcock, C.E., Huntington, J.L., Lymburner, L., Hostert, P., Gao, F., Lyapustin, A., Pekel, J.F., Strobl, P., Cook, B.D., 2022. Fifty years of Landsat science and impacts. Remote Sens. Environ. 280, 113195. https://doi.org/10.1016/j.rse.2022.113195

Wulder, M.A., White, J.C., Loveland, T.R., Woodcock, C.E., Belward, A.S., Cohen, W.B., Fosnight, E.A., Shaw, J., Masek, J.G., Roy, D.P., 2016. The global Landsat archive: Status, consolidation, and direction. Remote Sens. Environ. 185, 271–283. https://doi.org/10.1016/j.rse.2015.11.032

Wulder, M.A., White, J.C., Nelson, R.F., Næsset, E., Ørka, H.O., Coops, N.C., Hilker, T., Bater, C.W., Gobakken, T., 2012b. Lidar sampling for large-area forest characterization: A review. Remote Sens. Environ. 121, 196–209. https://doi.org/10.1016/j.rse.2012.02.001

Xu, Y., Goodacre, R., 2018. On Splitting Training and Validation Set: A Comparative Study of Cross-Validation, Bootstrap and Systematic Sampling for Estimating the Generalization Performance of Supervised Learning. J. Anal. Test. 2, 249–262. https://doi.org/10.1007/s41664-018-0068-2

Yuan, Q., Shen, H., Li, T., Li, Z., Li, S., Jiang, Y., Xu, H., Tan, W., Yang, Q., Wang, J.,

Gao, J., Zhang, L., 2020. Deep learning in environmental remote sensing: Achievements and challenges. Remote Sens. Environ. 241, 111716. https://doi.org/10.1016/j.rse.2020.111716

Zald, H.S.J., Wulder, M.A., White, J.C., Hilker, T., Hermosilla, T., Hobart, G.W., Coops, N.C., 2016. Integrating Landsat pixel composites and change metrics with lidar plots to predictively map forest structure and aboveground biomass in Saskatchewan, Canada. Remote Sens. Environ. 176, 188–201. https://doi.org/10.1016/j.rse.2016.01.015

Zavala, M.A., Espelta, J.M., Retana, J., 2000. Constraints and trade-offs in Mediterranean plant communities: the case of mixed holm oak (Quercus ilex L)-Aleppo pine (Pinus halepensis Mill.) forests. Bot. Rev. 66, 119–149.

Zhao, F.R., Meng, R., Huang, C., Zhao, M., Zhao, F.A., Gong, P., Yu, L., Zhu, Z., 2016. Long-term post-disturbance forest recovery in the greater yellowstone ecosystem analyzed using Landsat time series stack. Remote Sens. 8. https://doi.org/10.3390/rs8110898

Zhao, K., Popescu, S., Meng, X., Pang, Y., Agca, M., 2011. Characterizing forest canopy structure with lidar composite metrics and machine learning. Remote Sens. Environ. 115, 1978–1996. https://doi.org/10.1016/j.rse.2011.04.001

Zhu, Z., 2017. Change detection using landsat time series: A review of frequencies, preprocessing, algorithms, and applications. ISPRS J. Photogramm. Remote Sens. 130, 370–384. https://doi.org/10.1016/j.isprsjprs.2017.06.013

Zhu, Z., Woodcock, C.E., 2012. Object-based cloud and cloud shadow detection in Landsat imagery. Remote Sens. Environ. 118, 83–94. https://doi.org/10.1016/j.rse.2011.10.028

Zhu, Z., Woodcock, C.E., Olofsson, P., 2012. Continuous monitoring of forest disturbance using all available Landsat imagery. Remote Sens. Environ. 122, 75–91. https://doi.org/10.1016/j.rse.2011.10.030

Appendices

Appendix 1. Supplementary materials paper I

Table S3.1. Modelling results for Tasseled Cap Angle (TCA) recovery categories at each stage.

Category	Variable	Stage 1		Stage 2		Stage 3		Stage 4	
		Coefficient	Std. Error	Coefficient	Std. Error	Coefficient	Std. Error	Coefficient	Std. Error
CR	Intercept	0.662	0.145						
	Pre-fire conditions	0.012	0.005						
	Fire severity	0.061	0.005						
	Elevation	-0.018	0.017						
	Slope	0.003	0.005						
	Aspect	-0,010	0,004						
	Drought Index	0,279	0,492						
		R^2: 0.77; Adj. R^2:0.76; AICc: 955.89							
CRSC	Intercept	0.651	0.142	0.384	0.351	-0,847	1,421	-0,565	0,341
	Pre-fire conditions	0.075	0.043	0.055	0.068	0,058	0,277	0,081	0,066
	Fire severity	0.553	0.046	0.265	0.332	0,064	0,362	0,122	0,327
	Elevation	-0.261	0.069	-0.135	0.143	-0,162	0,586	-0,068	0,140
	Slope	-0.046	0.040	0.025	0.058	0,157	0,238	0,043	0,057
	Aspect	0.034	0.034	0.008	0.048	-0,008	0,197	-0,015	0,047
	Drought Index	0.758	0.154	1.143	0.058	2,525	0,130	0,788	0,047
		R^2: 0.77; Adj. R^2:0.76; AICc: 1656.55		R^2: 0.81; Adj. R^2: 0.80; AICc: 4031.20		R^2: 0.75; Adj. R^2: 0.74; AICc: 11055.78		R^2: 0.73; Adj. R^2: 0.72; AICc: 4238.93	
CRS	Intercept	-0.495	0.068	0.196	0,053				
	Pre-fire conditions	0.093	0.025	0.024	0,009				
	Fire severity	0.260	0.032	0.040	0,055				
	Elevation	-0.132	0.064	-0.001	0,032				
	Slope	-0.006	0.026	-0.004	0,012				
	Aspect	-0.024	0.022	-0.002	0,008				
	Drought Index	1.849	0.065	0.075	0,086				
		R^2: 0.88; Adj. R^2: 0.88; AICc: 1746.11		R^2: 0.61; Adj. R^2: 0.58; AICc: 12831.31					
NCR	Intercept	-0.052	0.101	0.344	0,349	-0,540	0,294		
	Pre-fire conditions	0.079	0.032	0.033	0,064	0,048	0,054		
	Fire severity	0.449	0.039	-0.826	0,353	0,582	0,300		
	Elevation	-0.234	0.063	0.213	0,165	-0,201	0,141		
	Slope	-0.018	0.036	0.051	0,070	-0,001	0,059		
	Aspect	-0.041	0.029	0.021	0,051	-0,032	0,044		
	Drought Index	1.613	0.110	1.065	0,060	0,845	0,231		
		R^2: 0.83; Adj. R^2: 0.82; AICc: 1527.51		R^2: 0.78; Adj. R^2: 0.77; AICc: 7082.34		R^2: 0.74; Adj. R^2: 0.72; AICc: 6085.56			

Table S3.2. Modelling results for Tasseled Cap Wetness (TCW) recovery categories at each stage.

Category	Variable	Stage 1		Stage 2		Stage 3		Stage 4	
		Coefficient	Std. Error	Coefficient	Std. Error	Coefficient	Std. Error	Coefficient	Std. Error
CR	Intercept	0.416	0.040						
	Pre-fire conditions	-0.008	0.002						
	Fire severity	0.023	0.002						
	Elevation	-0.002	0.005						
	Slope	-0.005	0.002						
	Aspect	0.013	0.002						
	Drought Index	0.121	0.446						
		R^2: 0.71; Adj. R^2:0.69; AICc: 955.23							
CR2	Intercept	0.025	0.101	-0.076	0.046				
	Pre-fire conditions	-0.312	0.046	0.049	0.020				
	Fire severity	0.106	0.046	0.006	0.019				
	Elevation	-0.158	0.065	0.027	0.036				
	Slope	0.072	0.036	0.004	0.015				
	Aspect	-0.171	0.039	0.025	0.016				
	Drought Index	0.734	0.156	-0.609	0.170				
		R^2: 0.80; Adj. R^2: 0.79; AICc: 7870.95		R^2: 0.92; Adj. R^2: 0.92; AICc: 1227.11					
CRSC	Intercept	-0.322	0.120	0.612	0.214	0.358	0.229	-0.119	0.167
	Pre-fire conditions	-0.116	0.051	-0.091	0.116	-0.008	0.126	0.024	0.092
	Fire severity	0.094	0.044	0.206	0.099	0.140	0.108	0.053	0.079
	Elevation	-0.040	0.072	-0.098	0.248	-0.005	0.270	-0.059	0.198
	Slope	0.041	0.038	0.004	0.091	0.021	0.099	0.014	0.073
	Aspect	-0.148	0.031	0.103	0.070	0.106	0.077	0.050	0.056
	Drought Index	0.122	0.126	0.437	0.088	0.737	0.058	0.640	0.052
		R^2:0.88; Adj. R^2:0.87; AICc: 1959.93		R^2: 0.67; Adj. R^2: 0.65; AICc: 15831.16		R^2: 0.62; Adj. R^2: 0.60; AICc: 17032.23		R^2: 0.56; Adj. R^2: 0.54; AICc: 13009.93	
CRSC2	Intercept	0.765	0.065	0.324	0.198	0.099	0.047		
	Pre-fire conditions	-0.061	0.041	0.085	0.113	-0.008	0.026		
	Fire severity	0.045	0.039	0.139	0.106	0.018	0.025		
	Elevation	-0.127	0.062	-0.166	0.247	-0.017	0.057		
	Slope	0.014	0.030	0.030	0.087	-0.009	0.020		
	Aspect	-0.046	0.027	0.195	0.070	0.025	0.016		
	Drought Index	0.730	0.039	0.735	0.077	-0.150	0.075		
		R^2: 0.81; Adj. R^2: 0.80; AICc: 1064.20		R^2: 0.69; Adj. R^2: 0.67; AICc: 11669.50		R^2: 0,70; Adj. R^2: 0,69; AICc: 1451.47			

Table S3.2. continue

CRS	Intercept	0.146	0.061	-0.030	0.074
	Pre-fire conditions	-0.047	0.028	-0.002	0.031
	Fire severity	0.014	0.028	0.045	0.031
	Elevation	-0.030	0.058	-0.005	0.093
	Slope	0.018	0.022	-0.007	0.026
	Aspect	-0.021	0.019	0.034	0.021
	Drought Index	0.244	0.095	0.012	0.121
		R^2:0.94; Adj. R^2: 0.93; AICc: 2685.86		R^2:0.78; Adj. R^2: 0.77; AICc: 1967.95	

Appendix 2. Supplementary materials paper III

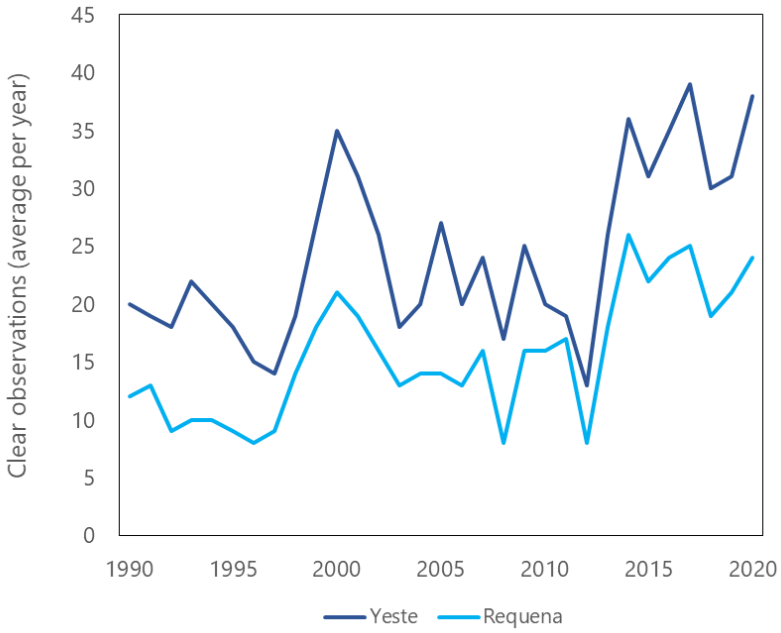

Figure S5.1. Clear sky observations per year (on average) for the study sites.

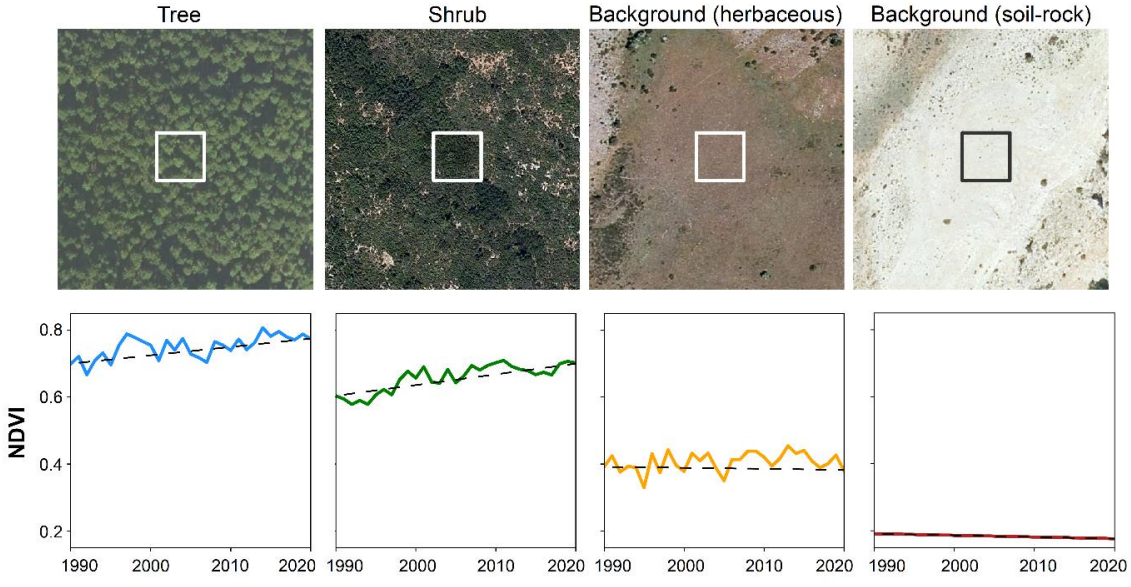

Figure S5.2. Examples of temporally stable pixels of pure tree and shrub cover types as well as pure or mixed background cover types based on visual interpretation of orthophotos (above) and stable time series (dashed line indicates the trajectory and colour lines annual NDVI time series).

Figure S5.3. Examples of validation pixels with estimated cover fractions.

Table S5.1. Number of pixels per cover class included in the library.

			Nº pixels	*Yeste*	*Requena*
Vegetation	Tree	*Quercus*	5	2	3
		Pinus	19	10	9
	Shrub	Shrub	14	7	7
Background	Soil	Bare soil	8	4	4
		Rock	2	1	1
	Herbaceous	Unirrigated grasslands	4	2	2
			Total = 52		

Appendix 3. Scientific production on forest remote sensing

The achievements of this thesis have been presented at the following conferences and symposiums:

- ForestSAT 2022, 29 August – 3 September 2022, Berlin (Germany). Contribution: *Shifts in post-fire forest cover composition from Landsat fraction images using machine learning regression-based unmixing.*
- 19th Congress of the Spanish Association of Remote Sensing, 29 June – 1 July 2022, Pamplona (Spain). Contribution: *Combinando datos LiDAR e imágenes Landsat para la evaluación de la recuperación de la estructura post-incendio en pinares mediterráneos.*
- SPIE Remote Sensing, 13 - 17 September 2021, Madrid (Spain). Contribution: *Extrapolating forest canopy cover by combining airborne LiDAR and Landsat data: The case of the Yeste Fire (Spain).*
- 8th Conference of Young Researchers of the University of Alcalá, 9 – 11 December 2020, Alcalá de Henares (Spain). Contribution: *Evolución de la recuperación post-incendio de pinares mediterráneos a partir de series temporales de imágenes Landsat y datos Lidar.*
- 3rd Symposium of PhD researchers on Geographical Information Technologies (SITIG-UAH), 25 – 26 November 2020, Alcalá de Henares (Spain). Contribution: *Analizando la regeneración post-incendio en bosques mediterráneos a partir de imágenes Landsat y datos Lidar.*
- 2nd Symposium of Geographical Information Technologies PhD program, 20 November 2019, Alcalá de Henares (Spain). Contribution: *Estimación de la regeneración post-incendio a partir de imágenes Landsat, datos Lidar y variables ambientales.*
- 18th Congress of the Spanish Association of Remote Sensing, 25 - 27 September 2019, Valladolid (Spain). Contribution: *Clasificación de trayectorias de regeneración post-incendio a partir de series temporales de Landsat: El caso de Yeste (Albacete).*

- SPIE Remote Sensing, 9-12 September 2019, Strasbourg (France). Contribution: *Classification of post-fire recovery trajectories using Landsat time series in the Mediterranean region: Spain.*

Appendix 4. Funding sources

This thesis was funded by the Spanish Ministry of Science, Innovation and Universities through the *Formación del Profesorado Universitario* pre-doctoral grant scheme (FPU17/03260).

During the doctoral research period, the author of this thesis received mobility grants to attend international conferences (*Bolsas de Viaje de la Universidad de Alcalá*) and did two research stays funded by the FPU mobility program for pre-doctoral researchers from the Spanish Ministry of Science, Innovation and Universities:

1. Earth Observation Lab, Humboldt-Universität zu Berlin (Berlin, Germany).
   - Supervisor: Patrick Hostert
   - Period: 01/05/2021 – 31/07/2021
   - Funding: FPU mobility grant (EST19/00215)

2. Climate and Ecosystems Research Group, Vrije Universiteit Amsterdam (Amsterdam, Netherlands).
   - Supervisor: Sander Veraverbeke
   - Period: 01/04/2022 - 30/06/2022
   - Funding: FPU mobility grant (EST22/00075

Universidad de Alcalá